PRESSURE WAVE PROPAGATION IN ADIABATIC TWO-PHASE FLOW

by

ROWLAND GRAYSON EVANS

PRESSURE WAVE PROPAGATION IN ADIABATIC TWO-PHASE FLOW

BY

ROWLAND GRAYSON EVANS

Submitted to the Department of Mechanical Engineering on May 17, 1968 in partial fulfillment of the requirements for the degree of Doctor of Science.

ABSTRACT

At present, there is a lack of reliable data on the propagation velocity of pressure waves in flowing gas-liquid two-phase systems in the void fraction range from roughly fifty to ninety-five percent. This is unfortunate because most commercial two-phase systems operate to some degree in this void fraction range, and because what little data exists is in disagreement with the present theory.

Classical methods of measuring acoustic velocity such as the acoustic interferometer are shown to be unsuitable for this void fraction range. A technique was developed in which the velocity and strength of shock waves traveling in the mixture were measured. Then, by extrapolating the results to a shock wave pressure ratio of unity, the local acoustic velocity is obtained.

Measurements of the acoustic velocity have been made in a flowing air-water mixture near the inlet and exit of a half-inch diameter vertical pipe fourteen feet in length. These measurements were correlated with the results of void fraction measurements made with quick-closing valves and phase distribution measurements made with an electrical resistance probe. The effect of inlet conditions was investigated by injecting the water along the wall through a porous section, and then repeating the measurements with the water injected at the center with an axial nozzle. Mass velocities used were from 0.257×10^6 to 1.31×10^6 lb/hr ft^2, void fractions measured were from 0.565 to 0.981, and flow regimes observed were slug, annular and mist flow.

The data indicates that the propagation of acoustic signals is done primarily through the core of the flow. Hence conditions in the core, particularly density inhomogenieties and inlet effects govern the propagation characteristics. The core propagation model developed here offers a logical explanation of the disagreement between existing data and theory. Further, it offers some hope of improving the predictions of exit choking in pipes.

Thesis Supervisor: Arthur E. Bergles
Title: Associate Professor of Mechanical Engineering

DEDICATION

This thesis is dedicated to the memory of the author's mother, the late Mrs. Helen Black Evans. Her ideals and vision provided the inspiration which made this work possible.

ACKNOWLEDGEMENTS

This study was carried out under the direction of Professors S. W. Gouse, Jr., A. E. Bergles, and P. Griffith. Their advice and support is gratefully acknowledged as having made the thesis possible.

Laboratory space and facilities were provided by the Engineering Projects Laboratory of the Mechanical Engineering Department. Fabrication of the various parts of the apparatus was done in this laboratory and in the Mechanical Engineering Department shops. The assistance of Mr. C. W. Christensen, Mr. R. E. Johnson, Mr. J. A. Calloggero, Mr. J. N. Orgettas, Mr. E. J. Clarke, and Mr. N. R. Andrews is gratefully acknowledged. The patient support of Mr. L. Mandeville was invaluable in the successful operation of the electronic equipment.

Professor Ragowski's sound advice on pressure transducers is greatefully acknowledged. Dr. L. Hoogenboom of Mechanical Technology, Incorporated, Latham, New York, provided transducer assistance.

Financial support for the thesis apparatus was provided by the United States Navy Office of Naval Research, Power Branch, through contract number 3963(15) under the cognizance of Mr. W. C. Karl.

Finally, the assistance of Miss Andrea Bickell in typing the text is gratefully acknowledged.

TABLE OF CONTENTS

Table of Contents contd.

LIST OF FIGURES

LIST OF SYMBOLS

A	arbitrary constant
c	Acoustic velocity (M/sec)
$\bar{c}$	Mean local acoustic velocity (ft/sec)
C_p	Specific heat at constant pressure (B.T.U./lbm^{o}F)
C_v	Specific heat at constant volume (B.T.U./lbm^{o}F)
f	frequency (cycles/sec)
k	Separation of constant for wave equation solution.
M	Mach number
p	Pressure (lbf/in^2)
P_r	Prandtl Number
R	Radius (ft)
t	Time (sec)
u	Local velocity in x coordinate direction (ft/sec)
$\bar{u}$	Mean local core velocity (ft/sec)
V	Velocity (ft/sec)
$\bar{V}$	Superficial Velocity (W/Area of Tube) (ft/sec)
w	Shock wave absolute velocity (ft/sec)
W	Weight rate of flow (lb/hr ft^2)
W_e	Weber Number
x	Coordinate direction (ft)
X	Flowing mass quality ($W_g/(W_g + W_l)$)
y	Coordinate direction (ft)

Greek Letters

α	Void Fraction
γ	Ratio of specific heats
δ	Film thickness (ft)
μ	Viscosity
ρ	Density (lbm/ft^3)
σ	Surface tension
τ	Characteristic time of a process (sec)
ω	Angular frequency (radius/sec)

Subscripts

co	Cut off
d	Viscous drag
g	Gas
l	Liquid
m	Misture
r	Relaxation
t	Thermal conduction
1	Conditions before arrival of shock wave
2	Conditions immediately after arrival of shock wave

CHAPTER I

INTRODUCTION

1.1 Background

The velocity of propagation of pressure waves is of importance in gas-liquid two-phase flow systems for several reasons. First, treatment of the flow oscillation problem in boiling heat exchangers requires a realistic calculation of the lag time required for pressure differences in the exit plenum to be felt in the inlet plenum, and vice versa. Second, the phenomena of choked flow is not adequately understood at present. In particular, the classical compressible fluid single-phase theory predicts that exit choking occurs when the fluid reaches sonic velocity at the exit. However, there is a discrepancy between the data observed and the acoustic velocity calculated using a homogeneous equilibrium model. Third, the rapid depressurization of a pressure vessel can cause large forces to develop on light internal baffles and pipes, causing structural failure. This occurs if the differences in void fraction are distributed in such a way that the depressurization signal is able to proceed faster on one side of the structure than on the other. Finally, it seems possible that a situation might exist in which exit choking could couple with heat transfer to cause a flow oscillation. This is postulated on the basis of the existence of a time lag between the effects of flow rate on vapor generation and

the effect of exit choking on flow rate. The effects interact because the choked flow rate has been observed to have an order of magnitude charge with a change in flow regime and of course the flow regime is determined by the amount of vapor present.

In reviewing these problems, it became clear that they had in common the need for accurate information on the acoustic velocity in two-phase flow. Further the discrepancies in the exit choking data suggested that the existing acoustic velocity predictions were inadequate. This motivated a review of the literature on the subject and the subsequent investigation.

1.2 Review of Two-Phase Flow Acoustic Velocity Literature

The literature on acoustic velocity in two-phase flow has been reviewed at least twice in the last four years[1,2]*. Therefore only a summary of the state-of-the-art will be given here although a chronological list of important references is included in the bibliography, references (3) to (38). This is not an encyclopedic listing and it specifically omits the extensive literature on attenuation.

The classical method of making acoustic velocity measurements is to place the medium to be tested in an acoustic interferometer or standing wave tube. A sound source at one end is

---

*Numbers in superscripted parentheses refer to references listed in the Bibliography on page

reflected from a rigid plug in the other end resulting in a standing wave in the tube, the characteristics of which can be very accurately measured. Then knowing the frequency of the source, velocities can be calculated with great precision. A check of the above cited literature reveals that all but one of the experimental investigators used some form of this technique. Foldy[7,8] generated a screen of bubbles in an open body of water and then measured the reflection and attenuation of a sound source near the screen. Both of these techniques are accurate and convenient to use. However, they are characterized by the requirement that the measurements be conducted in a static or near static sample of the media. Thus in order to use these methods for two-phase flows, the mixture must occur in a flow regime which possesses a statically stable distribution. Such a regime is defined as one which can be duplicated in all of its particulars in a quadi-static system in which at least one of the phases has no net flow. In addition, the distributions are often independent of diameter effects. A statically unstable regime relies on strong dynamic interaction forces occurring in conjunction with flow in a conduit to maintain the configuration of its phase distribution. Such a system cannot be reproduced without these dynamic forces, and therefore it is inherently incompatible with the above acoustic measurement techniques. It is clear therefore that flow regimes have a direct bearing on the ease with which acoustic

measurements can be made and so the known flow regimes were reviewed from this point of view.

1.2.1 Distribution Stability of Flow Regimes

Figures 1A and 1B are schematic diagrams of the flow patterns commonly occurring in vertical and horizontal adiabatic flow. Their more frequently used descriptive titles are also shown and will be used in the following review.

The stratified flow regime is stable because it is inherently a low velocity regime and so already a quasi-static system. Bubble flow is stable primarily because of the low relative velocity between the phases. The low density ratio and high surface area give bubbles such a high drag to mass ratio that they must follow the liquid matrix very closely.

In general, bubbly flow does not exist much beyond the point where the volume of gas exceeds the volume of liquid; i.e., about fifty percent void fraction. The actual transition point away from bubbly flow varies widely and is quite dependent on the general flow parameters and on the properties of the liquid phase. In particular, if the velocity is very low and if the liquid contains surface active agents, a foam flow can exist up to very high void fractions. This is also a stable quasi-static system.

Under certain circumstances, the bubbles agglomerate and form slug flow in which long bubble plugs are separated by liquid slugs. This can exist in the void fraction range from ten to sixty percent, depending again very strongly on fluid properties and flow conditions. At low velocities this is a stable regime in the sense that the gas plugs travel at a regular predictable rate and so can be set up in a quasi-static model. However, there is a strong diameter effect so that measurements would have to be made at the same diameter and a long enough length would have to be used to arrive at a meaningful average of the flow properties. As the flow rate increases, it causes further interactions which change the nature of the flow making the slugs less distinct. For this reason, slug flow regime can be considered stable only at low bulk flow rates.

Next a liquid drop configuration commonly called mist flow will be examined. To gain an understanding of this regime it is helpful to turn to the large body of literature on particulate flow which it closely resembles. It is found that there are two stable configurations for particles. One is the case where the relative fluid velocity is less than the particle terminal velocity and the particles are concentrated enough that they are intimately interacting with one another. This low void fraction configuration is known as a fluidized bed and no comparable analogy exists to it in gas-liquid mixtures. The other stable configuration exists at

high void fractions in which the relative velocity between the gas and the particles is equal to the terminal velocity and the concentration is so low that the particles do not interfere with one another. If the concentration is increased beyond a certain point, the particles begin to interact causing floculation which produces the unsteady flow regime called slugging flow. The mechanism of what happens is that when the concentration reaches a certain value the particles are so close together that they begin to pass into the wakes behind other particles. When this happens, the particle in the wake catches up with the lead particle. This is because the particle maintains its terminal velocity constant relative to the flow field which is less in the wake than in the free stream causing a relative velocity to exist between the particles. When they collide, the hydrodynamic forces cause them to stick together producing a new particle with twice the weight but only a slightly larger effective surface area. It, therefore, has a substantially higher terminal velocity than the other particles, and it drops out of suspension. Figure 2 is a partially complete stability map for particulate flow which shows the effects of the particle to fluid density as well as concentration.[39] Obviously, a similar interference mechanism can exist for liquid particles, and hence it is to be expected that this stability map will apply to them as well.

Forsland[38] and Isshiki[39] have suggested that drop size depends on the gas velocity in that whenever a critical drop Weber number is reached, the dynamic forces split the drop apart.

$$We_c = \frac{\rho_g \Delta v^2 \delta}{\sigma} \simeq 7.5 \qquad (1)$$

Thus the stability limits on drop size and concentration can be predicted. Forsland's measurements of drop size and quality in the mist flow regime (high quality film boiling) are in good agreement with the suggested stability concentrations of this map. Snyder's[42] data also shows void fractions above the stability limit although his observed drop diameters are somewhat smaller than Forsland's.

Thus it can be seen that for other than low flow rates, stable phase distribution configurations exist only in the bubbly flow regime at low void fractions and the mist flow regime at very high void fractions. In the broad range in between from about fifty to ninety-five percent void fraction, no stable configuration exists. The flow regimes which occur in this region are annular, semi-annular, spray or dispersed annular and high velocity slug flow. In all of these regimes, the way in which the phases are distributed are controlled by large dynamic interaction forces occurring as a result of flow in the pipe. The configuration of the distribution is affected by changes in component velocity, conduit geometry, inlet conditions and a host of other variables. Therefore, the

properties of these flow regimes cannot be duplicated in a standing wave tube and meaningful acoustic measurements must be made on the actual flow itself in a pipe under normal operating conditions.

It is appropriate to mention one other point that the distribution stability implies. It is the ease with which a mathematical model can be constructed to describe it. In bubble and mist flow, the phases can usually be considered to be uniformly distributed in one another. Consequently, the properties of the mixture can be accurately represented by an appropriately weighted average of the properties of the component phases. Further, the interactions between the phases can be accurately described by existing formulas. In separated flows, such as stratified or slug flows, the phases can be treated individually, independent of one another. In the unstable flow regimes, neither of these simplifications are possible because of the irregular and confused way in which the phases are distributed. The interactions between the phases are similarly chaotic and they do not admit to any theoretical analysis.

With this understanding of the interaction of the fundamental stability characteristics of gas liquid systems in acoustic measurement techniques, a summary of the literature can be undertaken with a better perspective. As expected the stable, uniformly distributed regimes have been investigated first. Curiously, the stable separated flows have not. The author is

unaware of any acoustic measurements having ever been made in stratified or low velocity stable slug flow. There does not seem to be much evidence of commercial application for acoustic velocity data in these regimes and the dramatic reduction in acoustic velocity observed in the distributed systems theoretically will not occur, thus precluding academic interest. However, whether the absence of experiments is due to these or other reasons is not known.

A summary of the bubble flow regime will be made first. At very low void fractions Silberman's[11] experimental verification of Spitzer's[6] analysis including thermal conduction, surface tension and bubble resonances is the best reference. At other void fractions Karplus'[13] work is the authoritative standard for the two-component bubble flow regime. His analysis is based on a homogeneous mixture model in which the bubble dimensions are small with respect to the wave length of the signal. It can be shown that the equations developed by all of the other authors can be reduced by the same assumptions to the simplified one which Karplus presents and verifies experimentally (Figure 3).

$$\frac{c_m^2}{c_g^2} = \frac{1}{\gamma\alpha(1-\alpha)\,\frac{\rho_\ell}{\rho_g}} \qquad (2)$$

It is important to notice that this data definitely confirms isothermal propagation at the low frequencies used in the experiment.

Single component, i.e., steam-water, bubble mixtures are covered by Walle et. al.[29] and Davies[31]. The additional factor of mass transfer is shown to produce several anomalies. Among these are the effects of frequency (governs the amount of mass transfer), amplitude (large amplitudes near the saturation point can condense all of the vapor phase), and wave shape (rarefaction waves are theoretically less stable than compression waves).

Now consider the mist flow regime. For many years investigators believed that the homogeneous equilibrium model which had worked so well for bubble flow was also valid for mist flow. However, in the early 1960's Collingham and Firey[21], Deich[25], and Bowles and Manion[33] obtained data which did not agree with equilibrium predictions. The fact that viscous drag and heat conduction for a drop are finite rate processes had been previously recognized by several authors[15,15,20,22, 26-28,30]. However, it remained for Temkin[34,35] in 1966 to develop a general unified theory. By calculating the relaxation time of the thermal and viscous exponential rate processes, he was able to predict the characteristic frequency below which equilibrium propagation occurred. Figure 4 shows the excellent experimental verification of this theory. His equation which is only valid for very high void fractions ($\alpha > 0.95$) is as follows:

$$\frac{c_g^2}{c_m^2} - 1 = \frac{\rho_\ell(1-\alpha)}{\rho_g \alpha} \left\{ \frac{1}{1+\omega^2\tau_d^2} + \frac{(\gamma-1)\frac{C_{p\ell}}{C_{pg}}}{1+\omega^2\tau_t^2} \right\} \tag{3}$$

$$\tau_d = \frac{2\rho_\ell}{9\mu_g} R^2$$

$$\tau_t = \frac{3}{2} \frac{Pr_g C_{p\ell}}{C_{pg}} \tau_d$$

In order to illustrate the order of magnitude of the effects involved, sample calculations have been carried out for a typical case. The relaxation frequencies for a steam-water mixture at atmospheric pressure with drops of 200 mircrons diameter are:

$$f_d = .931 \text{ cps} \qquad f_t = .291 \text{ cps}$$

These frequencies are very sensitive to drop size, but they do demonstrate why nonequilibrium effects were observed so easily in mist flow. Relaxation frequencies for bubble flow on the other hand can be expected to be several orders of magnitude larger. Although the above equations cannot be used for bubbles, it is clear that their high drag-to-mass ratio and the higher thermal conductivity of the fluid matrix will permit substantially lower relaxation times. Hence, isothermal, equilibrium propagation is much more likely to occur as has been observed.

Just recently Deich et al.[38] obtained some data on 10-30 micron water drops in steam and correlated it with τ_d. The agreement is as good as could be expected in view of the fact that he does not consider the effects of relaxation times due to heat and mass transfer.

Finally, comment should be made about propagation at the saturated vapor line. Metastable phase states often occur and their existence can cause confusing results for data collected in this area. The work of Deich et al[32] indicates that although there are conflicting statements as to what occurs here, there is no convincing evidence; and, on the contrary, there is some theoretical basis for believing that there are no step changes in specific heat or acoustic velocity.

In contrast to the abundent work available on the stable distributed flow configurations little has been said about the unstable void fraction range. Some authors have merely extended the equilibrium calculations through this range as for example in Figure 2. Bowles and Manion have made an unsupported extrapolation of their mist flow equilibrium data into this area (Figure 4). However, the only data known to exist is the recent work by Seminov and Kosterin[24]. They timed the passage of pressure pulses past two transducers arranged in the wall of a pipe containing the flowing two-phase mixture. However, the data shown in Figure 5 is actually in worse agreement with the predicted values than it appears. This

is because the predicted values were calculated using adiabatic rather than isothermal propagation which makes the predicted line about eighteen percent higher than it should be. In addition, some of the experimental techniques used in their investigation may be questionable, and no information on flow regime is given.

1.3 Discussion of Unstable Flow Regime

It is now clear that there exists a hiatus in the existing acoustic velocity theory and data in the unstable annular flow regimes from fifty to ninety-five percent void fraction. In view of the intractable nature of the flow conditions and the experimental difficulties that they cause, this area would probably have been studiously avoided were it not for the unpleasant fact that the vast majority of two-phase flow systems operate to some degree in it. Consequently, there is a great need for information on flows in this region; and because of this practical consideration, it was selected as the region for this investigation.

An appropriate beginning is to examine what is known about the flow regimes which exist in this void fraction range from the point of view of devising an experiment to measure acoustic velocity. Starting at about fifty percent void fraction, increasing the volume of the gas causes the bubbles to coalesce and eventually fill the core of the pipe with gas. Starting at the other end at ninety-five percent void fraction, the addition of more liquid causes aglomeration of some drops which

then precipitate out and form an annular film on the wall. The other important phenomena which influences the flow is the strong interaction at the interface of the high velocity core gas with the annular liquid film which produces wave action and entrainment. The flow pattern that emerges then is one of a relatively slow, thin annular film of liquid on the wall with a relatively fast inner gas core transporting varying amounts of liquid in the form of slugs, blobs, tendrils, droplets, etc. At moderate flow rates, the transitions are reasonably distinct and orderly. The normal progression is from bubbly to slug, then to semi-annular, then to annular, then to spray annular and finally to mist flow.[57] However, as flow rate rises, the process becomes increasingly confused until at very high flow rates there appears to be only one long transition from bubbly to mist flow with no discernable intermediate regimes[43-45].

If the drop critical Weber number and stability theories are applied to this regime, they indicate that the flow must be in the form of a core mist of specifically limited drop size and concentration and an annular film on the wall containing all of the rest of the liquid. This indeed is observed to be true in the limited area where the void fractions approach the mist flow stability boundary. For instance, if the core void fraction is calculated for Hinkle's[46] data using the assumption that the value of the slip is about two, it is found that the core void is always in excess of ninety-nine percent. However,

over most of the void fraction range drops, globs, and tendrils of liquid greatly in excess of the size and/or concentration limits of the theory have been also observed.[47,48] This does not indicate an error in the theory. Rather, it implies that such liquid masses are not in stable suspension in the gas, but only following short semi-ballistic trajectories until they impact on the wall film. In fact, splashes of just this sort have been observed by Hewitt.[47] It also is evidence of the fact that the theories do not take into account the source of the entrainment which is due to inlet conditions or shearing off of the crests of the roll waves by the gas in the core. As has been previously mentioned, various types of slug flow can exist at moderate and low flow rates near the lower end of this void fraction region. The hydrodynamics of stable, low velocity slug flow are completely different from the annular flow regimes, being governed by the long gas plugs[49]. At the very high flow rates, characteristic to exit choking, these stable slugs do not form in the flow[43-46], and so this regime will not be treated further. The unstable higher velocity slug flows may form depending on just how high a flow rate exists. In fact, the cutoff point beyond which they no longer appear is not precisely defined in the literature. This is because it becomes increasingly difficult to distinguish between slug, semi-annular, and wispy annular at high flow rates. This in turn implies that the hydrodynamics of these three regions is not too different at elevated flow rates.

If the model of a core of stable fine mist and large ballistic globs surrounded by a wavy annular liquid film is in fact valid, it is reasonable to expect that the Temkin relaxation theory will be applicable to some extent in the core. In fact his theory predicts that the annular film is isolated from the gas core by such a relatively small surface area (compared to the drop's) that it will play only a minor part in the relaxation processes in the core. Temkin's analysis predicts that above a certain relaxation frequency, the velocity of pressure disturbances is essentially equal to the acoustic velocity in the gas as long as the gas phase is continuous. It offers little insight into the part the ballistic drops play or the effects of the large roll wave disturbances.

1.4 Scope of Investigation

Once the background studies had been completed, the objectives of a possible investigation as well as the restrictions within which it would have to be conducted began to emerge. It was decided to attempt to measure the acoustic velocity in a gas liquid two-phase mixture in the void fraction range from roughly fifty to ninety five percent. Because of the unstable nature of the flow regimes in this range, tests would have to be conducted on a flowing mixture in a pipe under typical operating conditions. High flow ratios were selected in order that any information obtained would be more useful for exit

choking investigations. It was decided to use two components for this first investigation in order not to confuse the data with the anomalies caused by mass transfer. The two components were chosen to be air and water for convenience.

A complementary objective of the experiment was to attempt to establish the effects of two separate phenomena on the acoustic velocity. The first of these was the effect of the distribution of the phases on the "equilibrium" or low frequency propagation velocity. It was decided to determine the effects of changes in distribution caused by length by making measurements near the inlet and exit of a long tube. Changes in distribution caused by inlet conditions would be investigated by making the measurements with the water injected along the wall through a porous wall section and then repeating the measurements with the water injected on the centerline by an axial nozzle.

Secondly, it was hoped to establish the existence of Temkin's relaxation phenomena on higher frequency propagation. To this end it was decided to use high frequencies in the investigation.

Finally, it was anticipated that a new technique for measuring acoustic velocity would have to be devised. This was because of the requirement to conduct the measurements in a pipe under typical operation conditions.

CHAPTER II

APPARATUS AND PROCEDURE

2.1 Description of the Test Loop

The experimental apparatus was located in the M.I.T. Engineering Projects Laboratory and is similar in many respects to Hinkle's[46] apparatus. Figure 28 is a diagram of the system and the specific details of the components are discussed in Appendix A.

It is an air-water system designed so that it can be operated as either an open or closed loop. The air supply was controlled by a diaphram actuated regulator valve after filtration and oil removal. The water used was Cambridge City tap water because the effects of purity were expected to be insignificant and beyond the scope of this initial investigation. A centrifugal pump provided supply pressure which, after filtration, was fed to the injector through a throttle valve. Heat exchangers were provided to regulate the temperature of both phases. At the exit of the test section the phases were run through a separator. The air was discharged to the atmosphere and the water was returned to a collection tank where it could be measured.

The test section material was selected as plexiglas to permit visualization of flow conditions. An inner diameter of one half inch was selected as typical of installations in which

acoustic effects are important. The orientation of vertical co-current upflow was chosen for the same reason. It was desirable to have the test section as long as possible in order to exaggerate the effects of length. Fourteen feet was convenient and satisfied this requirement. A three foot long straightener section below the water injector allowed the air to reach a fully developed velocity distribution before entering the test section.

Pressures and flow rates of the phases were carefully measured as described in Appendix B.

2.2 Instrumentation

2.2.1 Selection of Pressure Signal

The ideal experiment would be to introduce a harmonic pressure wave into the flowing mixture and then observe the effects caused by changes in frequency. Then existing signal processing techniques could be used to filter noise and determine other useful information such as attenuation and phase shift in addition to the velocity. However, it is extremely difficult to obtain a single transmitter which is able to cover such a broad frequency range in air with much power output. Then, when it is remembered that the transmitter must be small enough to somehow be incorporated into the geometry of the system without disturbing flow conditions, it is hopelessly impossible. One compromise might be to select a single frequency which a very small crystal transmitter embedded in

the tube wall could produce. The primary disadvantage of this scheme is that one must be able to calculate how high a frequency is high enough, and at present there does not seem to be an analytic way of doing this. Another drawback is that the impedance mismatch between air and water is so great that a wall transmitter would probably be unable to push much energy past the liquid wall film into the core. Consequently, harmonic signals were eliminated and other types had to be considered. One was an impulse signal which theoretically contains infinitely high frequency components. This also would be able to take advantage of signal processing techniques, but no feasible way could be found to manufacture a sharp enough impulse in a two-phase flow.

The next approach was to consider what type of signal was actually involved in the phenomena which had motivated the investigation originally. In pressure vessel decompression, it appears that the signal is a very steep pressure drop while in exit choking it very nearly approximates a step rarefaction wave. Consequently, a step rarefaction pressure signal is probably the most appropriate to measure. Unfortunately, it is extremely difficult to produce such a signal, primarily because it is an unstable configuration in air and disperses as it travels. It is still difficult, but relatively easier, to produce a step compression wave.

Such a wave would be appropriate for investigating high frequency phenomena because a Fourier analysis indicates that it contains a spectrum of frequencies which, theoretically at least, extend infinitely high. As is well known from single phase compressible flow theory a step compression wave corresponds to a shock wave which under certain conditions, is a stable configuration. Consequently, a shock wave is attractive to use from a practical point of view. It must be remembered that for such a wave to satisfy the acoustic wave equation, the amplitude must be small enough to justify use of the standard acoustic approximations.[50] A shock wave, on the other hand, is a finite amplitude phenomena whose existence depends on just those property variations which the standard acoustic approximations assume as constant. Not surprisingly, the equations governing shock propagation are markedly different than those for acoustic propagation,[51] so that if a shock wave is to be used successfully, some means of extracting the desired information from it must be devised. The compressible flow theory shows that the speed of propagation of a shock wave is dependent upon the pressure ratio across it. In the limit as the pressure ratio goes to unity, the velocity of the shock wave approaches the acoustic velocity in the media. Therefore, if the velocity of several shock waves of different pressure ratios are measured, the results can be extrapolated to unity pressure ratio

The propagation of shock waves in a gas in which particles are suspended introduces some additional considerations. This problem has been investigated extensively by several authors [14,15,20,22,26-28,30]. The most recent application for these investigations has been rocket nozzle flow calculations. Figure 7 shows the typical results of one of these investigations[22] as well as the transformation required to translate the variables in the stationary shock frame of reference to a moving shock frame[51]. It is demonstrated that if the velocities of the shock wave are extrapolated to a pressure ratio of p_2/p_1 equal to unity, the velocity obtained is the equilibrium velocity of sound in the mixture. It is also shown that in the region immediately following the shock a so-called "frozen flow" condition exists in which the gas properties are identical with what they would be behind a shock if there were no particles present. Consequently, if V_y is extrapolated to a unity pressure ratio of p_2/p_1 equal to unity it will yield the "frozen" or non equilibrium sound speed. Thus this method offers the possibility of obtaining both the high and low frequency limit propagation velocities in a single experiment.

In measuring the velocity of the shock wave in the pipe a problem arises with regard to the local velocity of the mixture. It is obvious that an observer in the laboratory frame of reference will see the shock pass with a velocity equal to $w \pm u$ depending on whether the shock is traveling

upstream or downstream in the flowing mixture. What is not so clear is what value of the local velocity to use. It is not known a priori what type of weighted mean is appropriate for acoustic propagation purposes. Further the state-of-the-art and the large fluctuations in the flow would not permit very accurate predictions even if the correct mean were known. It was decided to solve the problem by measuring the apparent velocity of shocks traveling in both the upstream and then the downstream direction in the flow past the same point on the wall of the tube. Then the measurements could be extrapolated to unity pressure ratio to give $\bar{c}_m + \bar{u}$ and $\bar{c}_m - \bar{u}$. These are easily averaged to eliminate $\bar{u}$.

2.2.2 Selection of Shock Initiation Device

Among the requirements of a device to produce the shock wave in a two-phase flow are that it be mechanically convenient to use repeatedly, and that it produce a signal which coalesces into a plane fronted shock within a few diameters from the source. This is important because of the high attenuation of pressure signals in flowing two-phase mixtures which can, in fact, weaken the signal faster than the shock can form.

The first device tried was a spring operated quick closing valve, but its closing time, about 10 msec, was found to be an order of magnitude too slow. Next, a high voltage electric sprak discharging between two electrodes on opposite sides of the tube was considered. It could probably have caused shock

coalescence in the order of five tube diameters and would not have required the resetting of any parts. However, the production of a spark in the presence of a large amount of water was expected to be erratic and unsatisfactory. Another technique considered was to string two or three fine wires across the tube and vaporize them with a high voltage discharge. These exploding wires would have produced the most rapid shock coalescence, about three diameters, of any of the techniques considered. However, it was not used because there seemed to be no way of eliminating the mechanically tedious process of replacing the wires after each test.

The next approach was to adapt to our geometry the standard shock tube device of rupturing a diaphram. Cellophane was chosen because it shatters rapidly with small petals at the pressure levels anticipated. It is appropriate to mention that the strength of the cellophane varied widely with its age. In fact if lower strength was required, artificial ageing in a 200°F oven worked well. The diaphram will shatter properly only if the pressure behind it exceeds roughly fifty percent of the natural rupture pressure. The diaphram was mounted behind a side port in sort of a T arrangement to the main flow and was ruptured by a solenoid driven pin. (Figure 8) A slide arrangement was able to be devised which allowed the diaphrams to be changed quickly for a series of measurements. The diaphrams were mass produced by cementing the cellophane

between washers. Tests indicated that the disturbance would coalesce into a shock in between eight and ten diameters; somewhat slower than other techniques. Another drawback was that the side port would create some flow disturbance. However, it was felt that the mechanical simplicity of operation overrode these disadvantages. The extent to which experience vindicated the choice will be discussed later. It is to be noted, however, that the exploding wire method is still potentially the best if a good way of restringing the wires can be found.

2.2.3 Shock Wave Production

The efficiency of the diaphram system of shock wave production under actual operation in the flowing mixture will now be discussed. The results varied widely from very good in the high gas flow tests to unsatisfactory for the inlet of run three. The system was first tested with only air flowing in the pipe at about the velocity of run one in order to see if the shock wave interaction with the turbulent velocity profile [51] would cause any difficulties. None were observed over these short lengths so it was decided to proceed with the tests. Runs one and four were done first. It was noticed that a substantially higher pressure was required in the driver section behind the diaphram to produce shock waves of equivalent amplitudes as those observed in the preliminary all air tests. There are two effects observed. The first

was that the water reduced the brittleness of the cellophane so that it would tear rather than shatter. It also weakened the cellophane causing premature rupturing. These effects were counteracted by cutting down the length of time the diaphram was in contact with the water. The diaphram was not slid into place until just an instant before it was to be used. However, even when proper petaling had been obtained, shock strength was very much lower. This was probably caused by the presence of the wall film between the diaphram and the core. When the diaphram was ruptured, the shock had to blast its way through the film in order to get to the core. This of course absorbed a considerable amount of the shock wave's energy thereby reducing its strength. As expected the problem worsened as the water film thickness was increased for the other runs. Driver pressures were raised up to 125 psi in some cases as contrasted to the 10-15 psi required for the all air test. Even these extremes did not suffice at the inlet for run three. Here the highest water rate was being injected along the wall and the film was so thick that the shock simply could not blast its way through. As a result no observations could be made there.

Another curious observation was the inconsistent production of a shock at the exit for all of the medium and high water flow rate runs. At the inlet for these runs, if a shock could be produced at all, one was observed to occur nearly every time.

However, at the exit for these runs, shocks were only observed to occur about a third of the time. In view of the "open shutter" type of triggering system used, which will be discussed shortly, it is felt that if they had occurred more often they would have been seen. This ambiguity remains unresolved, but it will be discussed further in Chapter III.

Coalescence of the shock was also observed to be much poorer in the presence of the film. This was due to two effects. The first is, of course, the disruptive effect of the film on the pulse of air as it burst forth from the side port. The second was the effect of the local core flow velocity. As has been mentioned, adequate coalesence had been observed in stagnent air in from eight to ten diameters of travel up the tube. Obviously, if the media is flowing with some velocity, the shock will travel ten diameters relative to the fluid in a much shorter length of pipe if it is going upstream or a much longer length of pipe if it is going downstream. However, the transducers were constrained to remain a fixed distance away from the shock source in order that the positions at which the measurements were made could be correlated consistently. In retrospect it is observed that the transducers could have been located at a longer fixed distance from the source than originally chosen because the attenuation effects which were unknown in the beginning turned out to be less than expected. The effects of this foreshortening or lengthening were most

evident in the downstream series as anticipated. Only occasionally was continued coalescence of a shock observed in the upstream series.

It had been originally feared that the side port would cause an unacceptably large flow disturbance. No effects were observed in the tests which could have been attributed to this cause. The preliminary tests in the flowing air also showed no effects.

In conclusion, it can be seen that the arrangement of a ruptured diaphram discharging through a side port to initiate the shock wave was only marginally successful. Although it lived up to expectations with regard to its convenience, the quality of shock it produced varied too widely. In any future investigations a more careful investigation of the exploding wire technique is recommended.

2.2.4 Pressure Transducers

The requirements for pressure transducers to measure the amplitude and transit time of the shock down the tube are quite rigorous. Because of the high attenuation and dispersion inherent in a two-phase flow, the shock wave can be expected to decay over a short distance. Consequently, it is desirable to make measurements as soon after the shock coalesces and over as short a gauge distance as possible. Unfortunately, a short gauge length requires that the accuracy of the measurement of the signal transit time be extremely high. It is also desirable to

keep the transducer face width down to as small a fraction of the distance between them as is feasible, which imposes the constraint that the transducers should be very small. The transducers must be mounted so that they produce negligible flow disturbance and must be intimately coupled to the fluid. Small diameter pressure taps between the flow and a transducer are unsatisfactory because of attenuation and time lag in signal transmission. The lag problem can be overcome in theory by an elaborate calibration scheme, but this is so tedious and difficult from an experimental point of view that it should be avoided if possible. Large taps cause undesirable flow disturbances. Flush mounting is the desired configuration; and, of course, this also requires small diameter transducers. A fast rise time is important for accurate resolution of the short transit time and for adequate discrimination of the signal from the background noise. With these constraints in mind, a review of the available transducer types was made.

Piezoelectric transducers were investigated first as the most promising. One made by Chu[52] appeared to have satisfactory specifications for size, sensitivity, and frequency response and so it was obtained and tested. Unfortunately, the piezoelectric material had deteriorated with age and it was inoperative. Next a standard Kistler quartz crystal piezoelectric was tried. Although somewhat larger than desirable, it was adequate in sensitivity and frequency response. Unfortunately,

piezoelectric transducers are characterized by very low internal damping. As a result the response to the test signal, a shock wave in air, exhibited an oscillation with an amplitude of about seventy-five percent of the signal itself and a very slow decay. It was felt that the oscillation resulting from response to the large amount of ambient flow noise would mask the signal. An electrical filter could be used to exclude some of the ringing, but this is not entirely satisfactory since the signal itself is of very high frequency. As a result piezoelectrics were initially rejected.

The next type of transducer considered was a semiconductor strain gauge type made by Shaevitz Bytrex, Inc. The diameter was moderately large, the sensitivity was good, and the natural frequency was lower than desirable. However, it too had an internal damping ratio of about .01, and so it was no improvement over the piezoelectric.

It was next decided to investigate the possibility of making a transducer which would meet the required constraints. A circumferential strain gauge design was worked out but the mechanical difficulties of manufacturing it causes its rejection. Next a solid dielectric capacitance gauge design was worked out. It was an extensively modified arrangement of an end wall shock tube gauge originally made by Baganoff[53]. An extensive program was undertaken to determine a suitable technique for manufacturing it. The results were disappointing. So a firm

engaged in capacitance transducer manufacture, Mechanical Technology, Incorporated of Latham, New York, was engaged to make one along the lines of this design. Again, the results were disappointing.

As a result of these costly failures, the entire field of transducer types was reevaluated. The decision was made to attempt an actual series of measurements with a piezoelectric in a two-phase mixture to determine what modifications would be required under actual operating conditions to make the results usable. At this time it was discovered that the annular liquid film interacted with the transducer so that the coupled system had a very large effective damping ratio. Therefore, the response was no longer oscillatory and the major objection to piezoelectrics was removed. The larger than optimum diameter of the transducers was compensated for by a careful calibration of the system (Appendix II). The transducers were mounted flush to the tube wall in a shallow recess which was faired into the tube wall surface with silicone rubber compound. (Figure 9) The maximum surface discontinuity was observed to be about $\pm$ .005 inches and the layer was so thin it produced no detectable effects on the transducer's response.

3.2.5 Development of Trigger System

The development of an appropriate method to trigger the scope properly was a time-consuming process. The requirements

for such a trigger are that it be able to consistently turn on the scope a few microseconds prior to the arrival of the signal at the first transducer. In this way the root of the signal will be seen and the horizontal coordinate can be adjusted to give the maximum distance between the two traces displayed on the scope. This is highly desirable in order to improve the revolution accuracy of the travel time measurement. The external mode of triggering the scope was selected so that each trace would have its own channel allowing the differences in wave shape to be clearly seen.

The first attempt was to trigger off of the supply voltage to the solenoid. This was unsatisfactory because the time elapsed for the solenoid to activate, the diaphram to rupture, and the shock to reach the first transducer was two or three times the transit time of the shock between the two transducers. This bunched the traces too close together preventing an accurate measurement of the interval. The next attempt was to insert a delay line between the solenoid signal and the scope. This too failed when it was discovered that the arrival time varied from shot to shot by an amount in excess of the transient time so that the two signal traces rarely appeared on the scope at all. Consequently, it was decided to insert another piezo-electric just upstream of the test transducers and use its output to trigger the scope. A Kistler Model 601 was located for this purpose, but it was found that the signal strength

was insufficient to activate the external trigger of the scope even after maximum amplification by a Kistler Model 566 Charge Amplifier. Another amplifier with a very fast rise time was needed, but none of the locally available models were fast enough. Therefore an operational amplifier was constructed using a Philbrick Type P-55A operational amplifier. When it was inserted in series between the charge amplifier and the scope, it produced the required voltage but triggering was still erratic. It was finally discovered that when the solenoid switch was closed, the voltage surge in that circuit radiated a large electromagnetic noise signal despite the shielded wiring used. This was of sufficient strength so that when it was picked up by the leads in the triggering circuit, it turned the scope on. This problem was solved by elaborate shielding of the solenoid itself, a quieter switch and physical separation of all of the wiring. When finally adjusted, the system was able to trigger the scope so that about twenty microseconds of trace appeared on the screen prior to the root of the first transducer's signal when tested in air.

2.2.6 Data Recording System

The final arrangement as shown in Figure 9 consisted of two Kistler Model 601A and one Kistler Model 601 quartz piezoelectric transducers for the signal and the trigger respectively. A bank of three Kistler model 566 charge amplifiers was used

for amplification and the trigger signal was further amplified by an operational amplifier. The results were displayed on a Tektronix model 502A dual channel fast response oscilloscope. The scope was operated in the single sweep mode which was triggered externally as discussed above. The signal traces were then photographed with a Hewlett-Packard model 196A oscilloscope camera using Type 47 Polaroid film.

2.2.7 Transducer Performance

The Kistler Model 601A quartz piezoelectric transducers which were used on the experiment have a natural frequency of 130 kcps and a rise time to a step input of three microseconds. In the nitrogen shock tube calibration described in Appendix C, rise times of about nine microseconds were observed. This increase in rise time is due to the transit time of the shock wave across the face of the transducers and indicates that this active surface area is about .083 inches in diameter or about two thirds of the outside face diameter. The frequency of the "ring" or oscillation in the step response was also measured and found to very close to the expected 130 kcps. A slow beat was also observed indicating that the transducer had two components with natural frequencies very close to 130 kcps. The most obvious explanation is that the diaphram of the transducer had been designed to have about the same natural frequency as the quartz crystal.

As has been mentioned previously, the performance of the transducers was dramatically different when they were used in the two-phase mixture. The transducers apparently coupled themselves to the wall film so that the effective natural frequency was reduced by an order of magnitude. That is, the water film acted locally as an added mass to the diaphram of the transducer. Since the angular natural frequency of a system is defined as the square root of the ratio of its spring constant to its mass, it is clear that increasing the effective mass will reduce the natural frequency.

Examination of the pressure trace photographs of the experiment, Figures 20 to 25, yielded some interesting observations. Not all of the traces displayed an oscillatory response. In general, only the traces with very sharp rises displayed a ring. The frequencies of the oscillations were measured and they varied from about five to thirty-five kcps. The frequencies varied with the water flow rate and hence with the film thickness in the expected way; i.e., lowest frequencies occurred with the thickest films and vice versa. The frequencies were all about the same for a given flow condition for both upstrean and downstream observations. Occasionally, a small 130 kcps signal was superimposed on the lower frequency oscillation. Where it occurred, it often preceeded the arrival of the shock. Behavior of this type can be explained by the common phenomena of "ground wave" excitation of the crystal. A

so-called "ground wave" is mechanical noise, probably originating in this case from the diaphram rupturing device, traveling in the pipe wall and being transmitted to the crystal directly through the casing of the transducer. It is interesting to notice that this effect is observed only for low water rates or thin films. Apparently, the film dampens out wall noises too.

The other dramatic effect of the wall film transducer coupling was the dramatic increase in the effective damping ratio of the transducer. Overshoots for all signals were very small and often the oscillation died out after three or four cycles. This high damping was beneficial in two respects. First it allowed the amplitude of the response to be resolved more accurately and second, it prevented an oscillatory response to environmental noise from obscuring the signal.

The question can be raised as to whether or not the oscillatory response observed was due to surface waves on the film. As will be discussed, the transducers are actually measuring the boundary layer's response to the shock wave and this response involves disturbances of the layer's shape. Further evidence for this is given by the observation that the oscillations persist longer for the downstream observations than for the upstream. After a careful evaluation, it was decided that surface waves were probably not responsible. The strongest refutation is that the oscillations were not observed in all

cases. If the layer's response was characterized by surface waves, they should have appeared in all cases. Instead, it appeared only in the case of the fastest rise responses in keeping with classical dynamic response theory. The variability of the amplitude of the oscillations even for the fast rise response is entirely explainable by the variability of the effective damping by the film. The rise times of the signals also were in close correspondence to the observed frequency of the oscillation. Finally, it is felt that surface waves of an amplitude required to produce the observed signals could not possibly have had frequencies as high as several thousand cycles per second.

The very much lower effective natural frequencies produced by the film coupling caused two major difficulties. The first was that the root of the rise was so gradual that it was very difficult to discern where the wave began. Resolution of the transit time was therefore degraded considerably resulting in rather large errors. The second effect was the deterioration in trigger performance.

The triggering system has been previously described and in particular, the very short time available to turn on the scope was discussed. However, when the rise time of the signal itself approaches and exceeds the trigger time interval, the trigger signal will be late. Said in another way, a certain amplitude output is required from the triggering transducer in

order to turn on the scope. If the rise time of the signal is slow enough, this level of output will not have been reached before the root of the signal has arrived at the first of the test transducers. The net result of this is that the pressure trace for the first transducer will not show the root of the signal. Thus there is some ambiguity in determining which points on the traces to measure τ between. There are two possible remedies for this. The first way is to increase the power amplification of the trigger circuit so that a lower signal threshold can be used. This was tried but did not work because of the flow noise. The other way is to increase the distance between the trigger transducer and the first test transducer. Unfortunately, there was not sufficient time after the discovery of this effect in which to construct an entirely new transducer block.

The observed flow noise varied widely for the different runs, but in general it consisted of two types. (Figure 15) The first was a relatively high frequency jitter which was most prounounced at the exit and for the high gas flow runs. It was the amplitude of this component which determined the level at which the trigger threshold could be set. The desired mode of operation was to have the trigger turn on a single sweep when the signal arrived. Consequently, the trigger level had to be set high enough so that the noise would not trigger it before the signal arrived. The minimum level at which the

threshold could be set was ascertained experimentally for each run.

The second type of noise was a very large amplitude low frequency pulsating type flow noise which will be described further in the flow regime classification section. The amplitude was so large it exceeded the signal amplitude, and so it was impossible to set the trigger level above the noise and still see a signal. (Figure 7D) This dilemma was resolved by keeping the trigger threshold set at a level which would exclude the majority of the jitter and simply leaving the camera shutter open a short period of time. As a result the scope was triggered every time one of these pulsations arrived as well as by the signal. The camera then took a picture of several of these noise pulses superimposed on the signal. It was found that the frequency of the pulses was so slow that by careful coordination of the exposure with the initiation of the signal, only a few noise pulses would be seen on the picture. The evolution of this technique was a time consuming, frustrating experience and the quality of the resulting pictures poor. It was another object example of the intractable nature of this flow regime and demonstrates the extremes required to obtain data on it. It is recommended that in any future investigations an intensive effort be made to devise a more satisfactory data-recording system. One possibility is the use of high speed pictures of the scope trace.

2.2.8 Void Fraction Measurement Device

Correlation of the velocity measurements with void fraction was considered to be an important objective and accordingly the pros and cons of the various method of obtaining void fractions were investigated.(54) It was decided that the requirements of this initial investigation were best met by the technique of trapping a portion of the flow between quick-closing valves. The first proposal was to use rubber walled pinch valves because of their great simplicity of operation (Figure 10). A single air valve could be opened, quickly closing both of them simultaneously. A pair of valves were then obtained, fitted with permanent flanges and the rubber bores ground out to a $\pm$ .005 inch tolerance. The permanent flanges were necessary because it was found that the degree of compression of the rubber flange affected the inner dimensions of the rubber core. It was necessary also to anchor the rubber core firmly in place so that the inner bore could be accurately aligned with the test section bore. The calibration of the valves was very involved because of the need to account for the water displaced into the measuring section as the valve pinched shut. This, of course, changed as void fraction varied. Preliminary tests indicated that the valves closed with a repeatable displacement of about $\pm$ .1 ml, but only if the pressure difference between the chamber and the bore was maintained constant. However, when the valves were tested in

the apparatus under normal flow conditions, it was found that after the valves had closed, different bore pressures built up at the upper and lower valves. The external bore pressure on the upper valve was due to the hydrostatic head formed when all the water in the test section collected on top of it. The lower valve experienced a dynamic head due to the sudden stoppage of the flow and then a rapid rise to the no flow pressure output of the water pump. Consequently, the valves did not close uniformly in service. Finally, it was found that the body of the valve was so deep that the volume of water it contained when it was closed limited the maximum void fraction that was able to be measured to about ninety-one percent. For these reasons it was reluctantly decided to replace the pinch valves with ball valves. This necessitated the manufacture of an elaborate, cumbersome, spring operated trip latch mechanism shown in Figure 11. The maximum calibrated void fraction that the ball valves could measure was 98.2 percent, but the entire volume of water was visible, and so good estimates could be made for even higher voids than that. This was made possible by machining away the valve body so that only about one quarter inch of metal remained above the ball in the valve. The inner diameters of the valves were bored out to size to minimize flow disturbances and the stops for the valve handles were accurately machined so that the valve would open to the same position each time. Precautions

also had to be taken to keep the valve body tight so that leakage around the ball would not occur. This in turn increased the force required to turn the handle which required the use of a larger spring. Once the mechanics of the latch were worked out, this device operated reliably and accurately.

2.2.9 Flow Regime Classification

As has been discussed the way in which the phases are configured is likely to play an important part in the pressure wave propagation. Establishment of flow regime boundaries is an approximate process at best. Furthermore, the effects of flow geometry and fluid properties on flow regimes presently is not understood very well, if at all. Consequently, existing flow regime maps can be used only for qualitative indications in a very general way of what might be expected. It was decided that more definitive information on the distribution of the phases at the operating points used for this investigation was needed than was available from existing maps. For these reasons it was decided that some measurements of the phase distributions would have to be undertaken.

In 1966 Bergles and Suo[43] reviewed the existing flow regime identification techniques. The following list is from their paper.

Techniques for Identifying Two-Phase Flow Regimes

Observation of flow within test section

(visual observations; still, motion, or x-ray pictures).

Observation of flow at exit to test section

(visual obervation; still or motion pictures)

Radiation attenuation

Hot-wire probes.

Sampling probes

Electrical probes (resistance or impedance)

Infer flow regimes directly from observables.

At the same time (and place) that the above appeared, Hubbard and Duckler[55] presented a new method for flow regime classification. This consisted of correlating the salient features of the measured energy spectral densities of pressure fluctuations with flow regimes.

Before proceeding with the selection of a technique, the amount and type of information needed for the purpose of this investigation were carefully reassessed. It was concluded that a convenient proven method of determining the character of the core of the flow was desired. The above techniques were reviewed from this point of view and the electrical resistance probe was chosen. First used by Solomon[56], it is simple, reliable and well proven, and it has the prominent advantage for this investigation of being able to indicate the degree of continuity of the gas phase in the core. Its disadvantages are that evaluation of the output traces is subjective to some degree and it cannot detect the size or presence of

entrained liquid thus precluding differentiation between annular, spray annular and mist flow. However, these aspects were overshadowed by its advantages, particularly for this initial investigation. The details of the probe are shown in Figure 12 and the results were interpreted by comparing them with the signal traces in references 43 and 57.

In addition flow noise traces were recorded because they were so easily obtained from the transducers already set up for the shock wave measurements. These were compared with those of Hubbard and Dukler, but no attempt was made to compute energy spectral densities.

Finally, the operating points were plotted versus several existing flow maps.

2.3 Operating Procedure

The inlet conditions of 40 psia and 70^{o}F were chosen so that comparisons with other results[46] would be possible if it was later found necessary. The flow rates tabulated below were the maximum possible for the given inlet pressure and temperature discharging to atmospheric pressure.

Run	W_ℓ lb/hr	W_g lb/hr	X	G lb/hr $ft^2 x10^6$
1	198	153.0	0.436	0.2575
2	592	81.0	0.1203	0.494
3	1765	20.0	0.0112	1.31
4	198	168.0	0.459	0.2685
5	592	81.0	0.1203	0.494
6	1765	19.55	0.0106	1.309

The procedure for each day's runs was as follows: First, the electronic equipment was calibrated as described in Appendix B. Then the water and air flow rates were brought up to the desired values and sufficient time was allowed for the system to achieve thermal equilibrium. Then the desired measurements were made. In order to make all of the various measurements at each of the locations (inlet and exit) the apparatus was shut down, the previous test device unbolted, the next device inserted, and the test section bolted together again. Then the apparatus was started up again and the next measurement taken. That is, the velocity, void fraction and resistance probe measurements were made sequentially one after the other at the same location in the apparatus for duplicate flow conditions. They were not made simultaneously. The tests were made over a ten week period and there was no trouble in obtaining repeatable results.

All of the tests were completed at one location before going to the other location in order to keep from turning the electronic equipment on and off any more than was absolutely necessary. This tended to preserve the calibrations of the equipment as discussed in Appendix B.

CHAPTER III

RESULTS OF THE INVESTIGATION

3.1 Flow Regime Data

The resistance probe was inserted at a point 0'8" and 12'8" above the tops of the injection chambers for the inlet and exit runs. The base lines for zero and one hundred percent water on the scope trace were checked before each run by running air and then water alone through the test section. Representative traces from the results are shown in Figures 14 and 15. The flow noise pictures are also shown in Figure 15, and the operating points are plotted on two flow regime maps in Figures 16 and 17 in which the slug flow to annular boundaries of several authors also have been plotted.

First consider the effects of the way in which the liquid was injected. The two injectors are shown in Figures 23 and 24 and their design and performance under operating conditions is discussed in Appendix B. The first immediate effect of the different injection systems was a change in the pressure drops in the flows. This effect has been previously observed[64]. It was manifested in this investigation by different flow rates for the same inlet and exit pressures. The axial injector produced a higher flow rate between runs four and one, no change between runs five and two and a lower flow rate between runs six and three.

In examining the resistance probe results, the traces show no differences depending on whether the liquid was injected axially or on the wall. This can be explained by the results of previous investigations of axial liquid injection. They found that the axial stream of liquid migrated to the wall within a very few diameters[64,65], and that the only residual difference in phase distribution further downstream was a larger number of fine droplets in the core[64]. It appears then that in the inlet traces in Figure 14, the liquid has already migrated to the wall before reaching the resistance probe and the fine droplets are not seen because this probe is incapable of giving any information on drops. The inlet probe traces for runs three and six (Figure 15) do show a considerable amount of liquid in the core. However, once again the observed patterns are the same for both the axial and wall injection systems. The pattern is evaluated as an annular flow with large closely spaced waves extending into the core. It is felt that once again the axial liquid has already migrated to the wall and that what is seen is a developing semi-annular pattern.

As is expected from the above, the exit traces also show no discernable differences between the axial and wall injected runs. The traces for runs one, two, four, and five are all similar to the spray annular traces of reference (57). As can be seen on the flow regime maps, these operating points are all

above the slug to annular transition line. In fact on the Baker[45] plot Figure (14), the points, fall just above the annular to mist flow boundary. As has been mentioned, pressure traces were obtained on the flow noise and these provide additional information which is used to supplement the resistance probe traces. For runs one and four, no large pressure pulsations were observed. This combined with the probe trace indicates that these operating points were in the mist flow regime. For runs two and five large pulsating pressure disturbances were observed similar in amplitude to those shown in Figure 16 for run six. This leads to the conclusion that these two runs were probably in the spray annular regime rather than the mist flow indicated by the Baker plot.

The traces for the exit of runs three and six are interesting because of the very sharply delineated zones of partial conduction. This implies the existence of distinctly defined local zones of high water content in the core. Knowing the gas velocity, these zones can be calculated to be in the vicinity of twenty-five to fifty diameters in length with quiescent periods of one to six times that length between them. It is very interesting to note that the pressure pulse has nearly the same duration as the resistance trace zone indicating some degree of correspondence between the two phenomena. The operating points fall below the slug to annular transition boundaries in Figures 16 and 17, but they are in the region

where it is difficult to distinguish between the different configurations. Therefore based on all of the above, runs three and six were evaluated as being high velocity unstable slug flow. It is significant to note that the resistance probes do not show complete conduction in the slug zone as is normally seen for low velocity slug traces[57]. This indicates that the slugs are composed of a roiled up, bubbly mixture. It is felt that the negative charge effect discussed in reference (57) probably did not play a part in the slug zones not showing 100 percent conduction because of the low purity of the tap water which greatly reduces this effect.

There is one further implication to be drawn from the observation that runs three and six were probably in slug flow. It will be recalled from the discussion of the performance of the diaphrams, that shock waves were observed only about one third of the time that they were initiated. This implies that the presence of the slug zones prevented the formation of a shock or attenuated it extremely rapidly once it was formed. That is to say that shocks may only have been seen in those cases where a quiescent zone extended over the whole length between the shock initiator and the transducer block. This point remains unresolved.

3.2 Void Fraction Measurements

The midpoint of the quick closing valve assembly was located 1'0" and 13'0" above the tops of the injection chambers

for the inlet and exit measurements respectively. The measurements observed are as follows:

	INLET			EXIT		
	Mean	Variation		Mean	Variation	
Run	α	Min.	Max.	α	Min.	Max.
1	.943	.942	.943	.975	.973	.978
2	.846	.845	.846	.916	.915	.917
3	.579	.570	.591	.707	.552	.815
4	.960	.959	.963	.981	.981	.981
5	.834	.830	.840	.896	.862	.915
6	.565	.560	.565	.677	.517	.810

In general it can be seen that void fractions at the inlet were considerably lower than at the exit and the amount of variation was highest at the exit for the highest water rate runs. It was noticed that in those exit readings in which there was a large spread, the data seemed to clump around certain values. For instance in run five exit the values grouped around .865 and .911 and in run six exit around .554, .650, and .791. This is just the sort of effect to be expected if a varying number of roll waves were trapped. It is also a graphic demonstration of the high degree of axial inhomogeniety which can exist in this flow regime.

3.3 Observed Pressure Trace Phenomena

3.3.1 Film Propagation Analysis

There are a great many phenomena which were observed in the pressure traces and careful examination of them has led to several significant conclusions. It is appropriate to begin by examining what signal a wall transducer is likely to feel. The model selected is a two-dimensional system similar to Figure 13 in which a pure gas mass overlies a thin liquid film. Consider first the case where there is no bulk flow of either gas or liquid and a group of plane acoustic waves of unspecified frequency is propagating in the gas. The velocity of sound in the liquid is very much higher than in the gas, and it is pertinent to inquire, (a) if some of the signal in the gas might propagate into the liquid film, and (b) it might then race ahead of the wave front in the gas. To answer the second part of this, the acoustic wave equation can be solved in the liquid film.

The equation for two dimensions is:

$$\frac{\partial^2 p}{\partial x^2} + \frac{\partial^2 p}{\partial y^2} + \frac{1}{c^2}\frac{\partial^2 p}{\partial t^2} = 0 \qquad (4)$$

Assume a harmonic solution $p = X(x)\,Y(y)e^{-i\omega t}$ and separate variables

$$\frac{X''}{X} + \left(\frac{\omega}{c}\right)^2 = -\frac{Y''}{Y} = k^2 \qquad (5)$$

The solutions of this equation are as follows:

$$X = e^{i\sqrt{(\omega/c)^2 - k^2}} \quad \text{(waves traveling in (+) x direction} \tag{6}$$

$$Y = e^{\pm iky} = A_1 \cos ky \pm i A_2 \sin ky \tag{7}$$

The boundary conditions (idealized) are that the pressure at the free surface be zero and that the velocity normal to the rigid wall be zero. They are stated as follows:

$$(1) \quad p(x, y = \delta) = 0 \tag{8}$$

$$(2) \quad u_y(x, y = 0) = 0 \text{ or } \frac{p(x,0)}{y} = 0 \tag{9}$$

where δ is the thickness of the liquid film. The first boundary condition requires that A_2 equal zero and the second yields the following:

$$0 = A_1 \cos k\delta \tag{10}$$

$$k = \frac{\pi}{2\delta}(2n + 1), \; n = \text{integer} \tag{11}$$

The general solution is then

$$p(x,y,t) = A \cos((2n\pm1)\frac{\pi y}{2\delta}) \; e^{i\sqrt{(\frac{\omega}{c})^2 - [\frac{(2n+1)\pi}{2\delta}]^2}\, x} \; e^{-i\omega t} \tag{12}$$

Notice that if $\frac{\omega}{c} < \frac{(2n+1)\pi}{2\delta}$, the radical becomes imaginary, a wave type propagation in the x direction is no longer possible and amplitude is sharply attenuated with distance. This defines the "cut off" frequency below which sound will not propagate in the film.

$$f_{co} = (2n+1)\frac{c}{4\delta} \tag{13}$$

For the fundamental propagation mode, i.e., n = 0 the "cut off" frequency in a water film of one tenth inch thickness is 141,000 cps. This equation also demonstrates that the higher propagational modes have correspondingly higher "cut off" frequencies. For frequencies below "cut off" the relaxation length is defined as the length in which the signal is attenuated by a factor of e^{-1}.

$$x_r \equiv \frac{1}{i\sqrt{(\frac{\omega}{c})^2 - [\frac{(2n+1)\pi}{2\delta}]^2}} \tag{14}$$

$$x_r \simeq \frac{2}{\pi}\delta \text{ for } f << f_{co},\ n = 0 \tag{15}$$

Thus low frequency pressure waves die out in a length equal to little more than the film thickness. The very high frequencies can propagate, but they are affected a great deal by attenuation. In the discussion of attenuation modes in reference 50 it is pointed out that viscous drag and thermal conduction near a wall are several orders of magnitude larger than the thermal

and viscous attenuation effects in the bulk of the flow. These effects are confined to a thin layer near the wall but in the present case the majority of the propagation is in just this region. The effects are aggravated by the cosine amplitude distribution, the high frequency and the higher propagation modes. Consequently, one can expect that high frequency propagation in the annular wall film of liquid is severely attenuated by wall effects.

In actuality, the prospects of propagation are far worse than pictured here. This is because the film is not stagnant as assumed, but in general is a turbulent flow under extremely high shear forces with a churned up, wavy surface. These factors alone are capable of dramatically attenuating any acoustic wave. Consequently, the picture that emerges is that little or no acoustic energy is capable of being transmitted any large distance in the film. This leads to the far reaching conclusion that if a pressure signal is to be transmitted down a pipe in the annular flow regime, it must, of necessity, propagate down the core.

Now the question of whether the signal in the core can ever get transmitted into the film is examined. Classical acoustic wave theory states that the transmission of wave energy across an interface between two media depends primarily on the impedances of the media and the angle of incidence.[50] In the case of air and water, the acoustic impedance, defined

as c, is severely mismatched by a factor of 10^4. Further, the angle of incidence (measured from the perpendicular to the interface) is 90^o in this instance. By Snell's law when the angle of incidence exceeds the critical angle, total reflection of wave energy occurs which is the case here. Consequently, pressure signals in the core in general cannot be transmitted into the liquid film by standard acoustical theory. The interaction consists instead of surface deflections. In fact if the film is stagnant, what occurs when a step pressure wave passes over the surface is that the surface depresses by an amount such that the difference in hydrostatic head exactly balances the pressure in the signal. In this case no change in pressure would be detected on the bottom. When the film is moving, surface deflection is still the predominant reaction; but, of necessity, it must produce deflection in the flowing stream lines. The resulting curvatures are able to support pressure differences which can be felt on the wall. In conclusion, then it can be seen that the interaction between pressure disturbances in the core and the wall film are generally not acoustic phenomena but rather the interaction of bulk flow over a thin boundary layer. The situation is then analogous to single phase boundary layer flow with the notable difference of extremely high layer density. It is from the literature in this field of boundary layer interactions that explanations can be found for the observed phenomena.

3.3.2 Shock Wave-Boundary Layer Interaction

The interaction of a shock wave with a boundary layer has been intensively investigated in the literature. Initial interest in the problem was concerned with shock stall of lifting surfaces in which the high adverse pressure gradient of the shock wave causes separation of the boundary layer[50]. An excellent review of the subject is contained in Lee's lecture notes[57] and two prominent works in the field are references 59 and 60.

A qualitative summary of the effects of a shock wave moving upstream over a compressible boundary layer such that it imposes an adverse pressure gradient is as follows. The boundary layer can exist in either a subcritical or supercritical state. The subcritical state is associated with laminar or very low turbulent boundary layer flow and the super critical to turbulent flow. In the subcritical state the curvature in the streamlines propagages upstream for some distance initiating a shock wave of its own. This causes the so-called "lambda" bifurication of the shock wave near the boundary layer. Depending on flow conditions the boundary layer may separate and then reattach a short distance downstream. Pressure profiles as shown in Figure 13, are characterized by a double hump type of rise.

If the boundary layer is supercritical, perturbations cannot propagate upstream and a jump from super to subcritical occurs

at the base of the shock wave. This jump occurs over a very short length; i.e., one or two boundary layer thicknesses. No bifurcation results, and as can be seen in Figure 13, the pressure rises abruptly.

In examining the photographs of the upstream shock wave pressure traces of this investigation a remarkable similarity to the compressible boundary layer results was observed. The double rise type response was observed in several cases indicating a subcritical condition. The abrupt rise or supercritical response which was also observed occurred most frequently. Thus, it appears that the experimental evidence substantiates the boundary layer type of interaction model for the response of the liquid film to core disturbances.

One very interesting and unexpected result also emerges from the subcritical interaction traces. It is that the presence of the subcritical state indicated by these traces implies the existence of a laminar boundary layer. These were observed to occur at the inlet for both axial and wall injection at the intermediate mass flow rate tests. These admit to the plausible explanation that the film is thick, has a low superficial liquid velocity and has not yet had a chance to be accelerated by the gas core. At the high gas rate test, film thickness is smaller and the higher velocity core accelerates it faster. At the high liquid flow rate, the superficial liquid velocity is probably high enough to cause the liquid

flow to go turbulent even before the accelerational effects of the gas core can be felt. It would be interesting to verify these conclusions by some independent measurements.

Now consider the pressure traces of the downstream shock waves. There are several marked, consistent differences in the appearance of these as compared to the upstream case. The amplitude is somewhat lower, the initial rise often appears as a rounded bump, there is a pronounced dip just after the bump and the tail does not rise as fast. After the successful use of the compressible boundary layer literature in explaining the upstream case, it was reasonable to turn to this body of information again. However, after an extensive search of the literature, the author was unable to locate any reference in which the interaction of a favorable pressure gradient shock on a boundary layer had been investigated. Consequently, the observed phenomena remain unexplained. This appears to be another area in which the results of an independent investigation would be of importance in confirming the validity of the boundary layer interaction model.

The result of the above observations is the realization that the pressure transducers are not measuring the characteristics of the shock wave itself, but rather they are measuring the liquid boundary layer's response to the shock wave. Therefore, it is appropriate to inquire if this introduces any error in the measurement of the desired quantities; namely, velocity

and pressure. All of the theoretical and experimental investigations of the upstream adverse pressure gradient in the compressible case indicate that it is a stationary process. That is, the application of a simple change of reference frame such as is shown in Figure 7C will transform the phenomenon to a steady-state process. This means that even though the shape of the curve representing the boundary layer response is different from the shape of the pressure profile of the shock itself, each point on the two curves remains fixed relative to one another. This means that there is theoretically no error in measuring the velocity of the shock if the transit time is measured between corresponding points on the response curves. In actual practice, there is some difficulty in picking out the corresponding points on any pair of curves due to the changes in the shock and boundary layer characteristics during the transit time interval. However, this falls into the realm of experimental error. The important conclusion is that there is no fundamental reason for error in the velocity measurements.

The experimental observations of the compressible case seem to indicate that the amplitudes of wall pressure traces are slightly lower than the pressures observed in the actual shock. This implies that some of the shock energy is dissipated in passing through the boundary layer shear field, which is

not too startling. The present experiment is interested in the case where the pressure ratios are extrapolated to unity. The result of the above attenuation would then be to merely change the slope of the extrapolation curve, not the point to which it was extrapolated. Hence there appears to be no fundamental error involved in the pressure measurements.

Inasmuch as the downstream favorable pressure gradient shock interaction phenomena remain unexplained, no definite unequivocal statements about the errors involved can be made. It does seem reasonable to expect that if it is indeed another type of boundary layer reaction, the fundamentals of the process will not be too different from the upstream case. This feeling is reinforced by an examination of the experimental pressure traces. They show reasonably small changes in the character of the output of the two transducers for any one run. In addition, the values of the velocities obtained with those traces are reasonable.

2.4 Velocity Measurement

The mean points about which the velocity measurements were taken were 0'8" and 12'8" above the tops of the injection chambers for the inlet and exit runs respectively. The steps in reducing the data consisted of measuring the amplitudes of the two traces and the distance between corresponding points on the two traces. These points were often difficult to determine and hence probably introduced some error. The

pressure amplitudes of the two traces were averaged and then used to calculate the pressure ratio across the shock. Then the log of the velocity was plotted versus the log of the pressure ratio and a straight line of the correct slope was drawn through the data. Run six inlet had such a large spread that a simple average had to be used. No data was obtained for run three inlet because of the previously discussed inability to initiate a shock wave. The observed velocities are tabulated here and compared with the acoustic velocity in air corrected for 100 percent humidity in Figures 18 and 19.

		INLET		EXIT	
Injection	Run	$\bar{c}_m$	$\bar{u}$	$\bar{c}_m$	$\bar{u}$
wall	1	1096.5	155.5	990.5	208.5
	2	1120.0	161.0	1143.0	219.0
	3	-	-	1071.5	119.5
axial	4	1136.0	185	1157	338
	5	1117.0	120.5	1051	217
	6	744.0	122	1054	110

The most important feature of all of this data is the very high velocities observed. This indicates that propagation occurred through the core and that the core was nearly pure air with a very high effective void fraction. No differences were able to be seen between the axial and wall injected runs.

The expected effect was that the larger amount of fine droplets resulting from the axial injector would produce lower velocities. However, the accuracy of these tests was insufficient to make a definite evaluation although some evidence of this is seen in runs two and four, and five and six at the exit.

Large inlet effects were observed in the results for run six inlet. It has been noted that the flow regime was a developing semi-annular flow with large liquid waves in the core. The acoustic velocity was quite low and fluctuated widely. The lack of data on run three inlet prevented a comparison with the wall injected case, but it is felt that the fine drops from the axial injector probably contributed to some degree to the low velocities observed. The conclusion may be drawn that inlet conditions which produce a distribution of liquid in the core will have a large effect on the acoustic velocity.

The final conclusion concerns the axial inhomogeneity of the flow. At the exit for runs two, three, five and six and at the inlet for run six, the measured values fluctuated by an amount which was much larger than could be explained by fluctuations in the core gas velocity. This indicates that axial inhomogeneities such as roll waves can have a very large effect on the acoustic velocity. The effect of slugs is not clear because the question of whether any shock waves were

ever observed to propagate in the slug zone is unresolved.

The errors involved in the above are substantial. The largest is due to the inability to obtain a valid statistical sample. The difficulties associated with triggering in the presence of noise and the limitations of the diaphram shock initiation system conspired to reduce the range of test pressure ratios, particularly in the downstream case. Runs one and four were not as effected and a moderate increase in the number of runs could have corrected this. However, any improvement in the other runs can only be achieved by completely revising the entire triggering and shock initiation systems.

Fluctuations in the gas core velocity introduced a large dispersion into the transit time measurements and again the effect was most severe at the exit for the lower void fractions. However, the largest variation in velocity measurements was due to the effects of axial inhomogenieties. For instance at the inlet for run six, the dispersion was so bad that a statistically accurate sample would have required several hundred measurements. Not only was this completely infeasible, but a moment's reflection leads to the conclusion that it would not have produced any meaningful additional information. For instance the data for run six inlet indicates that inlet conditions can produce distributions with substantial liquid in the core which can govern the acoustic propagation characteristics.

It is clear that the actual propagation value for a particular installation will depend entirely on its geometry, etc, which will be different in general from that used here.

There is one additional error which should be mentioned. As seen in Figure 7B the pressure ratio that should be used in the extrapolation technique is p_2/p_1. Ideally, the transducer arrangement would have measured p_2/p_1, but the effect of the liquid boundary layer in reducing the response of the transducers probably caused a pressure somewhere between the two to be measured. The effects of this error are greatest at the exit. Also, the pressure fluctuations in the pipe, particularly at the lower void fractions, caused the absolute value of p to be in error. Finally the slope of the extrapolation line through the data is probably slightly different from that in air. These last two effects would have been taken care of by a proper statistical sample.

3.5 Comparison with Existing Data

The observation that acoustic propagation in this flow regime is primarily a core phenomena leads to the conclusion that propagation velocities can only be correlated with core void fractions rather than the aggregate void fraction as has been done in the past. That is to say, the liquid in the wall must be subtracted from the total liquid flow rate before the appropriate void fraction can be computed. This fundamental

conclusion should be supported by the existing data of other authors.

First consider the work of Semenov and Kosterin. They snapped a spring loaded gate valve shut at the top of a vertical test section and measured the time for the disturbance to travel back down the pipe. From this author's experience, a mechanical valve is far too slow to initiate a shock wave. Instead a relatively slowly rising ramp signal is generated which can be expected to disperse as it travels due to the dependence of acoustic velocity on frequency. This was observed in their paper together with a comment on the difficulties it caused in resolving the arrival time of the signal. In fact, this signal's rise is so slow that even its higher frequency components should still not have greatly exceeded Temkin's relaxation frequency and its lower frequency components should start to decelerate the annular film. Therefore the measurements should represent the equilibrium acoustic velocity in a core which is not completely decoupled from the wall film. Consequently, the discrepancy between the data and the predicted equilibrium velocity cannot be explained by frequency effects. Now consider the effects of phase distribution. If a void fraction of say sixty per cent is chosen, the data is well above the theoretical value. Now if the water in the liquid film were discounted, the core void fraction would be very much higher; typically in excess of

ninety percent. This would shift the observed data to the right just about the correct amount required to bring it over to the equilibrium curve. Thus the conclusions of this investigation offer a logical explanation for the discrepancy in their data.

In Figure 26 the mean gas velocities calculated from some recent well documented choking experiments by Fauske[68] are presented. If the analogy with classical single-phase compressible flow theory is correct, these velocities should represent the mean local acoustic velocity in the media. The apparatus used in his experiment consisted of short pipes fed by a "T" mixer. Therefore, based on the results of the present investigation, inlet effects are expected to be present. Indeed at the lower void fractions, the data approach very closely to the equilibrium prediction indicating a rather homogeneous mixing of the phases in the core. In fact, all of Fauske's data is below the data of the present investigation as a result of the entrance effects. Yet they are still far above the equilibrium theory so that they would also shift to the right the correct amount if the core void fraction were used.

CHAPTER IV

CONCLUSIONS

The following general conclusions about acoustic propagation in flowing two-phase gas-liquid mixtures in the void fraction range from roughly fifty to ninety-five percent based on the results of this investigation can be drawn:

1. Little or no acoustic energy is capable of being transmitted any great distance in the liquid film.
2. The propagation of acoustic signals in the axial direction in this flow regime is done through the core.
3. The characteristics of the core govern the propagation phenomena. Two corrolaries of this conclusion are:
   A. Axial inhomogenieties in the core structure such as roll waves produce large fluctuations in the acoustic velocity.
   B. Inlet conditions which produce substantial distributions of the liquid phase in the core have a drastic effect on propagation.
4. The effects of phase distribution on acoustic velocity observed in this experiment provide an excellent explanation of the discrepancies observed in existing data. Specifically, the very much higher velocities predicted by the core propagation model have been observed.

APPENDIX A

DETAILS OF THE APPARATUS

Figure 21 is a schematic diagram of the system, and Figure 22 is a photograph of the lower part of the apparatus. The water supply section consisted of a thirty gallon water storage tank, a Hayes Model 3906 centrifugal pump rated at 50 gpm @ 50 psi, and a Dollinger Staynew Model ESL2, Cotton, Style BWC, filter rated at 95 per cent efficiency to remove an average minimum particle size of 3 microns. The piping and fittings were all of PVC plastic or bronze to minimize corrosion. The water flow rate was measured using Fischer Porter Flowrators. The water used was tap water.

The air supply was from a Joy reciprocating compressor rated at 320 scfm at 200 psig. The air was filtered through a Cuno Micro Clean Type 2278B3 filter rated to trap 5 micron or larger particles. An Alenite Model 323300-3 regulator valve was used to maintain supply pressure constant. The air was then passed through a series of four Purolator Type AS101 separators to remove any traces of oil. Air flow rate was measured using standard ASME orifices in a two inch nominal size pipe. Temperature of both the air and water was controlled by passing the fluids through American Standard model BCF type 7M502D5 heat exchangers.

The test section was made of plexiglass pipe of .500 $\pm$ .005 inch inner diameter and one eighth inch wall thickness. The butt

joints were all socket type flange connections similar to those on the resistance probe section (Figure 12). They were accurately machined and fitted so that the maximum joint asperity was observed to be about $\pm$.005 inches. The joints were sealed with "O" rings. The plexiglass tube was bolted to an angle iron and plywood frame with wood brackets spaced one foot apart. This close spacing was used to counteract the natural tendency of the plexiglass to bow. A three foot straightening length was used at the entrance to ensure that the air had reached a fully developed state prior to the injection of the water.

At the exit a pair of one inch Wright-Austin semi-steel "T" type flow separators were installed. The water from the separator was fed to a pair of collection tanks and then returned to the storage tank. The air was exhausted to the atmosphere. In practice, the capacity of these separators proved inadequate at the higher water rates.

The entire system was designed to withstand a pressure of 100 psi. However, normal operating conditions were 40 psia at the inlet. A variable pressure relief valve was connected to the inlet of the test section. This was used to limit the pressure surge to 55 psia when the quick closing valves were snapped shut to measure void fraction.

The air supply to the diaphram rupturing device (Figure 20) was taken off of the main line and reduced to 125 psi by an

Alenite Model 323300-3 regulator valve. This then led to two parallel air regulators. One was a Schrader No. 3463 non-relieving regulator which was used to maintain a five psi pressure differential between the driver chamber and the line flow across the diaphram slide so that the "O" ring seals would not leak. The other was another Alenite Model 323300-3 which was set to the desired driver pressure. It was followed by a lever operated ball valve. When this valve was opened, the non-relieving feature closed the Schrader regulator thus allowing the driver chamber to be charged up to the desired pressure. The solenoid then was used to rupture the diaphram, the test was recorded, and the ball valve closed. This reduced the chamber pressure low enough so that the slide could be operated easily allowing a fresh diaphram to be slipped into place. Occasionally, the desired driver pressure was in excess of the diaphram rupturing pressure. In these cases, the solenoid was not used and the diaphram was allowed to rupture naturally by opening the ball valve. This system resulted in convenient operation and repeatable results.

The two injectors used to admit water into the test section are shown in Figures 23 and 24. The injection section is nearly identical to that used by Hinkle.[46] The porous bronzeplug was made to order by Sintered Metals, Incorporated of Boston, Mass. It performed satisfactorily. The axial injector was similar in design to one recently used by Gill and Hewitt[64] in England.

As can be seen in the figures, the two are interchangable in the test section. The design of an axial injector invòlves the selection of nozzle parameters such as length, shape, and exit diameter which control the velocity and turbulence of the water jet. To date, no known investigations have been made of the effects of these parameters on the resulting two phase flow. As a result, the available body of literature on atomization cannot be used since it is not known if it is more desirable to inject the liquid at the same velocity as the gas or to attempt to create efficient atomization. Indeed this ignorance reflects the present inadequate ability to categorize inlet effects in general on two-phase gas-liquid flows. The investigators[64,65] which have used axial nozzle injectors have apparently used arbitrary convenient shapes and so that is what was done here. In operation, it performed best at the high gas rates. For runs one and four, the water jet expanded so that the first drops impinged on the wall at the very top of the conical injection chamber. For runs two and five, impingement first occurred about a half inch from the top. For runs three and six the chamber flooded. It appeared that the major part of the water entered in the test section immediately, but a small amount circulated in a slow eddy in the injection chamber.

Some vibration of the test section occurred, particularly at the exit for the high water rates. However, the supporting

frame was rigid enough that the amplitude of the pipe's vibration never exceeded a sixteenth of an inch.

APPENDIX B

MEASUREMENT OF FLOW PARAMETERS AND CALIBRATION OF EQUIPMENT

Water rates were measured with Fischer Porter Flowraters. Runs three and six used a type B8-27-10/70-CG and the other four runs used a type FP-3/4-21G-10/83. These flowraters were calibrated with a weigh tank prior to the runs and the resolution error for both of them was about one half per cent. There was sufficient pressure drop in the water supply system that fluctuations in flow rate were very small. In all cases they were kept within plus or minus a tenth of a gradation.

The air was metered with standard ASME orifice plates in a two inch nominal size pipe. The I.D. of the pipe was measured to be 2.071 $\pm$ .011 inches. Runs three and six used an orifice with a diameter ratio of .101 and all of the other runs used a ratio of .2415. Flange taps were used with a water manometer and all details of the meter were carefully checked to ensure that they complied with the ASME standards. Resolution accuracy of the manometer was plus or minus a tenth of an inch. The pulsating nature of the flowing mixture caused the air supply flow rate to oscillate somewhat. The amplitude of this oscillation varied from about a half inch of water for runs one and four to as much as two inches for runs three and six.

Air and water pressures were read using Bourdon type gauges. They were carefully calibrated with a dead weight

gauge tester prior to use. They were rated at $\pm$ 1/4 per cent accuracy over the full range and their resolution was $\pm$.1 psi. The gauges which measured pressure in the two-phase mixture were fitted with an air purge system to eliminate errors carused by water in the gauge lines.

Temperatures were measured with standard mercury thermometers having a scale resolution of .2°F. The apparatus was always allowed to tun until thermal equilibrium had been achieved and the runs were all made with the temperature of both the air and water within a half degree of 70°F.

Calibration of the oscilloscope and the charge amplifiers was given particular attention for two reasons. The equipment tended to drift out of calibration very quickly and the accuracy of the experimental results was extremely sensitive to this. The rated accuracy of the vertical amplifier and the sweep speed of the oscilloscope was only within 3 per cent. This was considered to be an unacceptably large error. Further, it was discovered that this represented the range of the drift due to a few day's operation or the simple act of turning the equipment off. Hence it was found necessary to institute the following calibration procedure. The equipment was not turned off unless absolutely necessary and whenever this did occur, everything was recalibrated again. In addition, everything was recalibrated prior to each day's runs. The sweep speed was calibrated with a Tektronix type 181 time mark generator which had a rated accuracy of .03 per cent and

a drift of .005 per cent per hour after warmup. The sweep was calibrated at the speed that was to be used for the test, generally 50 μsec/cm. The calibration signal source within the scope was calibrated with a Ballentine Laboratory model 421A precision calibration which had a rated accuracy of .1 per cent and a linearity of .05 per cent. Then, the zero and drift settings of the two charge amplifiers were adjusted. Next, the scope's calibration test signal was fed into the charge amplifiers and the output checked on the scope. This was done with the rest of the circuit, including the transducers, still connected up as they were for the test. Thus, it is felt that the calibration accuracy of the amplifiers and scope was better than 1 per cent.

The frequency response of the scope on the 50 mv/cm setting was 400 kcps. This was substantially better than the transducers. The tests were normally run with the vertical amplifiers in the A.C. mode. This feature automatically adjusts out any D.C. bias on the signal so that the mean voltage of the signal is brought down to the base line. The frequency response of the A.C. base line adjustment was about 15 cps.

The quick-closing valve void fraction measurement device was calibrated by first measuring the volume of the sight glass assembly several times. Repeatability of this measurement was within .1 ml. This total volume was then used to calculate the volume to be poured into the sight glass to

calibrate the intermediate fractions. Every tenth percentile was calibrated and the procedure was repeated at least twice. Finally, the distances between these points were measured and marks cut into the tube for every whole percentile. The Accuracy of the calibration is estimated to be a fixed amount equal to plus or minus one tenth of a gradation, i.e., as good as the resolution of the void fraction measurements.

The inherent accuracy of the device should also be discussed. So long as the valves closed simultaneously, which was ensured by the lever arm arrangement, it was felt that the speed of closing had no effect on the accuracy. The device measures the average over a fixed length at a given time rather than the desired time average at a given point. If the flow is changing rapidly with length, a length average is clearly suspect. This what is known to be occurring near the inlet[64,65] and the remedy is to shorten the length of the sight glass. Another source of error is the effect of axial inhomogenieties, primarily roll waves, which were particularly noticeable at the exit. This requires that a long enough section be used in order to average out the inhomogenieties. These length requirements conflict and so the final length of eighteen inches was selected because it was about the minimum that would permit void fractions up to 98 per cent to be visible in the sight glass. Selection of this length meant that the midpoint of the sight

glass was four inches higher than the mean point for the velocity and the resistance probe measurements. The error introduced by this was considered negligible at the exit and comparable to the error involved in the length average at the inlet.

APPENDIX C

CALIBRATION OF TRANSDUCERS

As has been discussed in section 2.2.4, the success of the experiment rested in large part on the ability of the transducers to accurately measure both the amplitude and the time of passage of the shock wave. Therefore a great deal of attention was paid to calibrating them properly. In addition, it was desirable to verify experimentally the validity of this technique for accurately measuring the velocity of sound.

The transducers were installed in a plexiglass block assembly (Figure 9) which had been bored out to .500 $\pm$ .005 inches. This block could then be inserted in the test section of pipe with the usual socket flanges. The block was split longitudinally so that when unbolted, the active face of the transducers could be examined. The distance between the leading edges of the two transducers was measured by means of an optical comparator and found to be 2.487 $\pm$ .005 inches. The recesses in which the transducers were mounted were then faired into the tube wall with a silicone rubber compound. When dry, the surfaces were inspected with the optical comparator. The fairings were somewhat rougher than the adjacent tube wall surface, but the maximum asperity was estimated to be less than five

thousandths of an inch.

It was decided to conduct the calibration test series under conditions which were as similar to the actual operating conditions as possible. Accordingly, a small shock tube was constructed from the same plastic tubing used in the test sections of the apparatus (Figure 31). Nitrogen was selected as the medium in order to avoid the effects of humidity while retaining shock velocities similar to those in air. The shock tube was piped with a purging system which was let run for several minutes before each test. The absolute pressure in the drivier section was measured with a mercury manometer. Temperature in the receiver was measured with a standard glass thermometer to an accuracy of $\pm$ .1^{o}F. The driver section was three feet long and the receiver six feet. This allowed a relatively long time interval before the arrival of end wall reflections. Cellophane diaphrams were used, and they were ruptured with a hand operated rod. The shock tube was bolted to a steel angle iron frame and accurately aligned with a surveryor's transit.

The transducer block was then inserted in the receiver section and the ancillary electronic equipment connected. The oscilloscope and the charge amplifiers were calibrated in place just prior to the runs.

Predicted values were calculated using the well known shock tube equations[51]. The attenuation of a shock wave

in a shock tube has been treated in the literature[66,67] and its effect on these experiments was investigated. Corrections were calculated based on Donaldson and Sullivan's work because their experimental data was obtained in a shock tube of almost identical proportions as this one. Their results are also presented in a convenient form. The attenuation at the test length of twenty-three inches from the diaphram was computed to be 1.14 per cent. This was less than the variational error in the runs as well as the resolution error of the transducer output. Nevertheless, the predicted values were calculated using this correction. Just to make sure that the actual attenuation did not exceed the calculated values, a series of runs were made at only one foot from the diaphram. This data showed pressures which were essentially identical with the longer length data. Although the spread of the data was such (about 4 per cent) that a measurement of the actual attenuation could not be made, it did confirm that it was less than the experimental error.

The results of the calibration test series are shown in Figures 32 and 33. There is quite a little spread in the data. The major cause of this is the poor resolution of the amplitude of the trace on the scope. As has been mentioned, the piezoelectric's response is highly oscillatory and so the actual signal amplitude must be picked out

of this "ringing". A low pass filter could have been used very effectively to remove this oscillation. However, it was known that the actual measurements in the experiment were going to be made without a filter and so it was decided to try the calibration without it also. It turned out that this decision incurred an acceptably low error penalty.

The next major cause of error was the variation in diaphram rupture dynamics. The evidence that this exists is seen in the variation in measured velocities. That is, if amplitude resolution was the only error, the data would show no variation in τ for those duplicate runs, only amplitude spread. The cause of these diaphram variations was not investigated, but is felt that differences which occurred in their assembly could account for this.

The manufacturer of the transducers provided an output sensitivity calibration performed at the factory. As can be seen in Figure 32, it is somewhat at variance with the observed sensitivity. It is impossible to tell whether this is due to the shape of the input signal or the cumulative effect of the components in the charge amplifiers and the scope. The inability to use the factory calibration caused a compounding of the resolution error. This is because the same data was used to determine the new sensitivity as was used for the velocity correlation which was computed with the use of these sensitivity values.

When a straight line was fitted to the data by the least squares method, a systematic error of -14.3 feet per second or 1.2 per cent was observed. The first possible cause for this is an error in the distance between the transducers. However, 14.3 feet/second corresponds to a discrepancy of .030 inches which is nearly six times as large as the resolution error in the length measurements. It is recognized that differences in the manufacture of the transducers would probably result in the active surface areas of their faces being located a slightly different distance apart than their leading edges were. There is no reason to expect that this effect would exceed .010 inches which is again too little to explain the observed error. The calibration of the oscilloscope is discussed in Appendix B and it seems unlikely that this could have accounted for all of the error by itself. Another possible small contributor is the accuracy of reading the mercury manometer which was $\pm$ .02 inches. Finally, it should be mentioned that the flexibility of the pipe wall could have reduced the shock speed. The effect of wall flexibility on harmonic wave speeds in ducts is well known[50], and it always acts to reduce velocity. However, it is most difficult to estimate the effect for a shock wave; and in particular, for the geometry of the transducer block.

In conclusion the size of the systematic error is such that it seems reasonable to explain it as the cumulative effect

of all of the possible sources discussed. Furthermore, it is sufficiently small that it will not noticeably affect the experimental results.

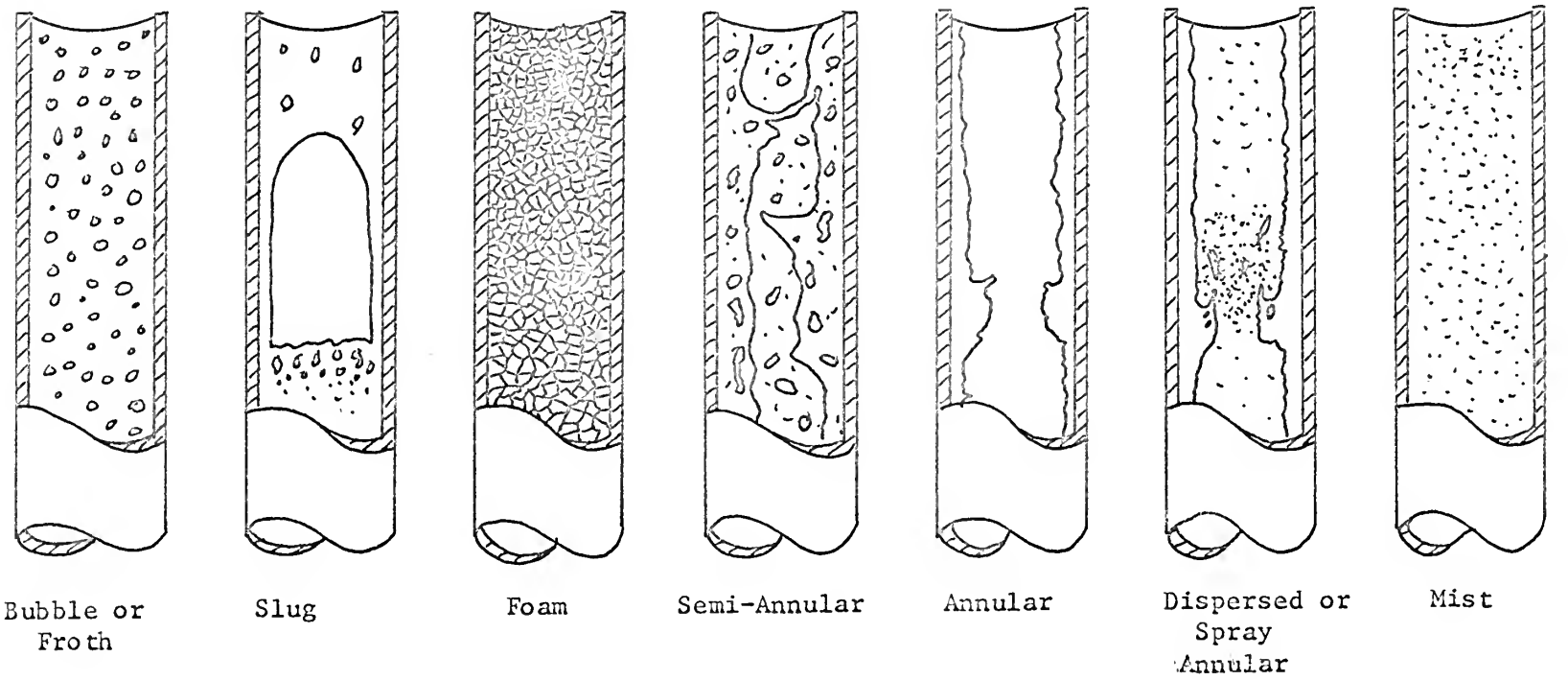

Figure 1. Flow Patterns in Adiabatic Two-Phase Vertical Upflow (69)

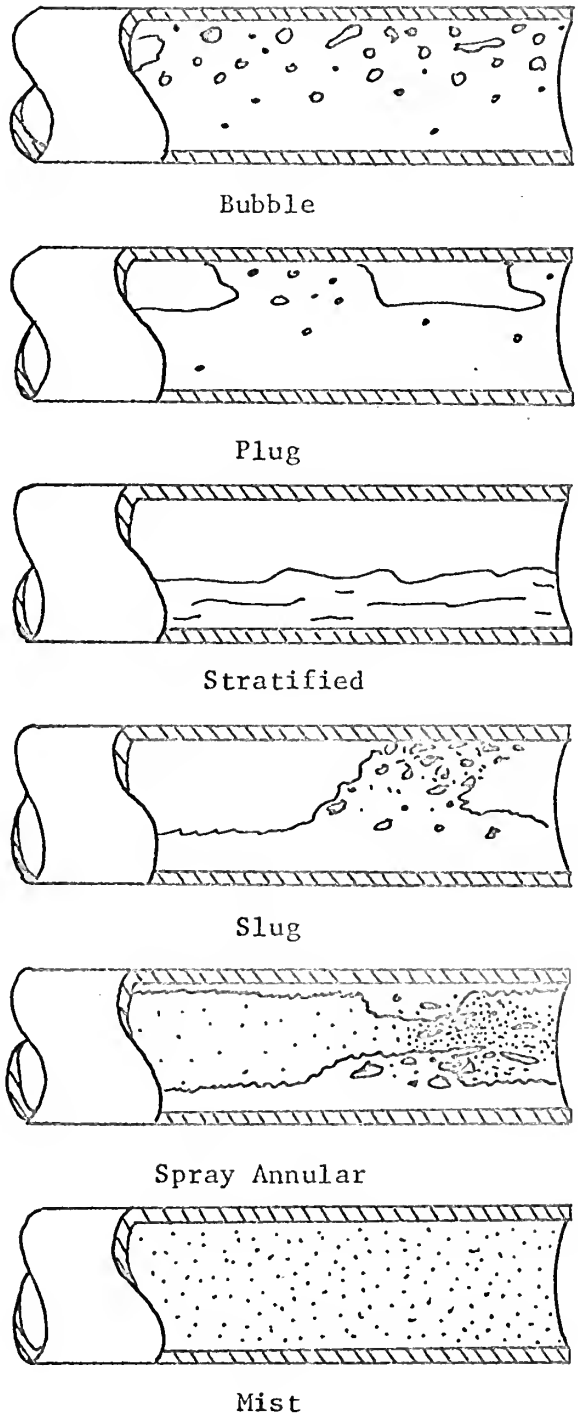

Figure 1B
Flow patterns in Adiabatic Two-Phase Horizontal Flow (69)

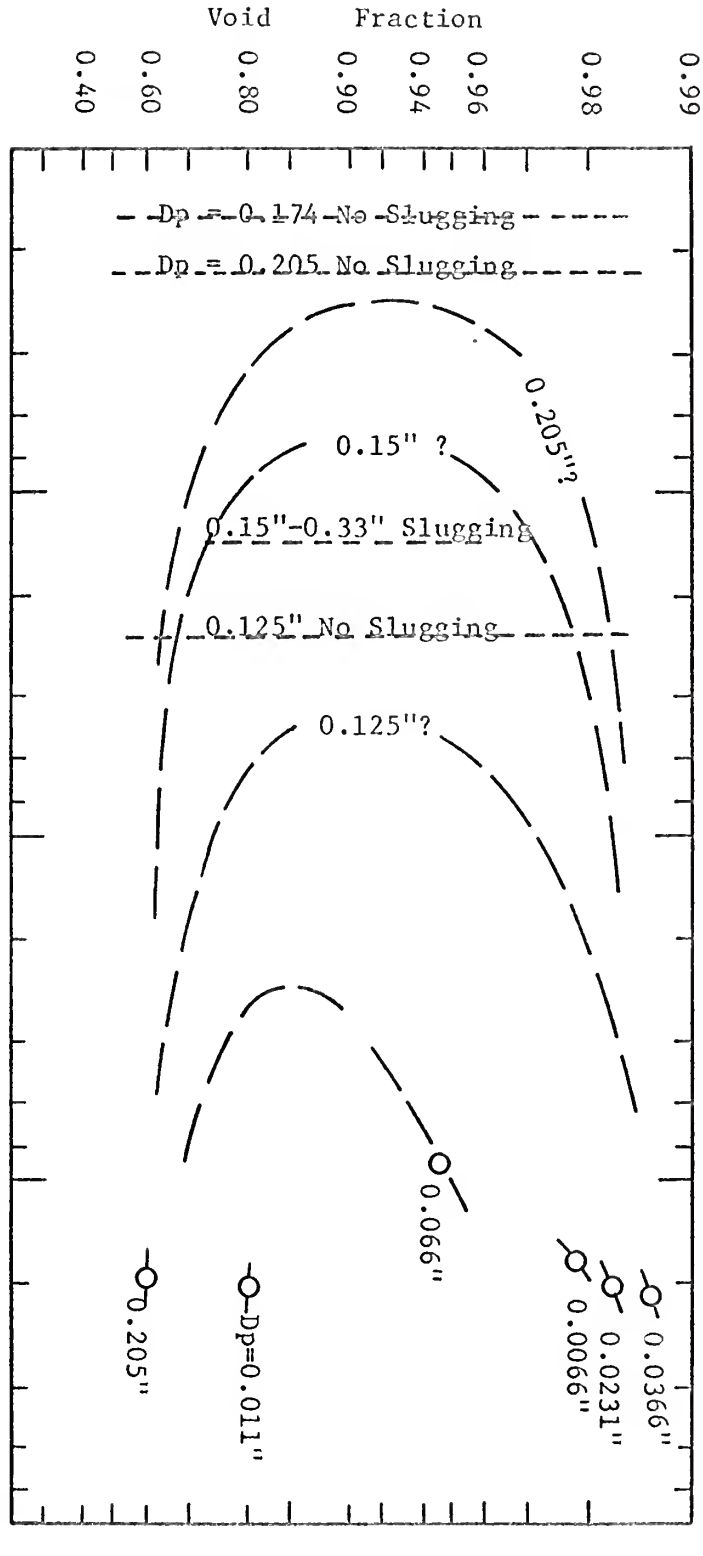

Figure 2 Stability Map for Particles Suspended in a Fluid

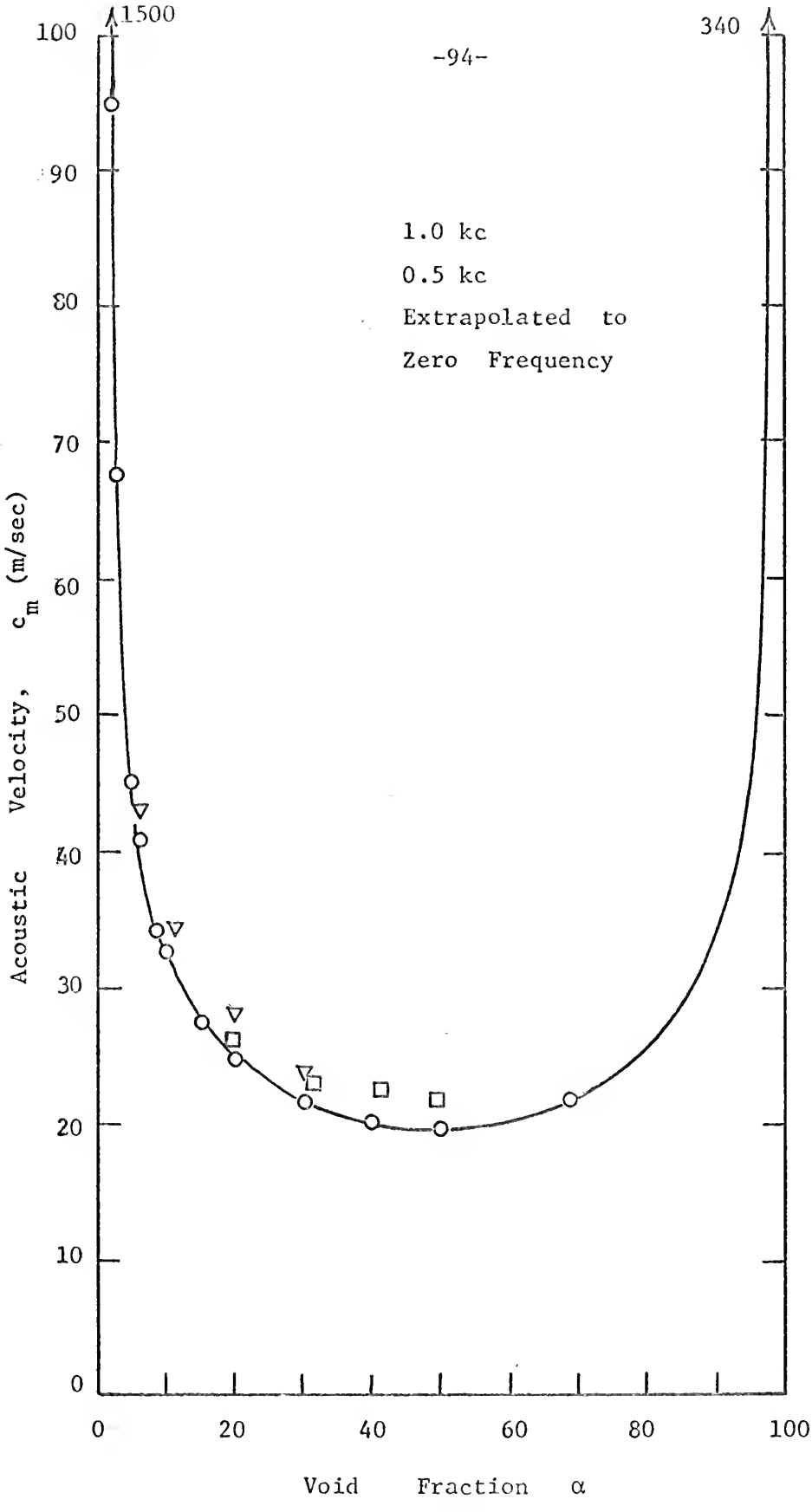

Figure 3
Theoretical and Experimental Values for Acoustic Velocity in Air-Water Mixtures (Karplus) (13)

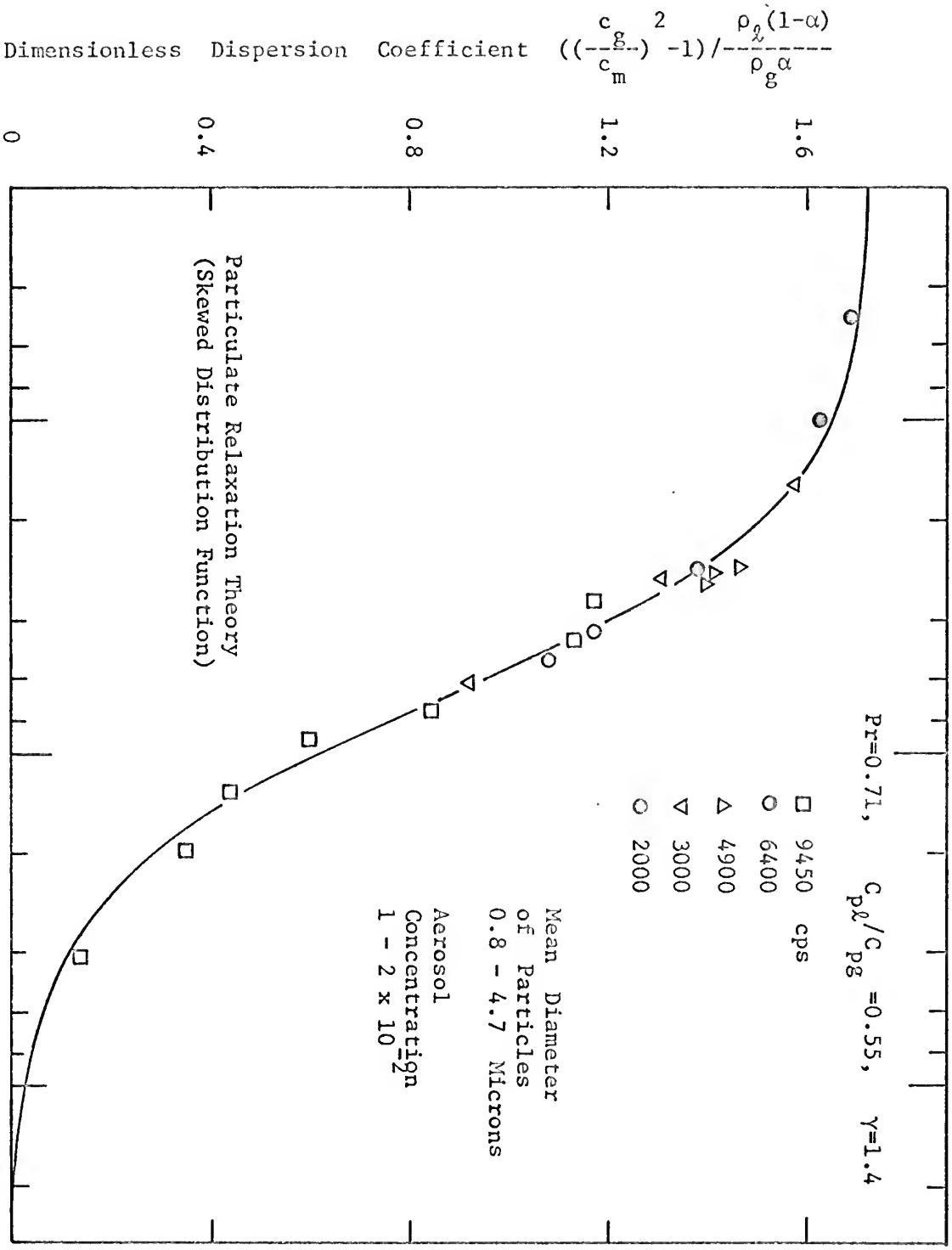

Figure 4 Theoretical and Experimental Values for Acoustic Velocity in a Mixture of Oleic Acid Particles and Nitrogen (Temkin and Dobbins) (35)

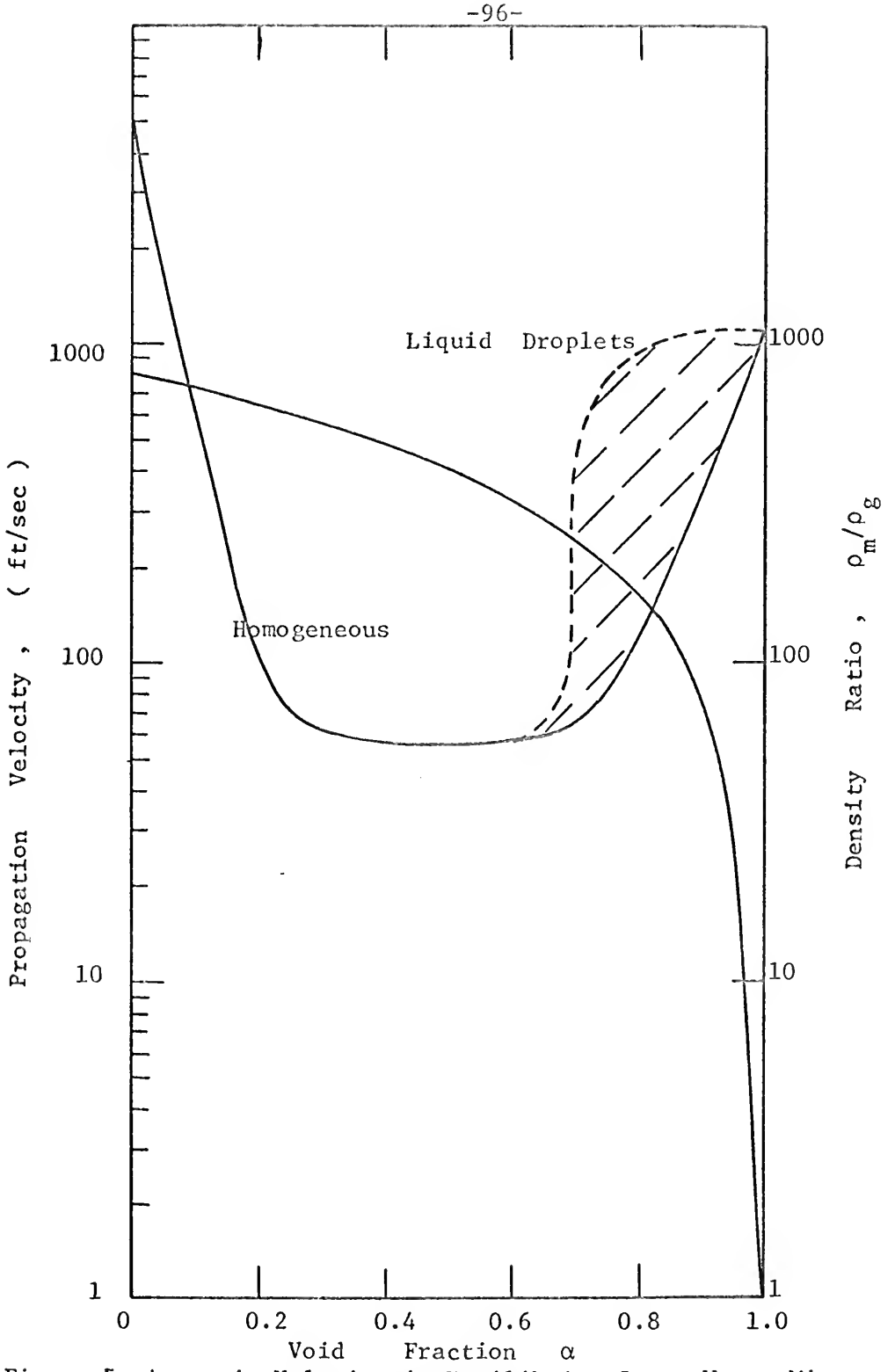

Figure 5 Acoustic Velocity in Equilibrium Steam-Water Mixtures (Bowles and Manion) (33)

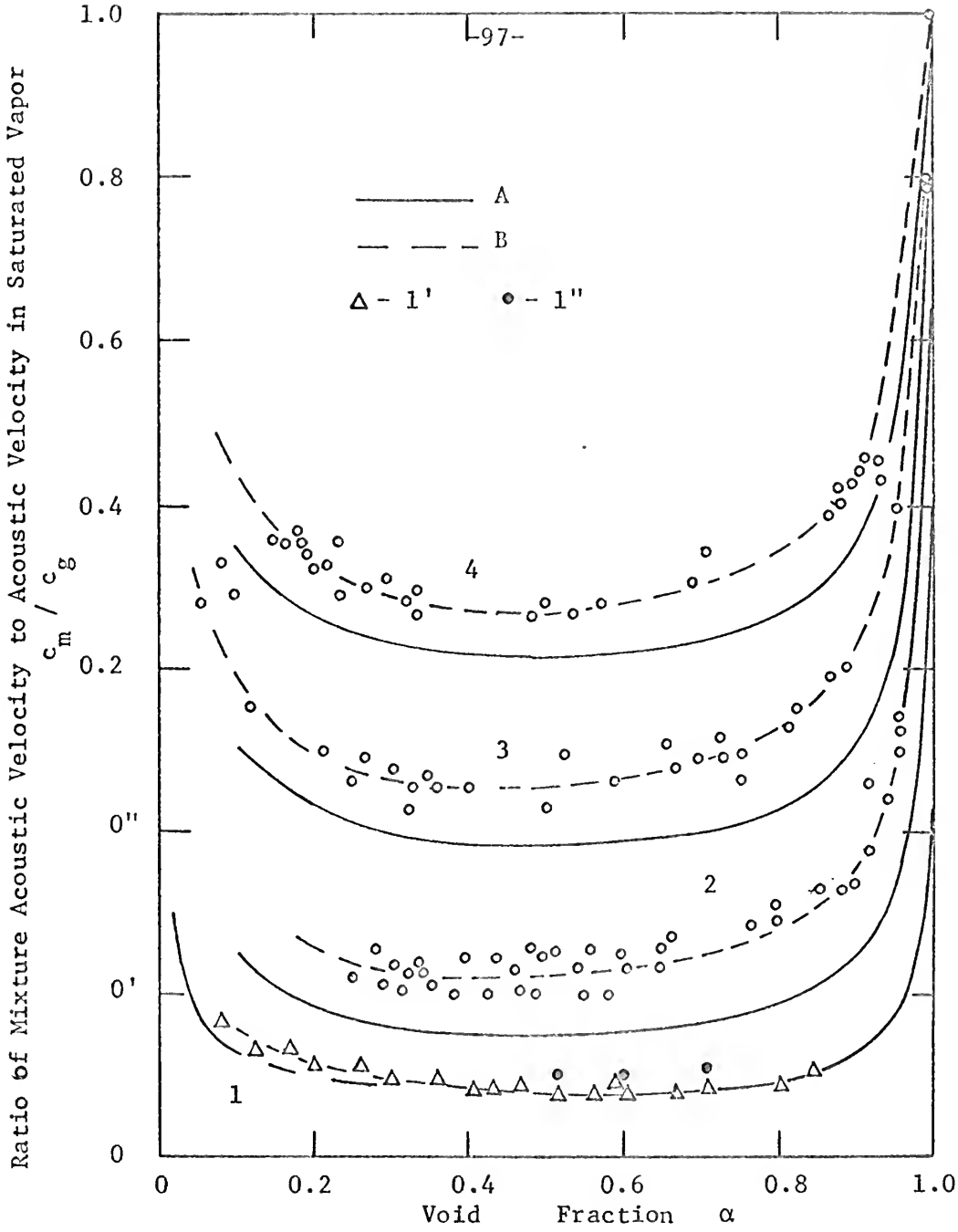

A - Theoretical , B - Experimental
1 - Air-Water system (1' - p=1.25 kg/cm^2, 1" - p=2 kg/cm^2)
2 - Steam-Water System, p = 10 kg/cm^2,
3-- Steam-Water System, p = 15 kg/cm^2, Coordinate Origin at 0'
4 - Steam-Water System, p = 20 kg/cm^2, Coordinate Origin at 0"

Figure 6 Theoretical and Experimental Values for Acoustic Velocity in Air-Water Steam-Water Mixtures (Semenov and Kosterin) (24)

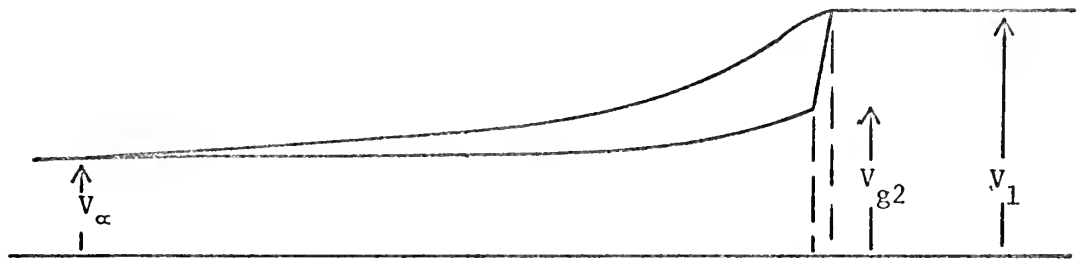

Figure 7 A Shock Wave Parameters, Effect of Particles on Velocity (Kriebel) (22)

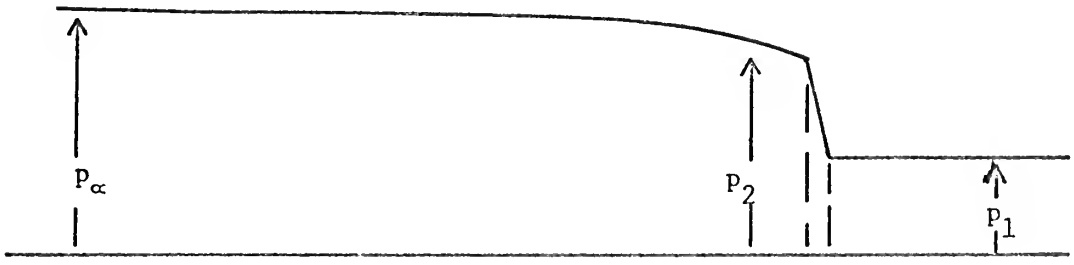

Figure 7 B Shock Wave Parameters, Effect of Particles on Pressure (Kriebel) (22)

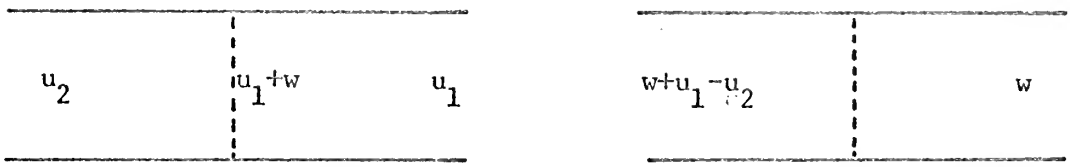

Moving Shock in Stationary Reference Frame

Stationary Shock in Moving Reference Frame

$$V_1 = w$$

$$V_\alpha = w \pm (u_1 - u_2)$$

Figure 7 C Shock Wave Parameters, Coordinate Transformation (51)

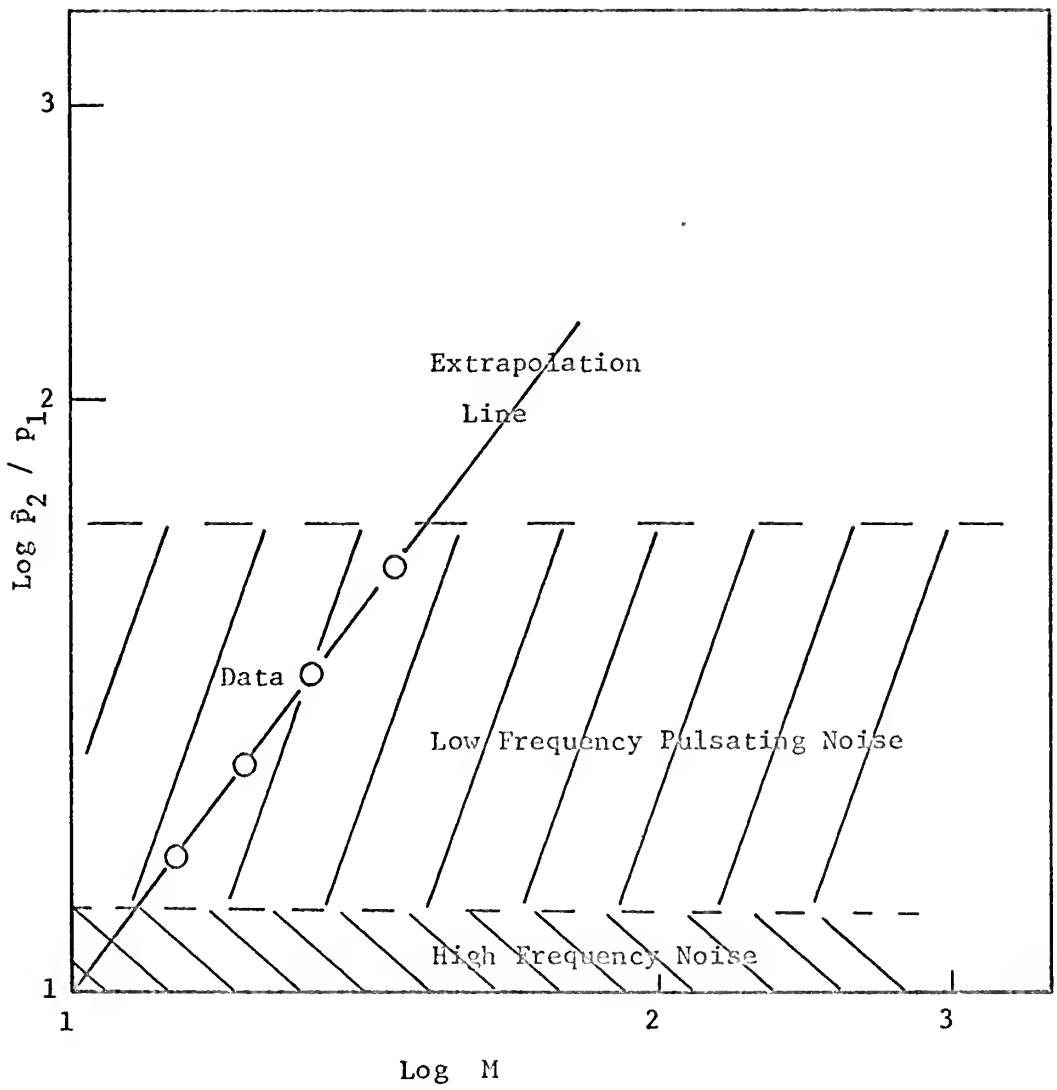

Figure 7 D Shock Wave Parameters, Effect of Noise

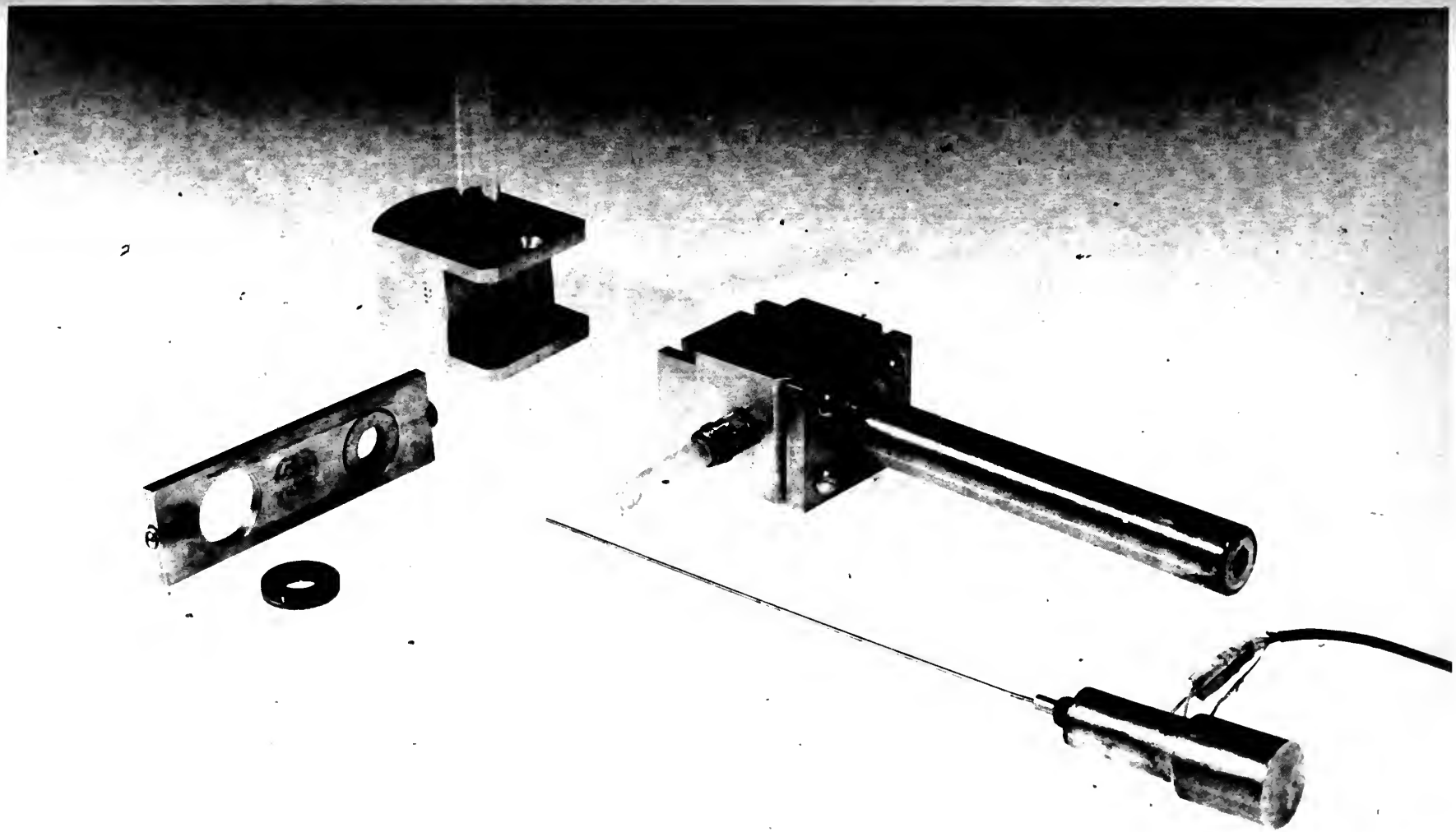

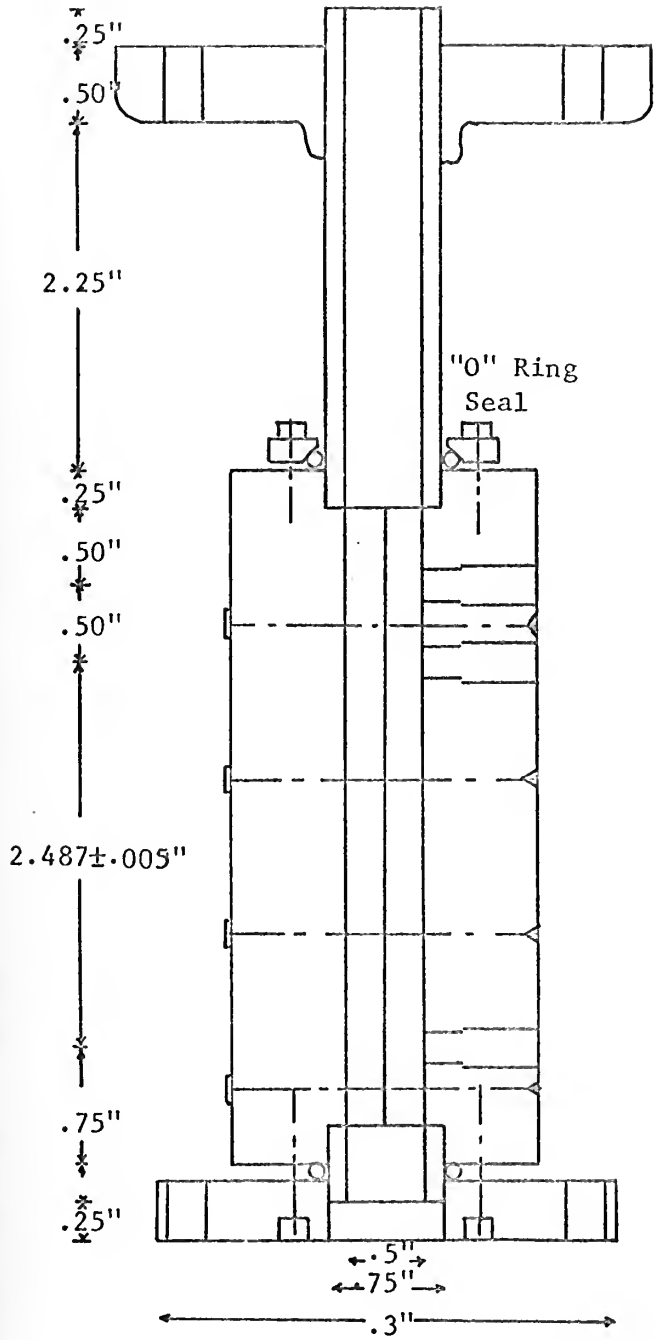

Cross Section of Assembly

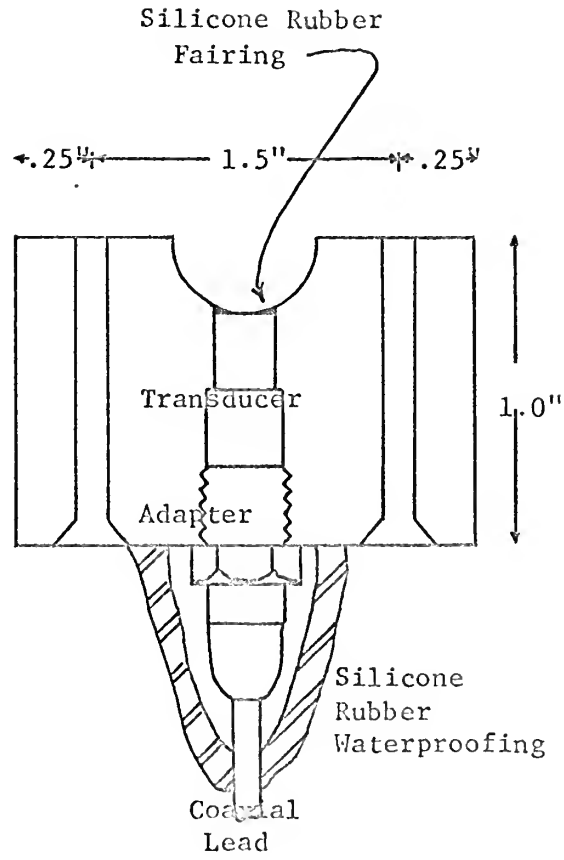

Details of
Transducer Mounting in
Half Block

Figure 9 Diagram of Transducer Block Arrangement


TOP
TOP

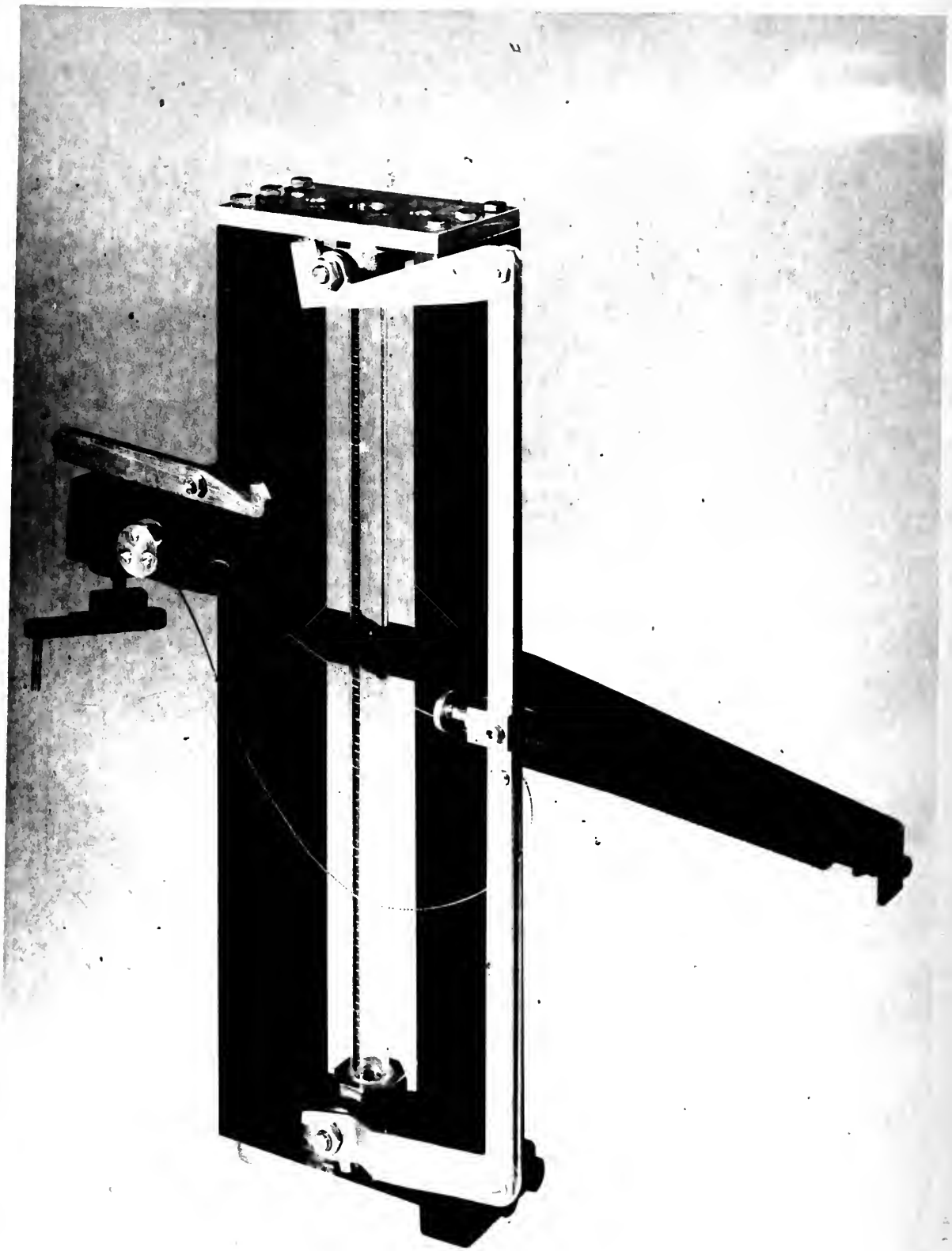

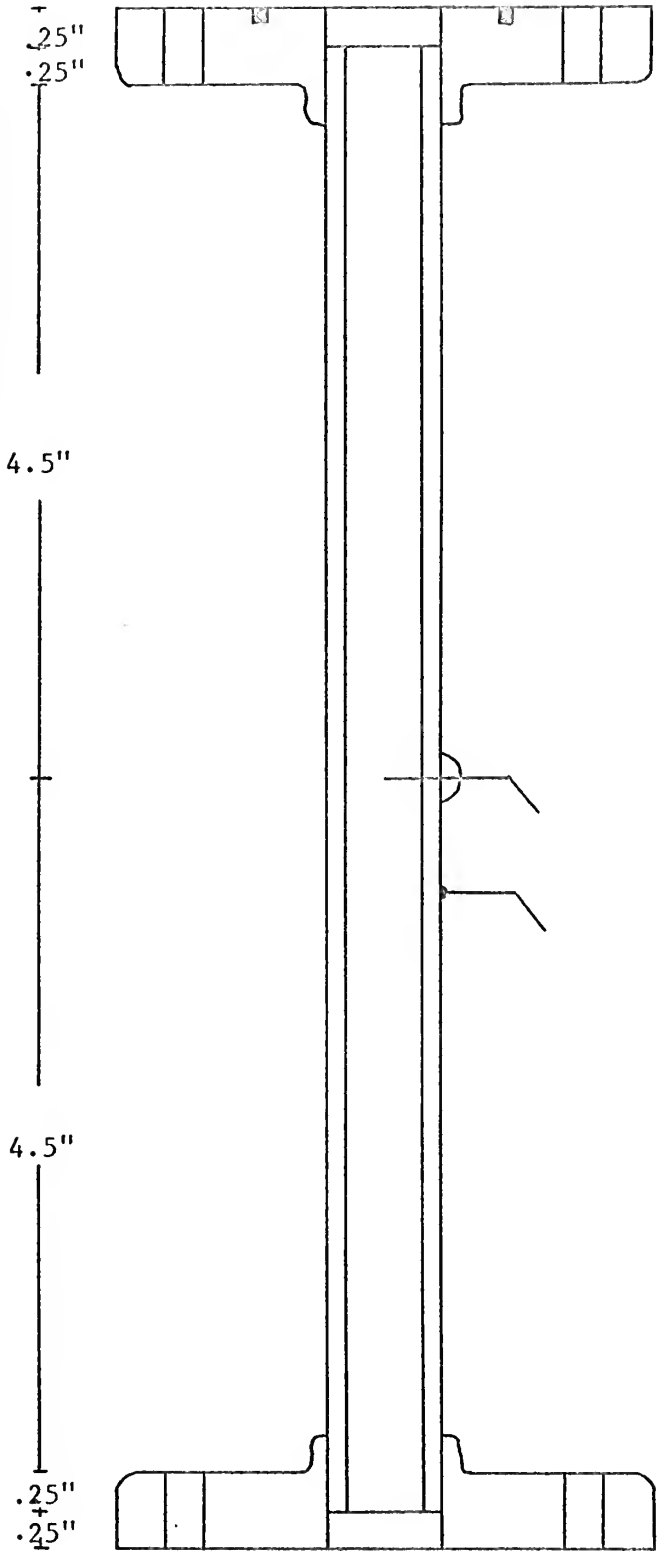

Cross Section

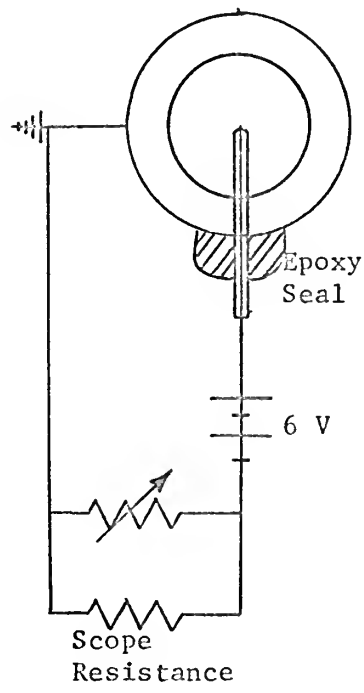

Details of Circuit and Probe

Figure 12 Diagram of Resistance Probe

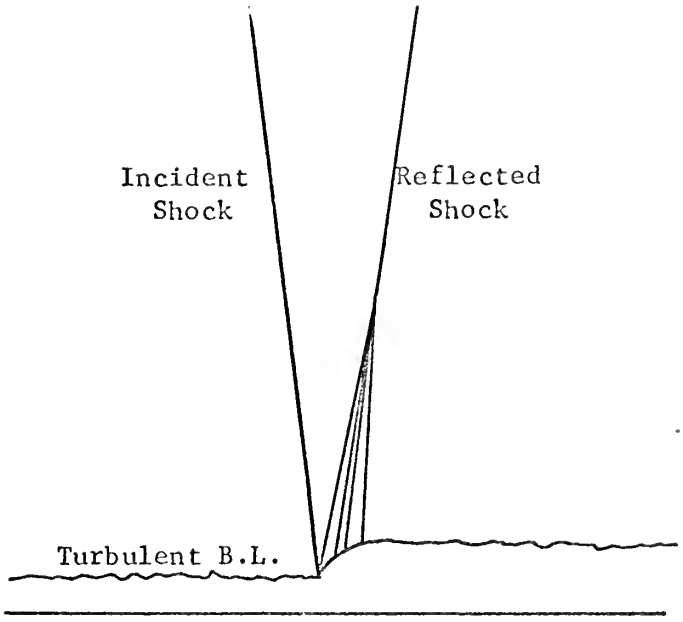

Super Critical Boundary Layer

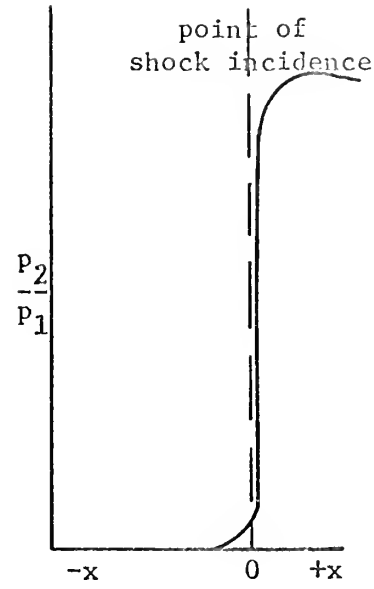

Wall Pressure
Distribution

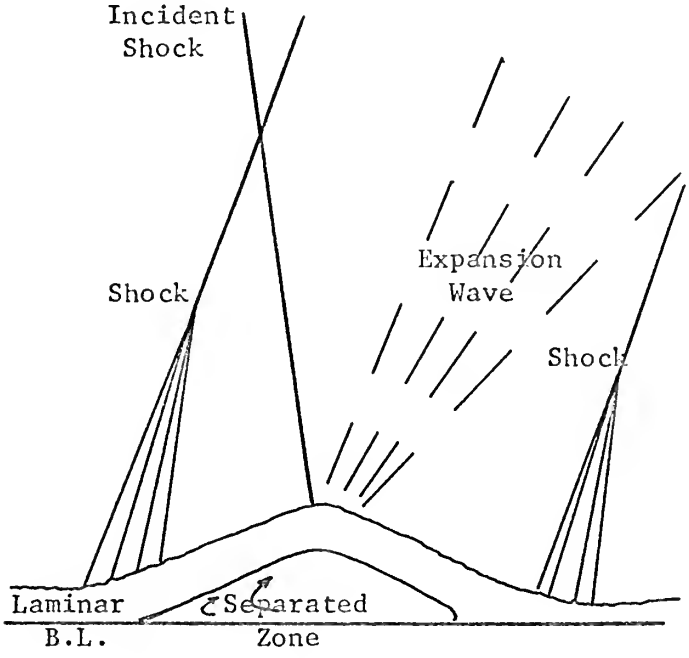

Subcritical Boundary Layer

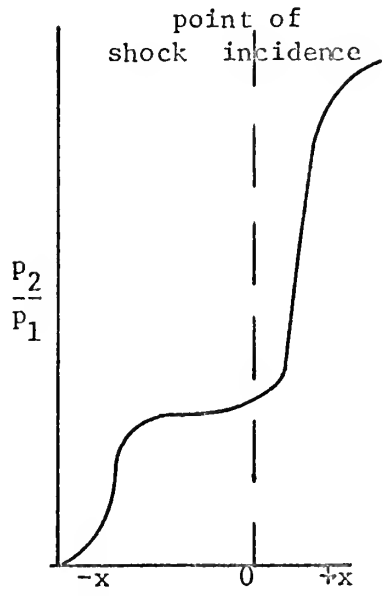

Wall Pressure
Distribution

Figure 13
Interaction of Shock Waves with Compressible Boundary Layers(51)

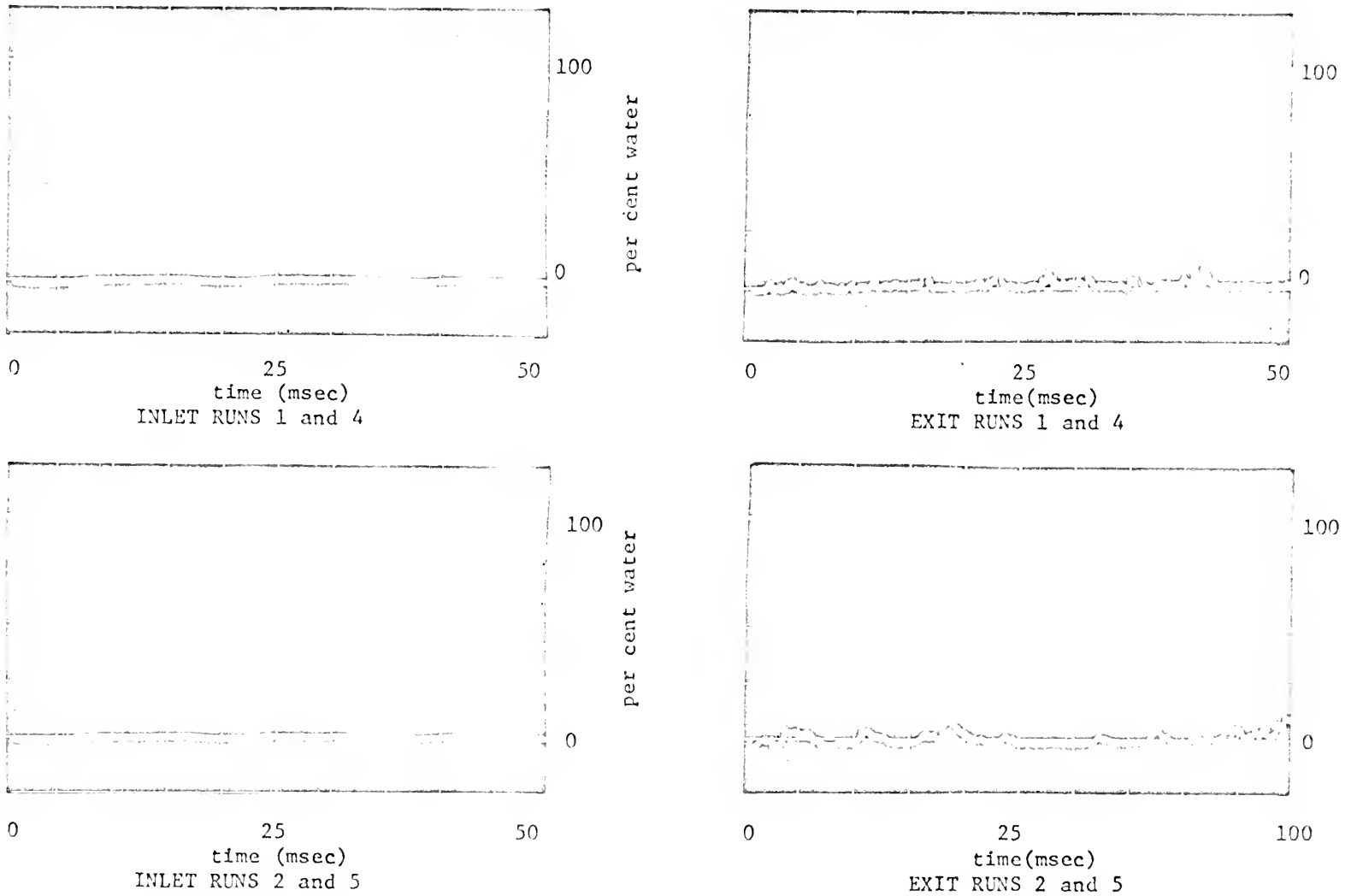

FIGURE 14 RESISTANCE PROBE DATA TRACES

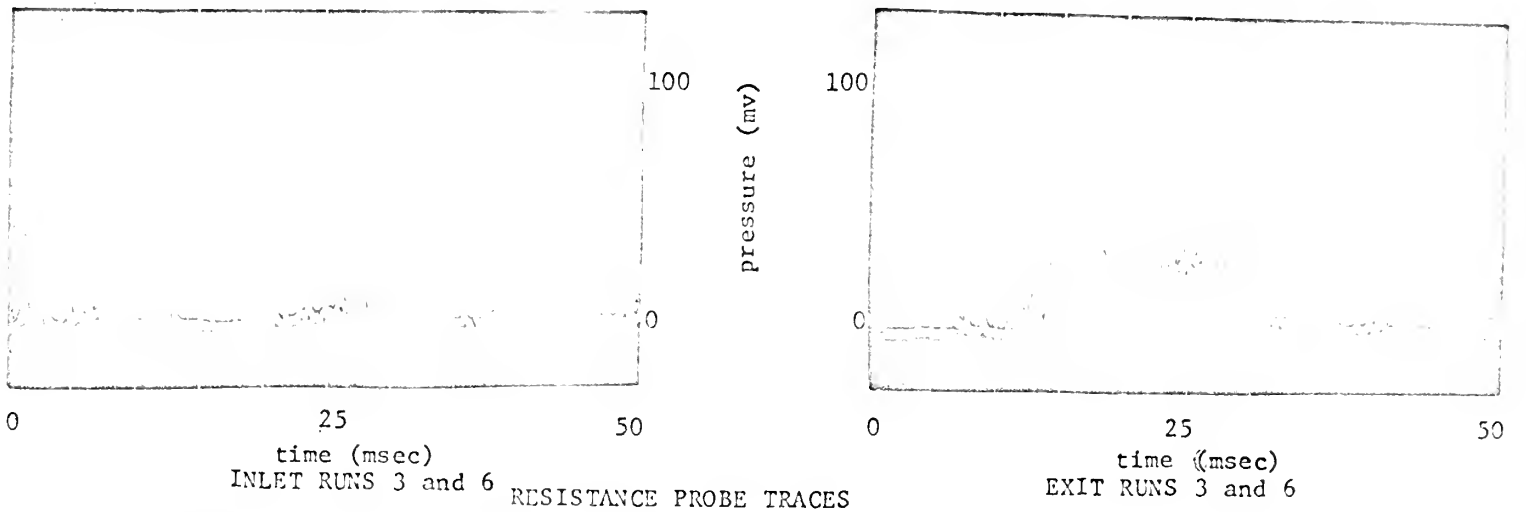

RESISTANCE PROBE TRACES

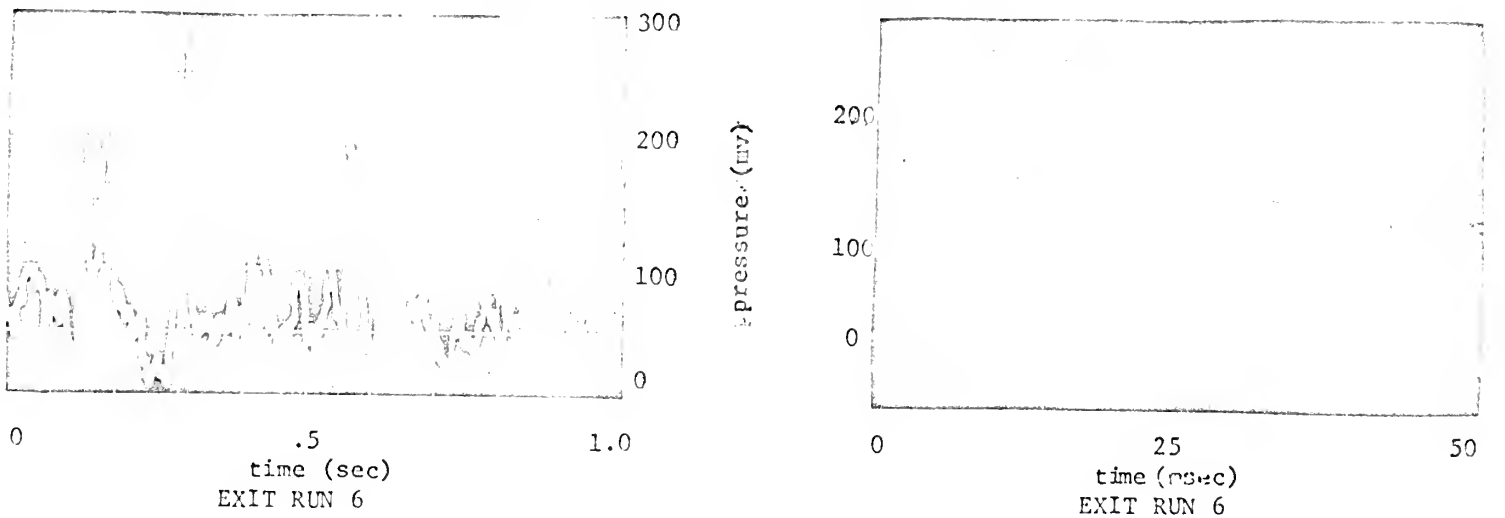

FLOW NOISE PRESSURE TRACES

FIGURE 15 RESISTANCE PROBE DATA AND FLOW NOISE PRESSRE FLUCTUATIONS

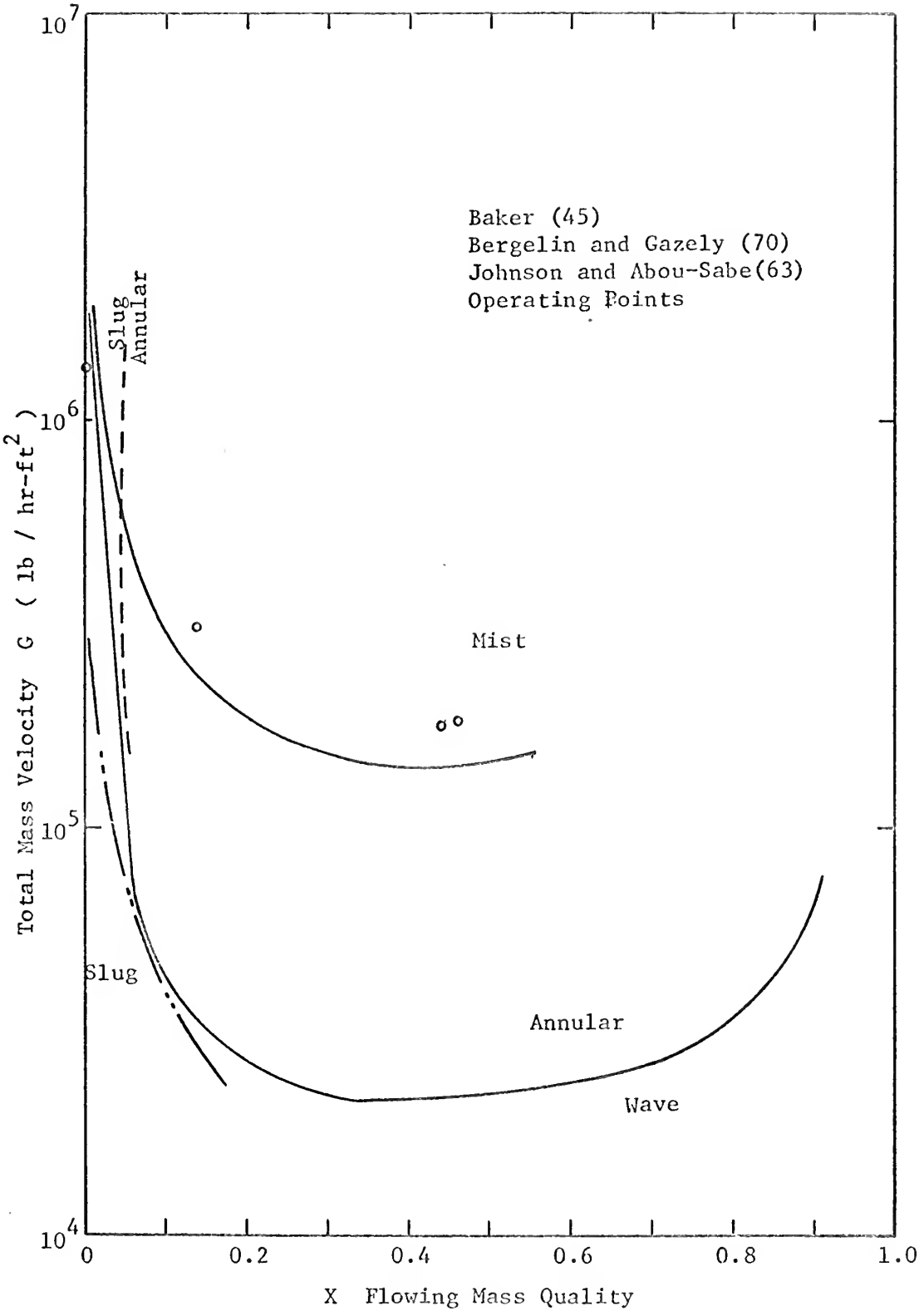

Figure 16 Flow Regime Map I

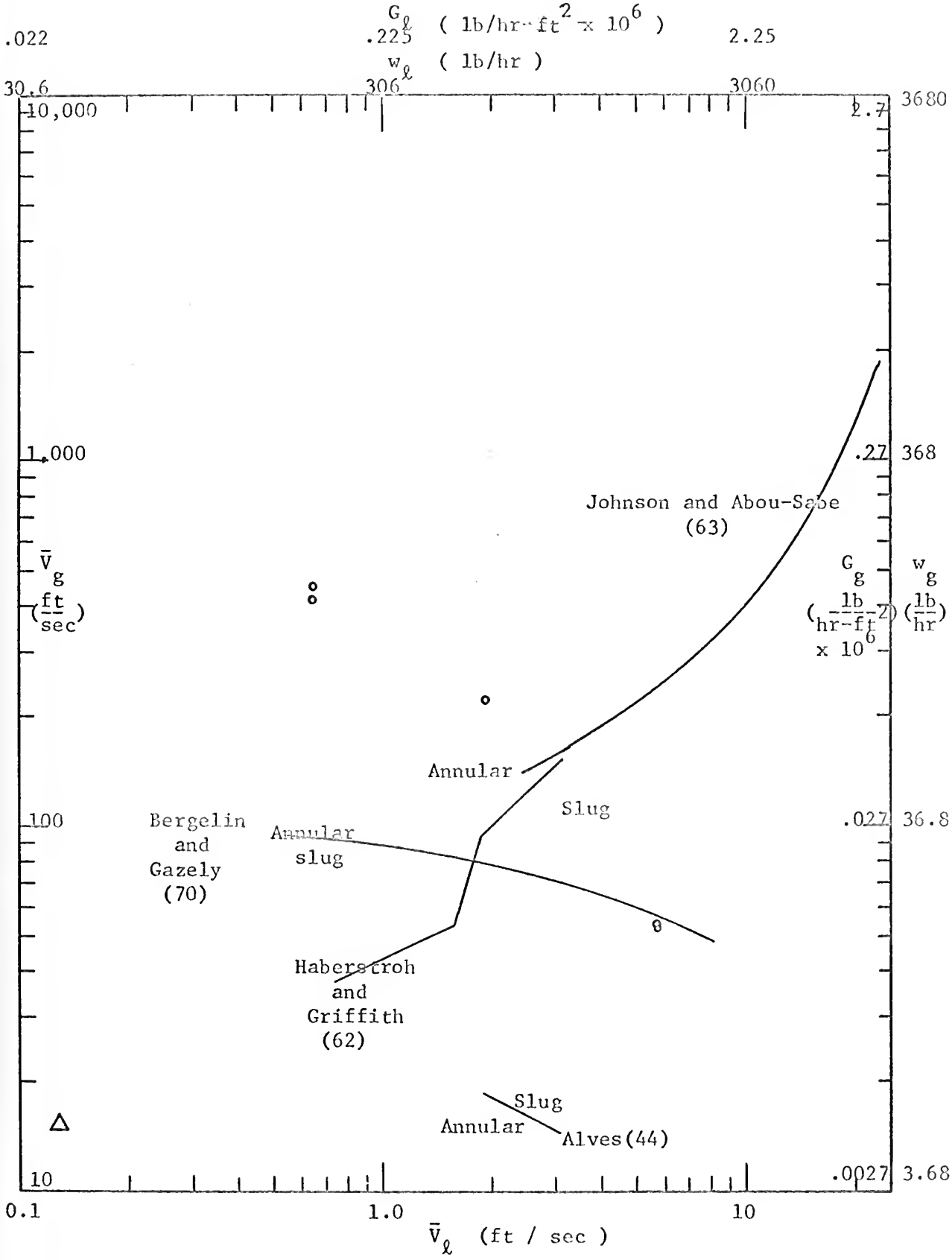

Figure 17 Flow Regime Map II

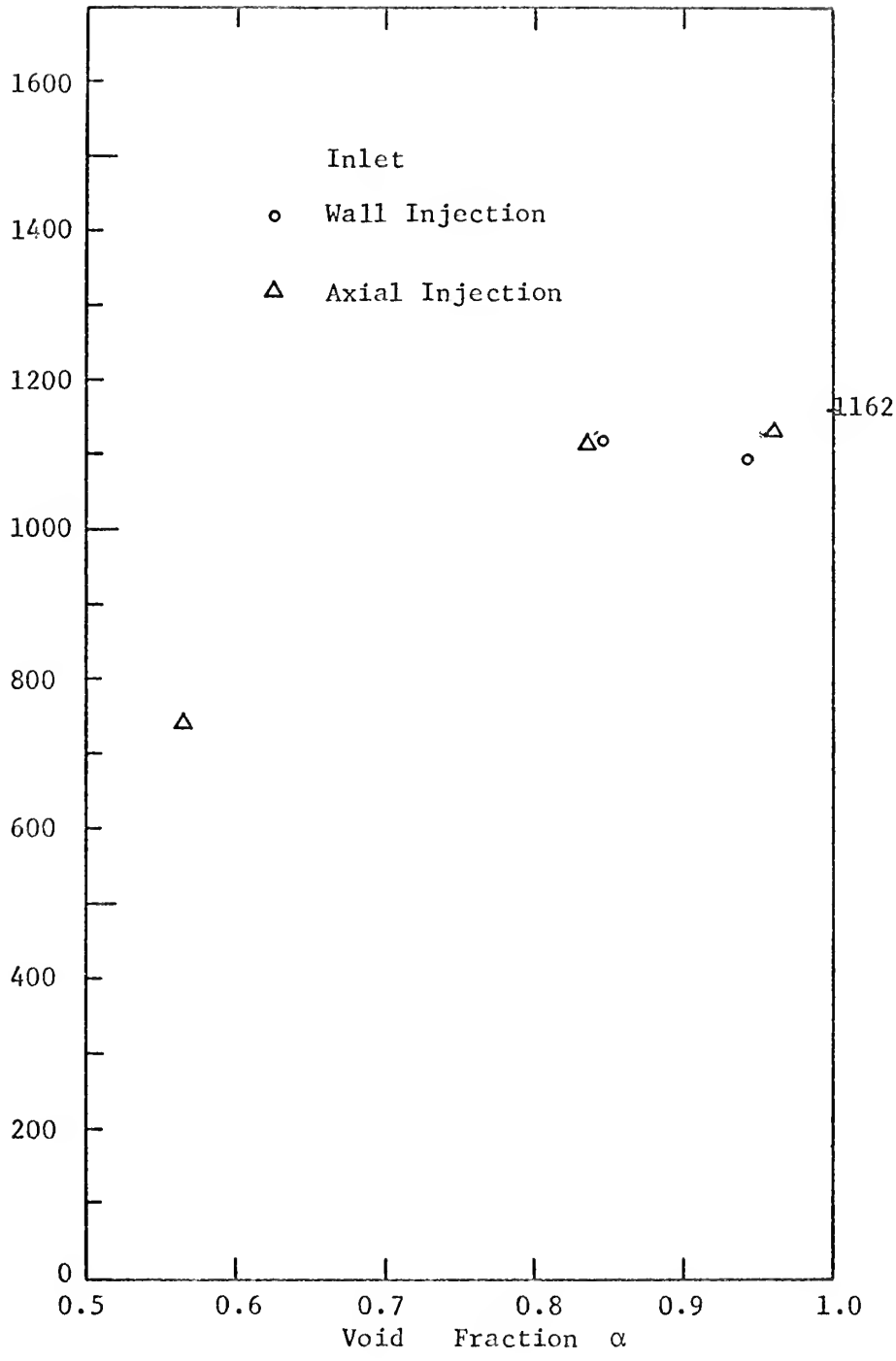

Figure 18
Acoustic Velocity Versus Void Fraction , Inlet Measurements

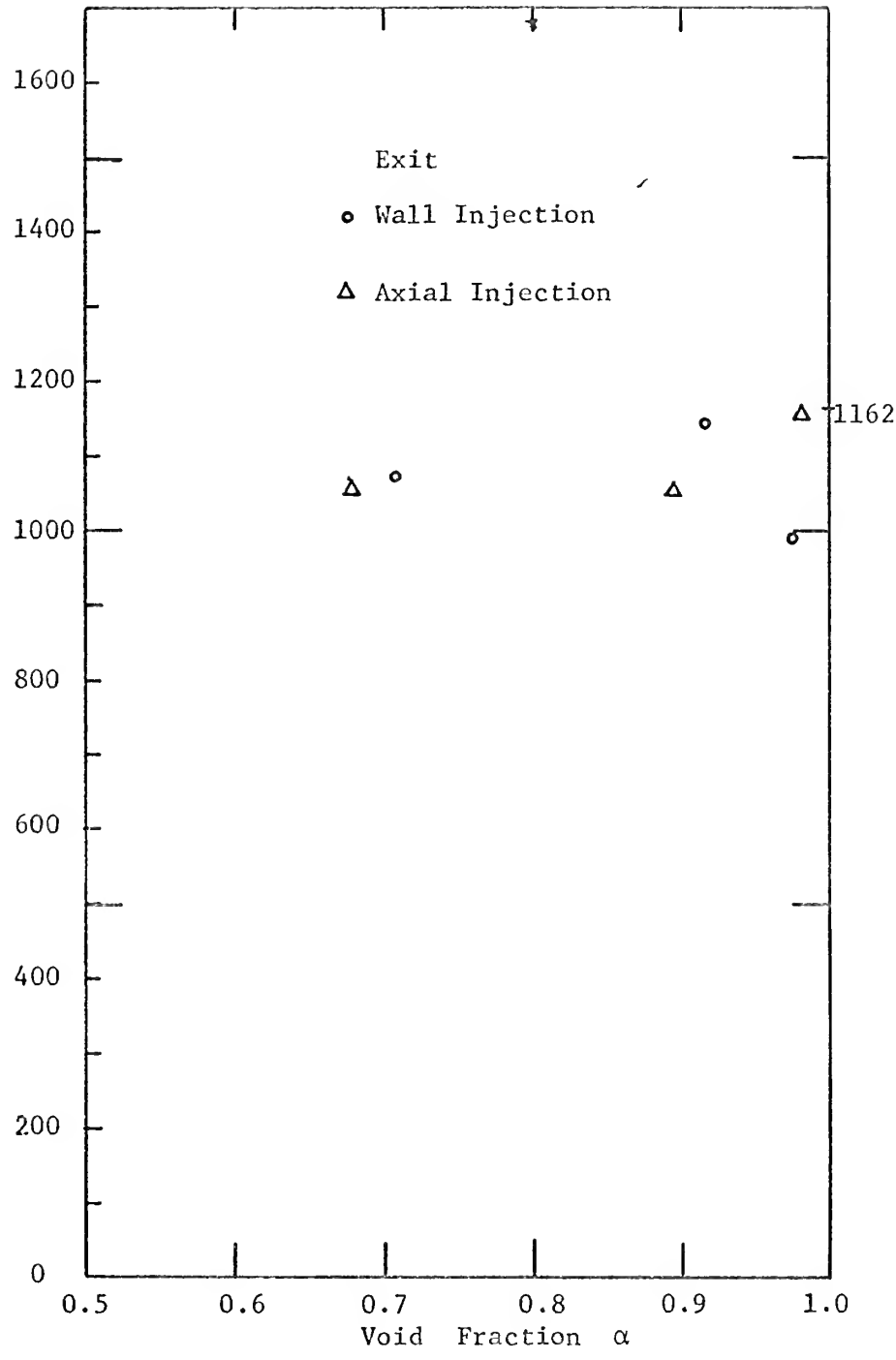

Figure 19
Acoustic Velocity Versus Void Fraction, Exit Measurements

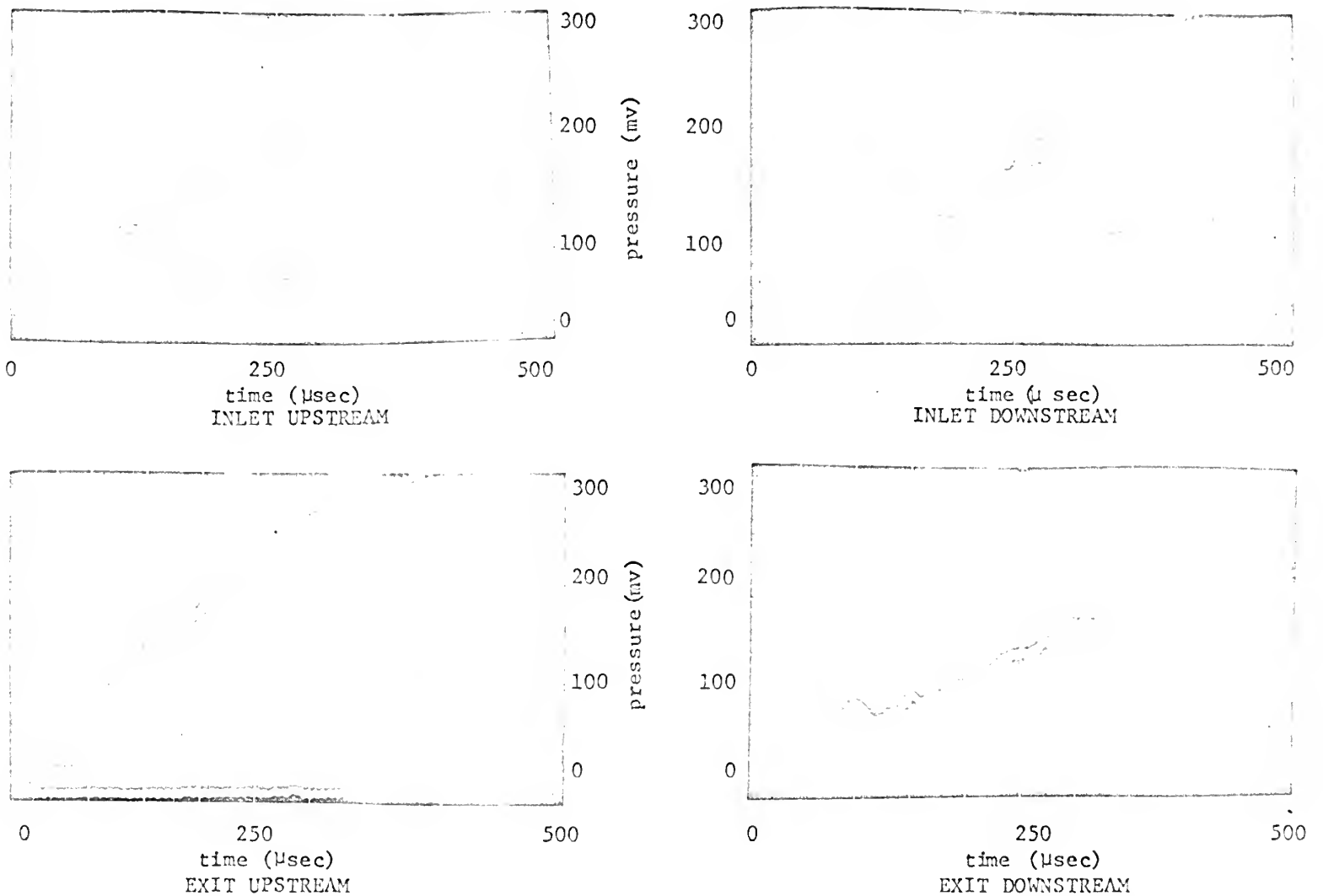

FIGURE 20 REPRESENTATIVE SHOCK WAVE PRESSURE TRACES RUN 1

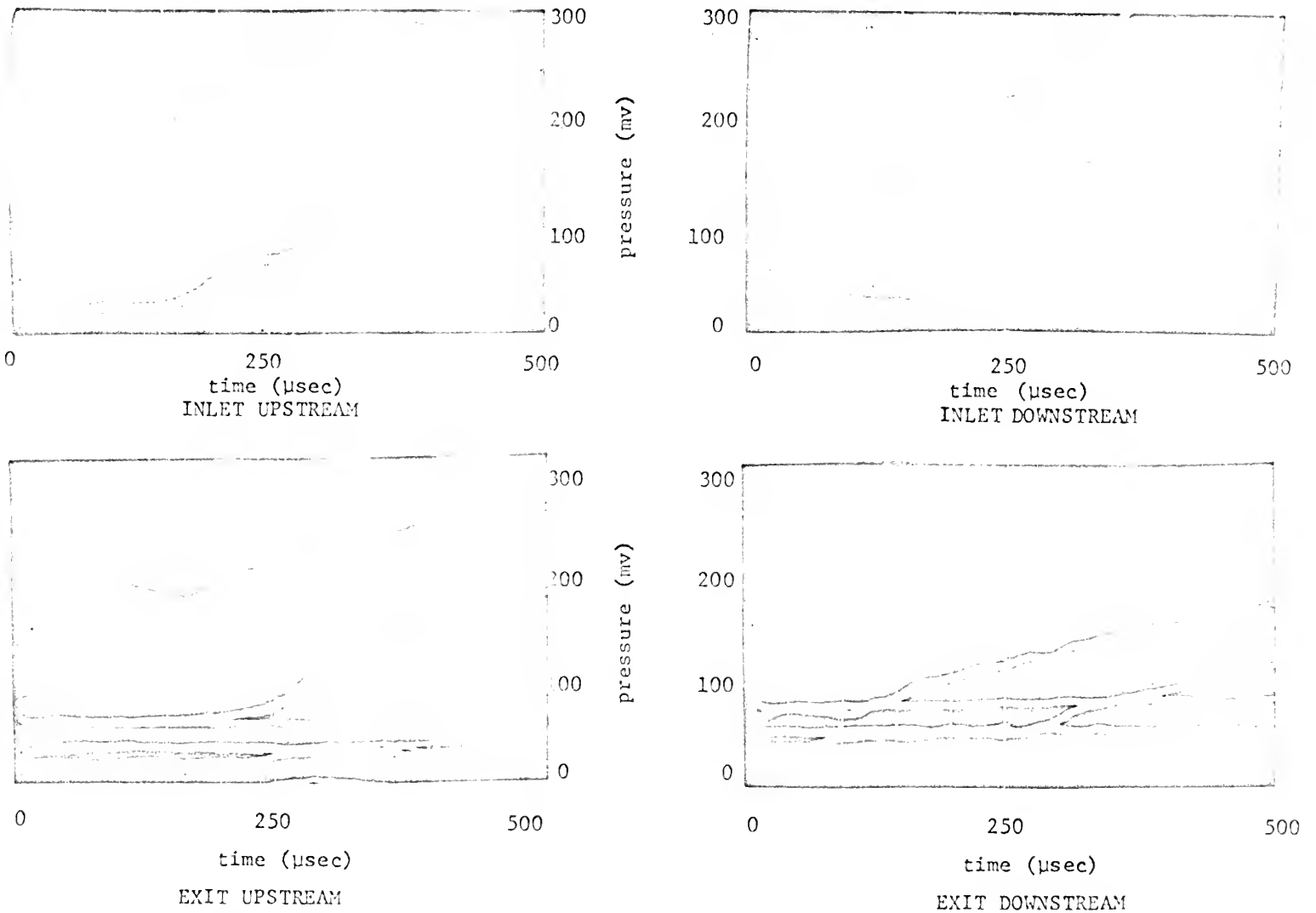

FIGURE 21 REPRESENTATIVE SHOCK WAVE PRESSURE TRACES RUN 2

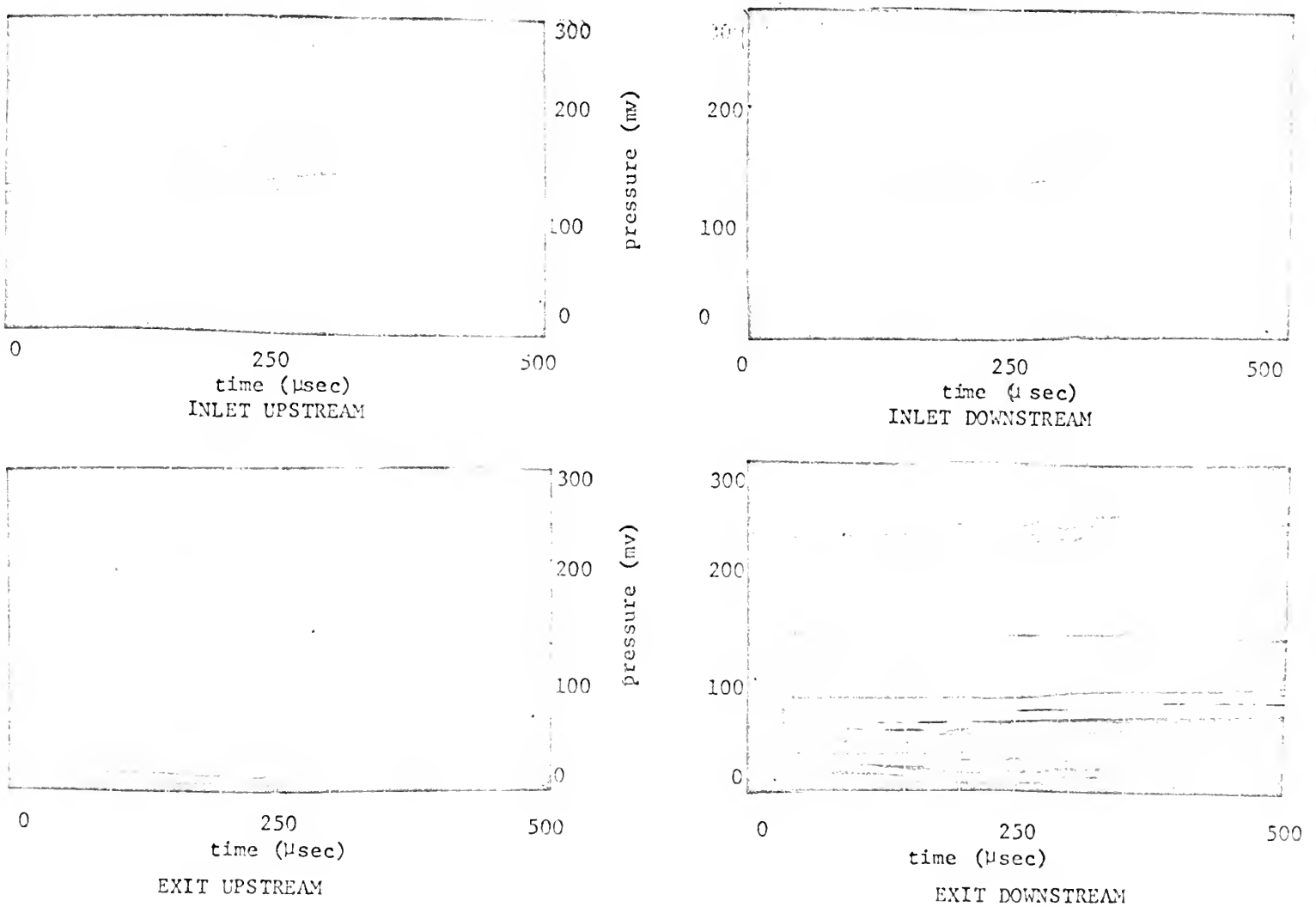

FIGURE 22 REPRESENTATIVE SHOCK WAVE PRESSURE TRACES RUN 3

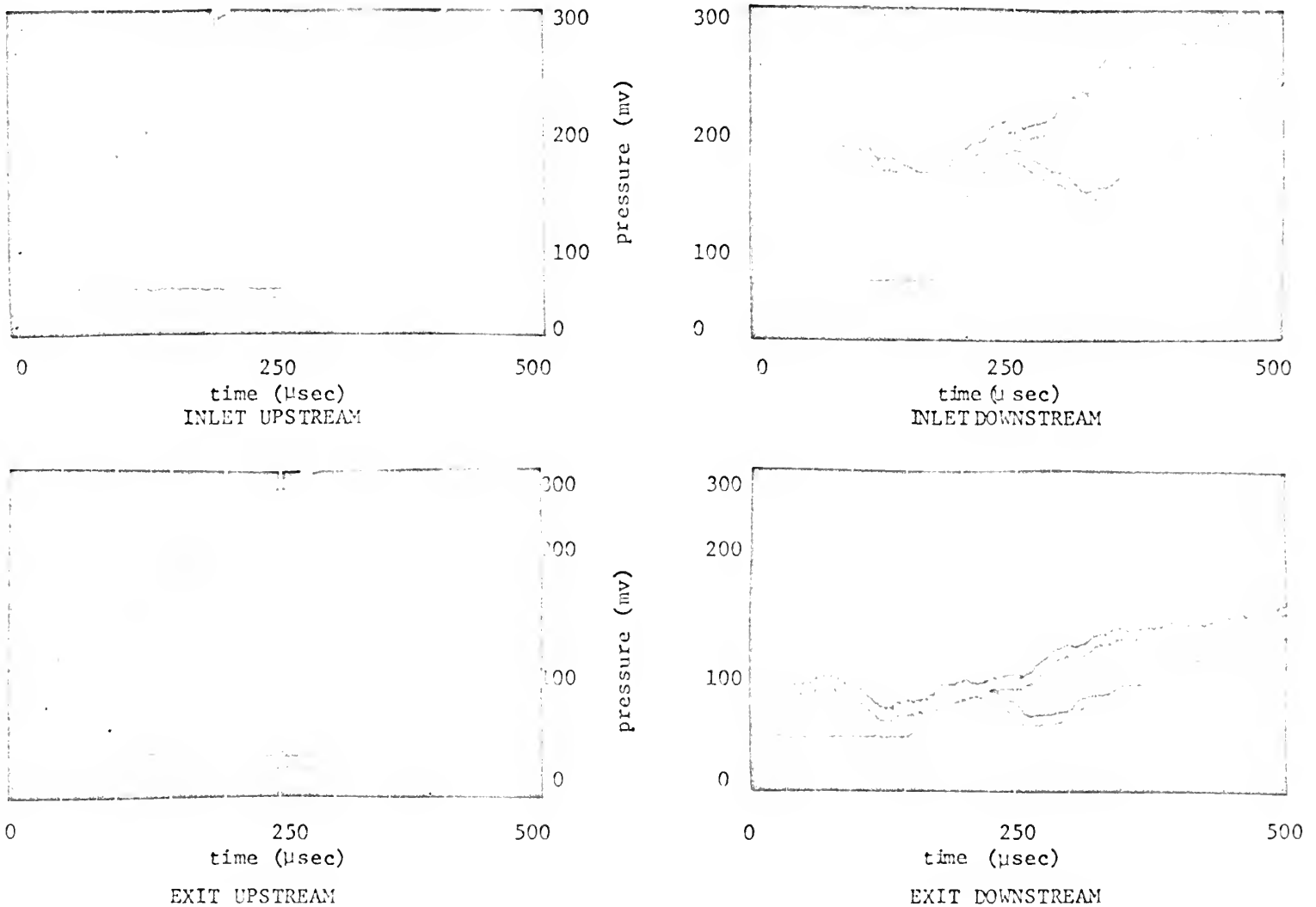

FIGURE 23 REPRESENTATIVE SHOCK WAVE PRESSURE TRACES RUN 4

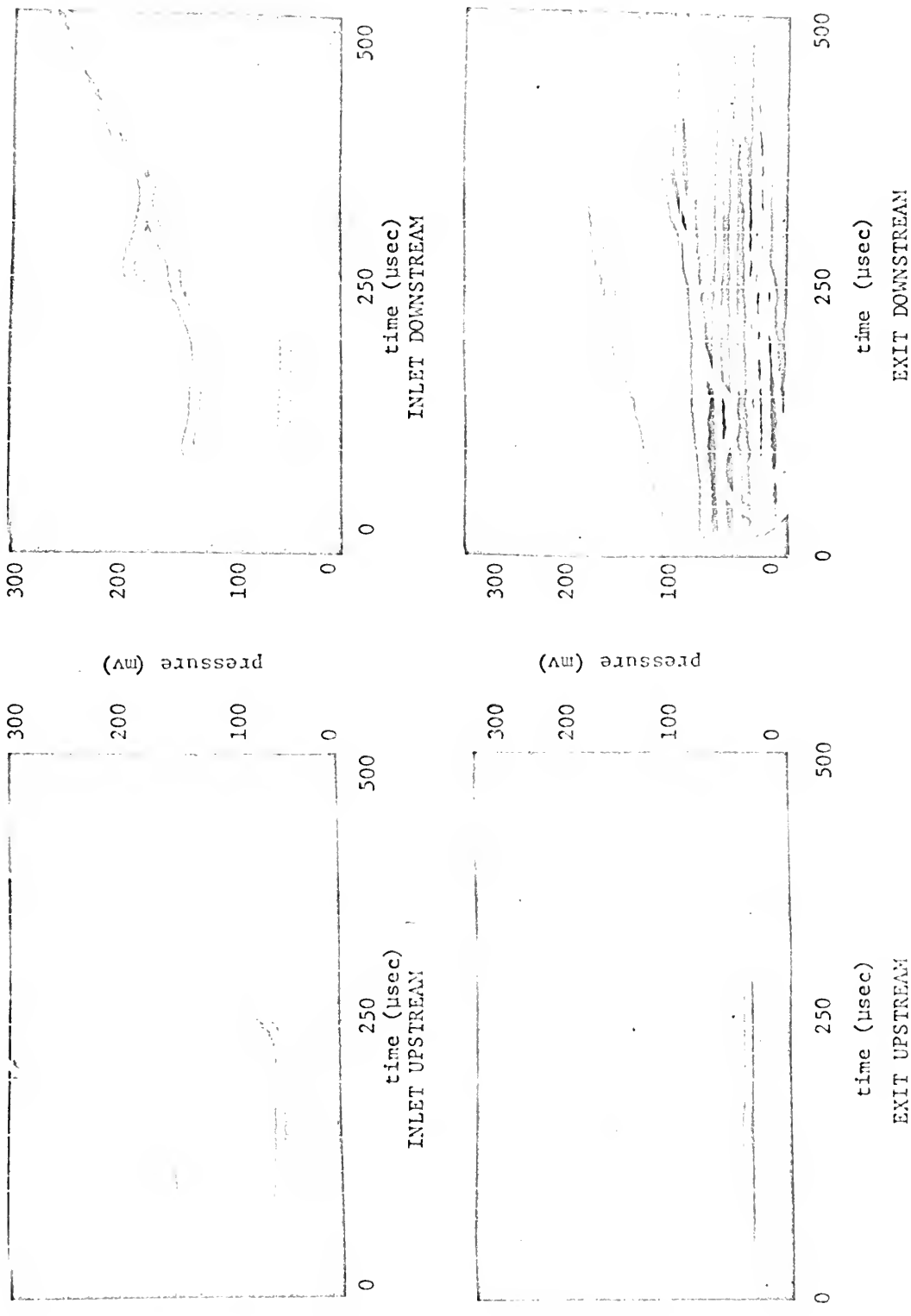

FIGURE 24 REPRESENTATIVE SHOCK WAVE PRESSURE TRACES RUN 5

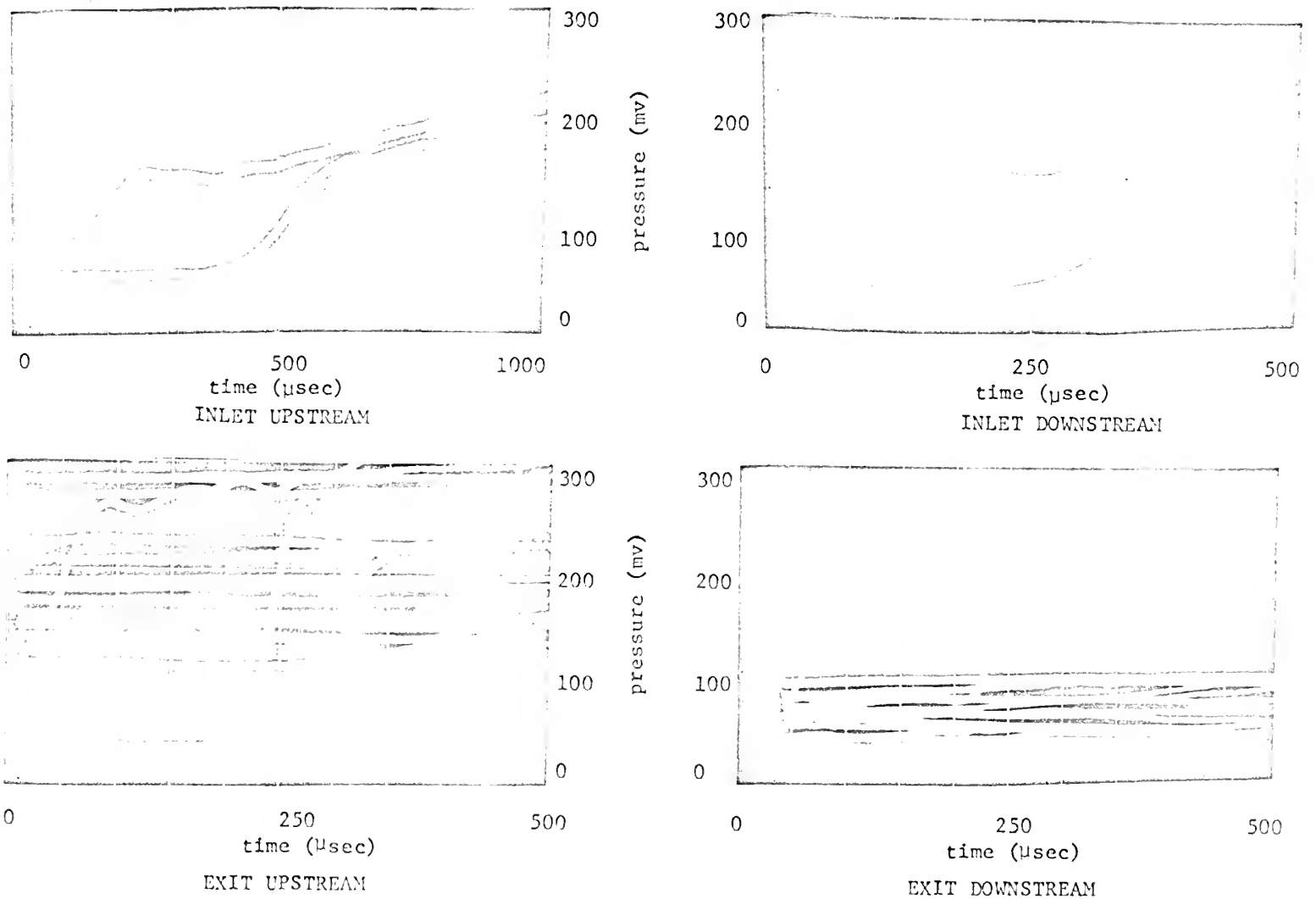

FIGURE 25 REPRESENTATIVE SHOCK WAVE PRESSURE TRACES RUN 6

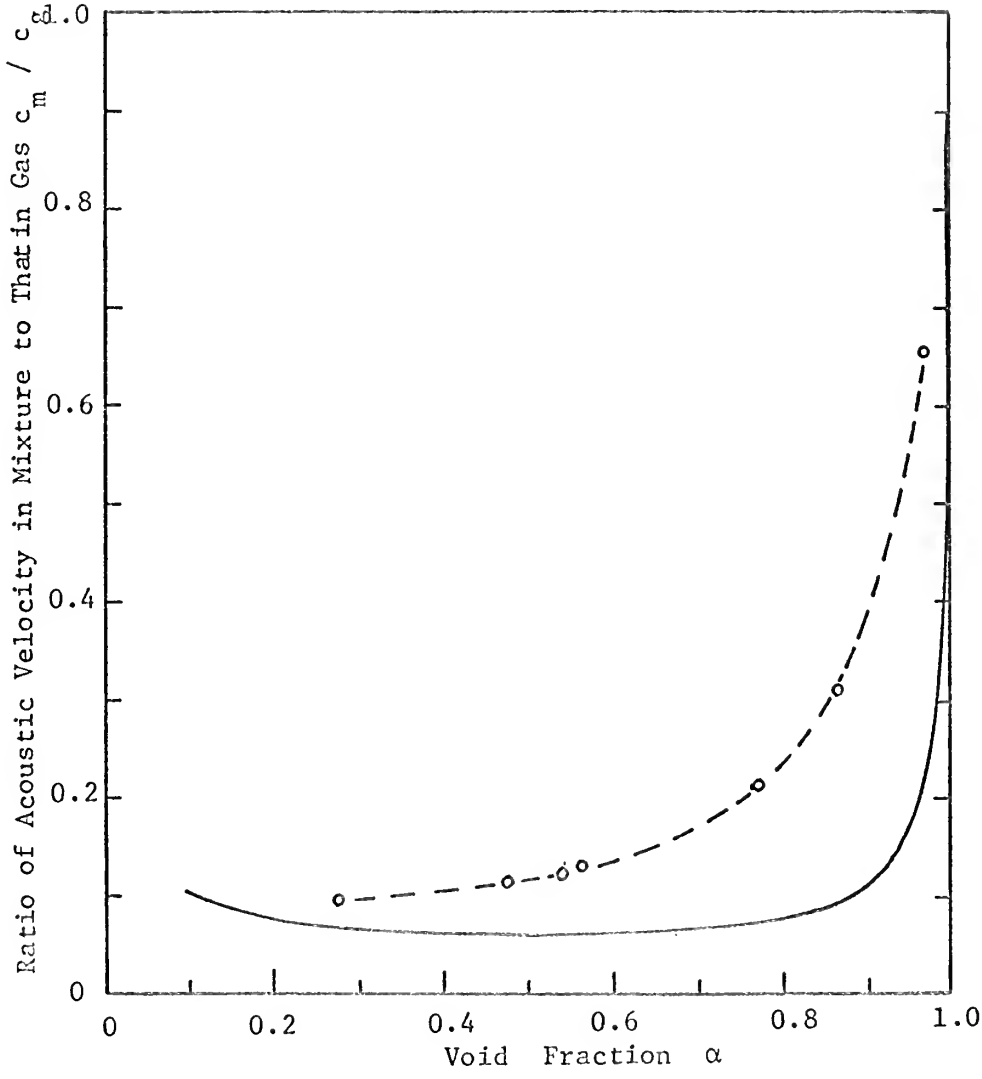

——Predicted Equilibrium Acoustic Velocity in Steam-Water at 17 psia

– – –Vapor Velocity from Critical Flow Data (Fauske) (68)

Figure 26
Mean Gas Velocity Versus Void Fraction for Exit Choking in Short Pipes (Fauske) (68)

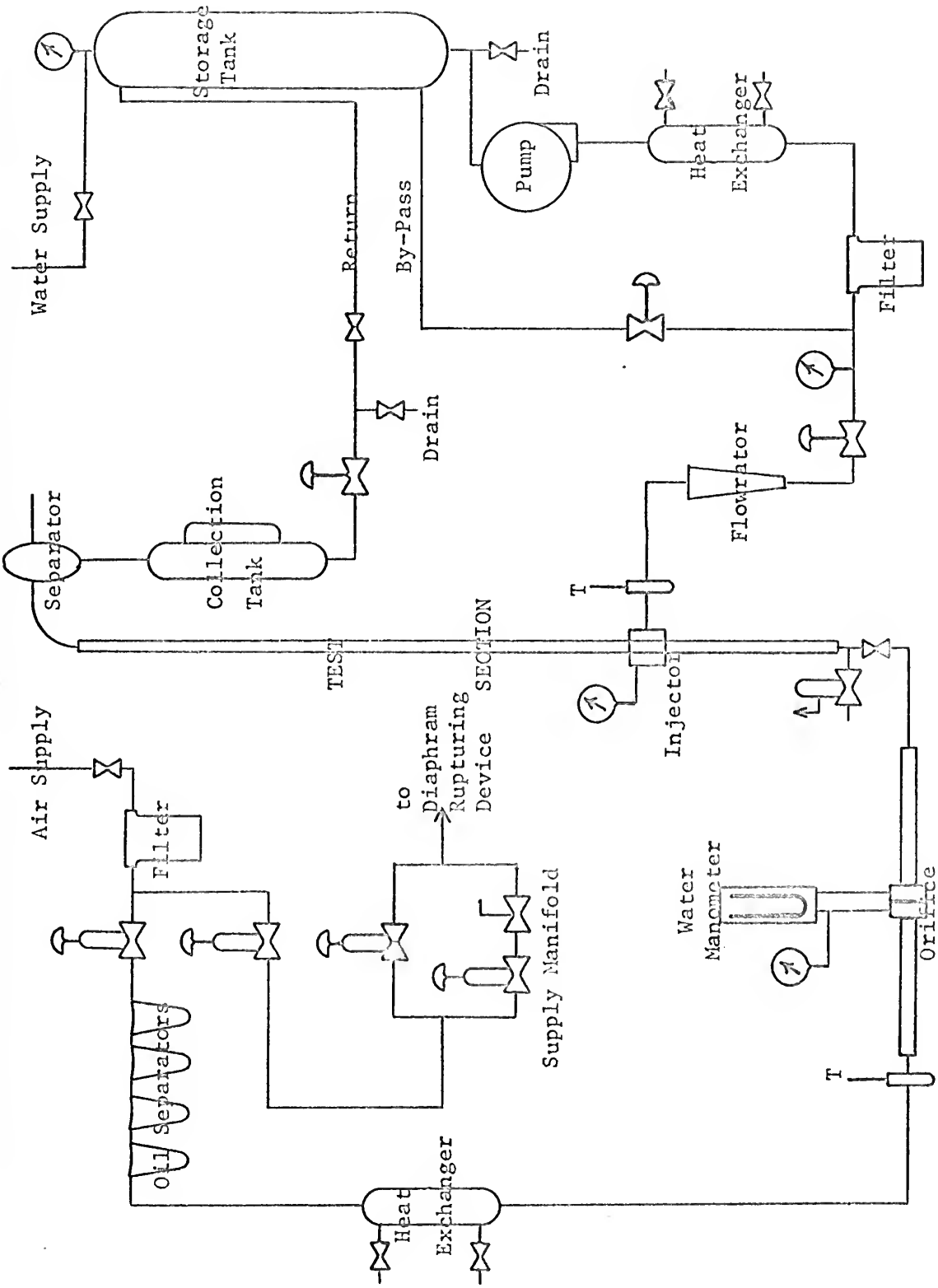

Figure 27 Diagram of Experimental Apparatus

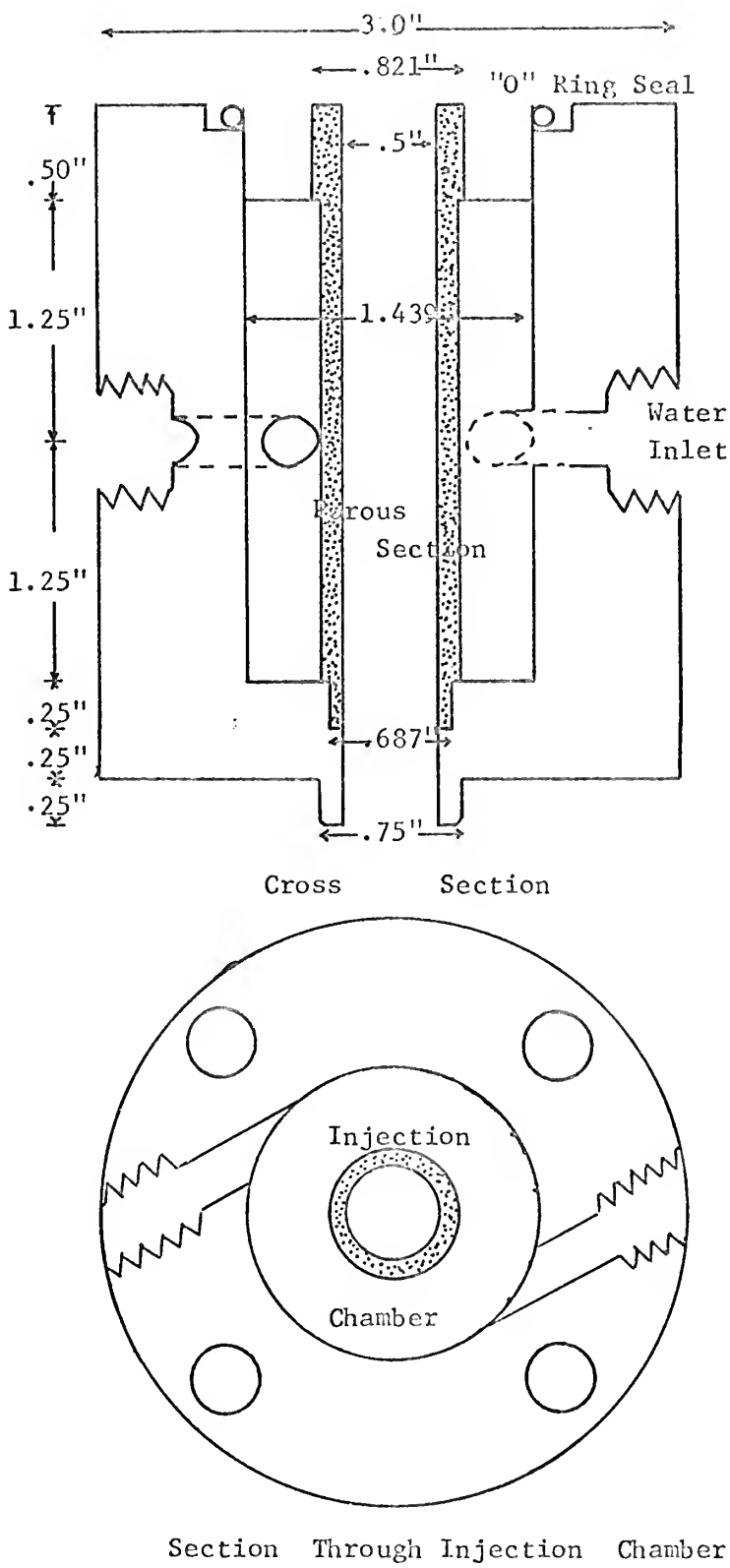

Machined from 3" Dia. Plexiglass Bar Stock

Figure 29 Diagram of Porous Plug Wall Injector

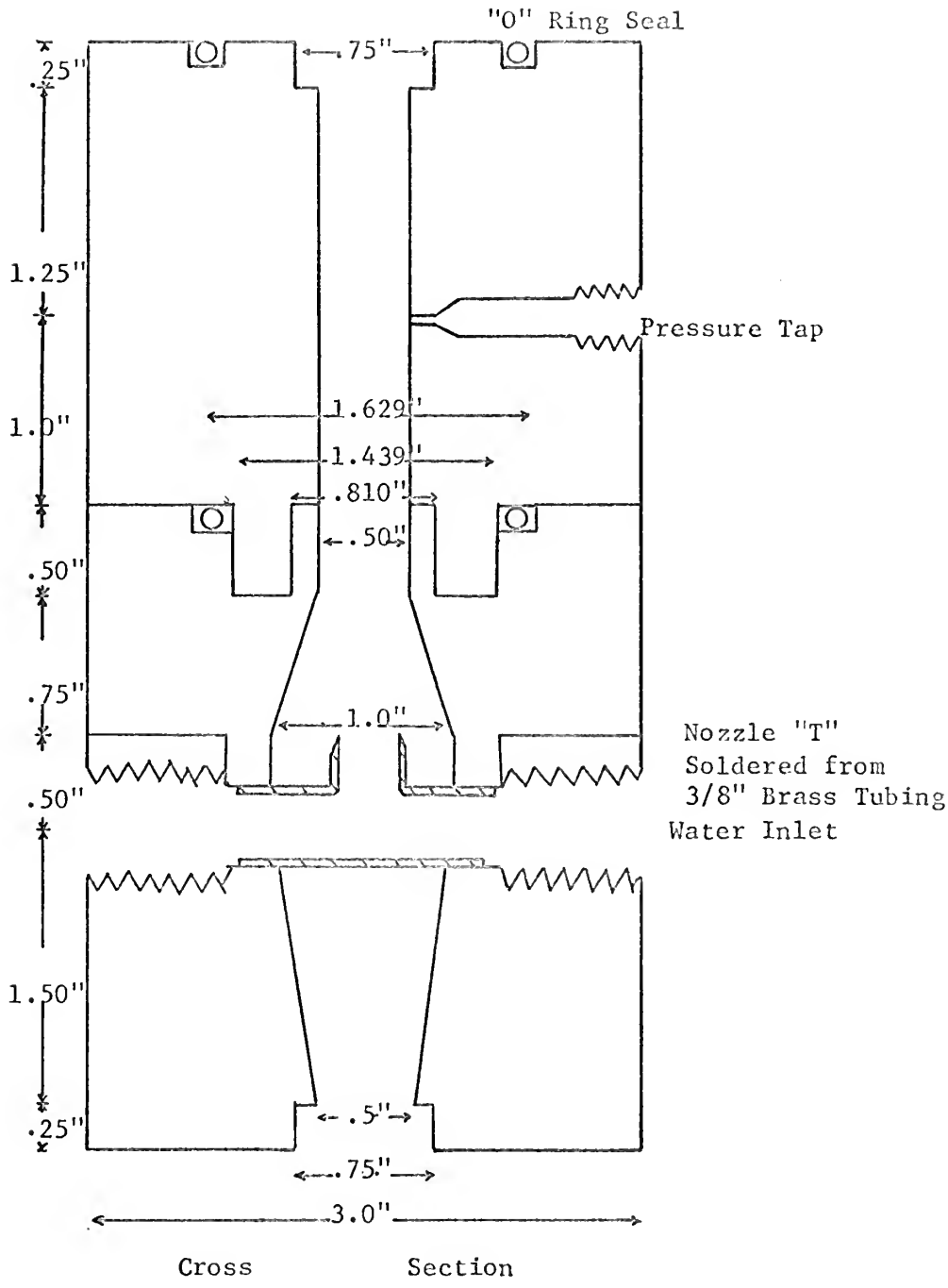

Figure 30 Diagram of Axial Nozzle Injector

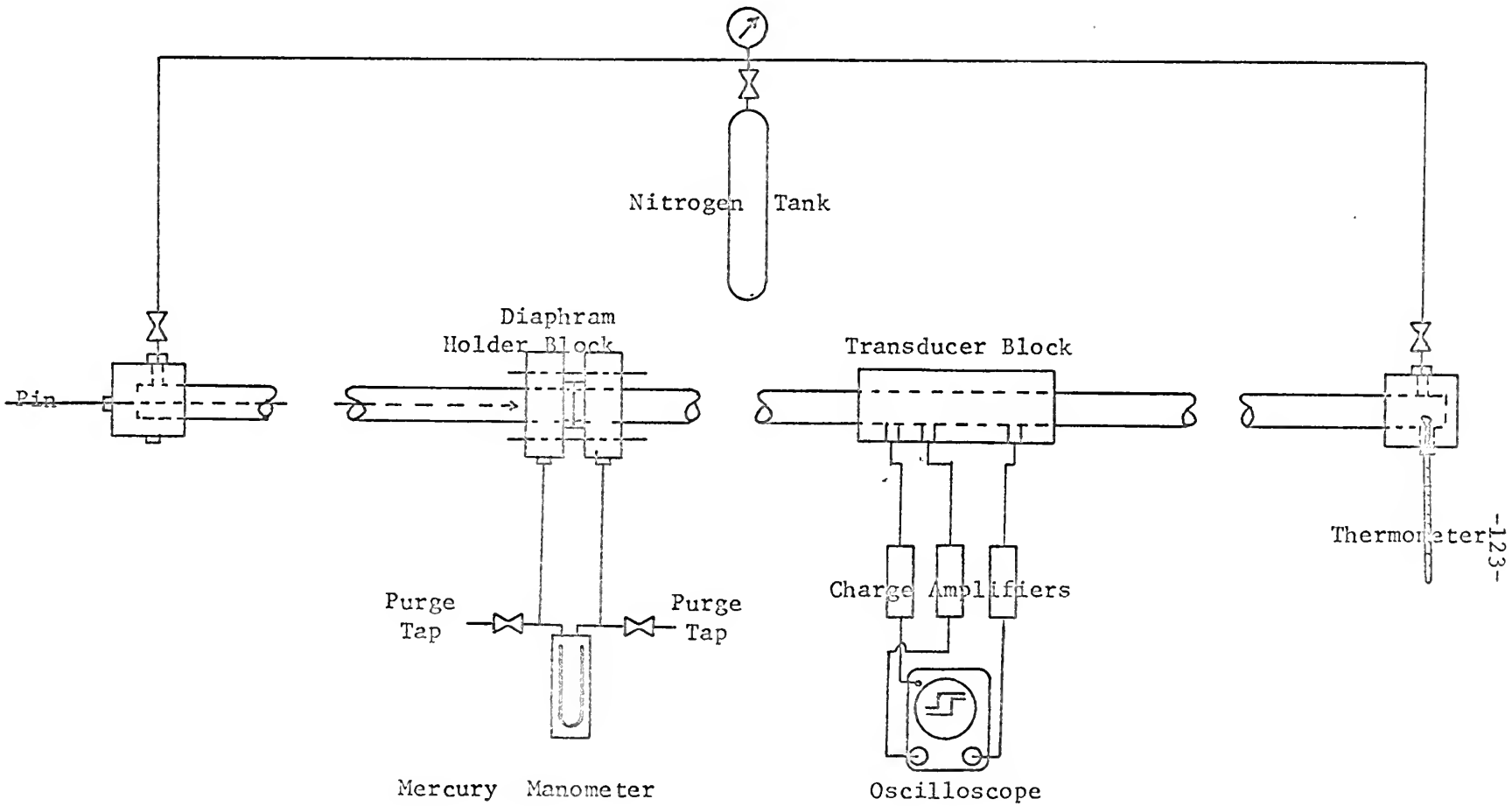

Figure 31 Diagram of Shock Tube Used to Calibrate Transducers

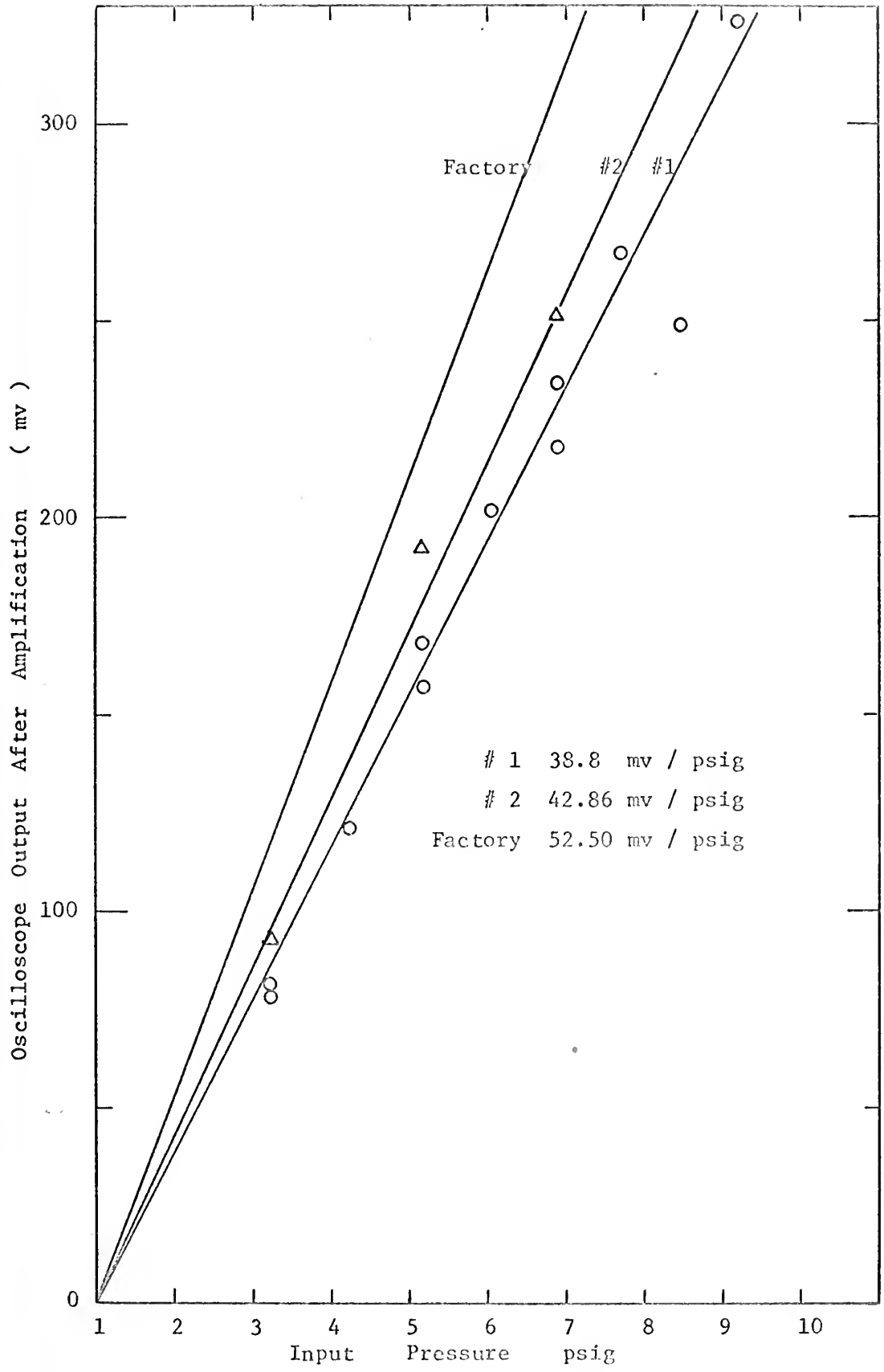

Figure 32 Transducer Sensitivity Calibration

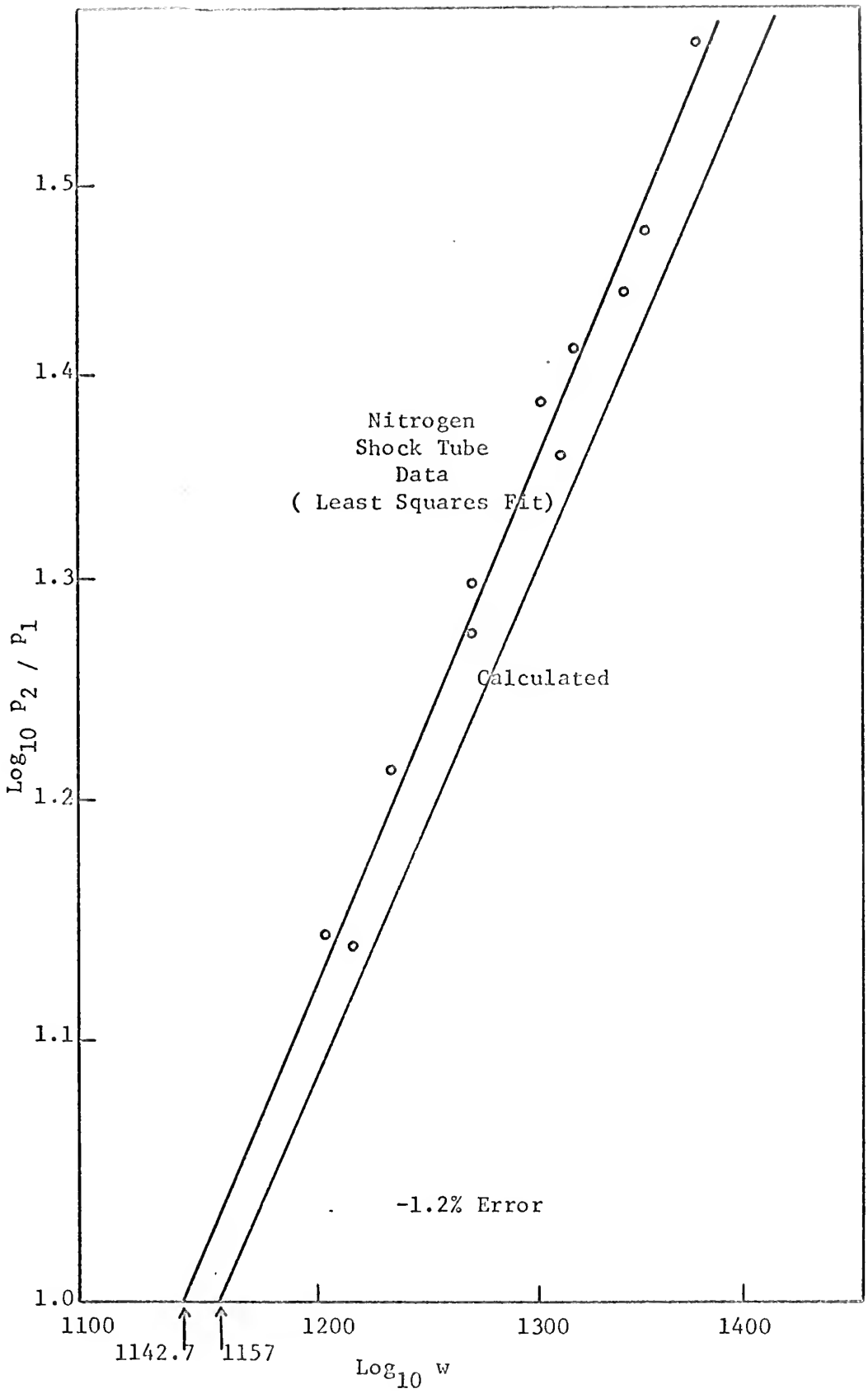

Figure 33 Comparison of Measured to Predicted Velocities Used to Calibrate Transducers

BIBLIOGRAPHY

1. Gouse, S. W., Jr., and Brown, G. A. "A Survey of the Velocity of Sound in Two-Phase Mixtures", ASME 64-WA/FE-35.

2. Gouse, S. W., Jr., and Evans, R. G., "Acoustic Velocity in Two-Phase Flow" Symposium on Two Phase Flow Dynamics, Eindhoven, Sept. 4-9, 1967.

3. Mallock, A., "The Damping of Sound by Frothy Liquids", Proc. Royal Society, Series A, 84, 391-96, 1910.

4. Wood, A. B., "A Textbook of Sound", Bell and Sons London 1st Ed. 1930.

5. Ackeret, J., "Experimental and Theoretical Investigatims on Cavitation in Water", Tech. Mech. and Therm. 1, #1, Berlin 1930.

6. Spitzer, L., "Acoustic Properties of Gas Bubbles in Liquids", NRDC Report No. 6, 1-sr 20-918, 1943, PB 31026.

7. Foldy, L. L, "Propagation of Sound Through Liquid Containing Bubbles, Part I, General Theory", OSRD Report 3601, Section 6.1, Ser. No. 1130-1378, April 1944.

8. Carstersen, E. L., and Foldy, L. L., "Propagation of Sound Through a Liquid Containing Bubbles, Part II Experimental Results and Theoretical Interpretations" OSRD Report 3601, Div. 6, Sec. 6.1, Ser. No. 1130-1629, June 1944.

9. Tangren, R. F., Dodge, C. H., and Seifert, H. S., "Compressibility Effects in Two-Phase Flow", J. App. Phys. 20, #7, 637-45.

10. Chambre, P. L., "Speed of a Plane Wave in a Gross Mixture", J. Acoustical Soc. Am. 26, #3, 329-31, 1954.

11. Silberman, E., "Sound Velocity and Attenuation in Bubbly Mixtures Measured in Standing Wave Tubes", J. Acoustical Soc. Am. 29, #8, 925-33, 1957.

12. Campbell, I. J., and Pitcher, A. S., "Shock Waves in a Liquid Containing Gas Bubbles", Proc. Roy. Soc. 243, Ser A, 1235, 534-45, 1958.

13. Karplus, H. B., "The Velocity of Sound in a Liquid Containing Gas Bubbles", Coo-248, June 11, 1958.

14. Zink, J. W., and Delsasso, L. P., "Attenuation and Dispersion of Sound by Solid Particles Suspended in a Gas", J. Acous. Soc. Am. 30, 765-771, 1958.

15. Carrier, G. F., "Shock Waves in a Dusty Gas" J. Fluid Mech., 4, 376-382, 1958.

16. Andonin, V. I., and Novikov, I. I., "The Speed of Sound on the Vapour-Liquid Phase Equilibrium Curve. The Speed of Sound in Saturated Steam", Prik. Mat. U. Teor, Fiz #1, 1960.

17. Sychev, V. V., "The Speed of Sound in Water and Steam on the Saturation Curve", Inzh, Fig. Zhur., 4, #6, 1961.

18. Karplus, H. B., "Propagation of Pressure Waves in a Mixture of Water and Steam", ARF 4132-12, Jan. 1961.

19. Hsieh, D., and Plesset, M. S., "On the Propagation of Sound in a Liquid Containing Gas Bubbles", Phys. of Fluids, 4, #8, 970-75, 1961.

20. Soo, S. L., "Gasdynamic Processes Involving Suspended Solids", A.I.Ch.E. J. 7, 384-391, 1961.

21. Collingham, R. E., and Firey, J. C., "Velocity of Sound Measurements in Wet Stream", I&EC 2, #3, 197-202, 1963.

22. Kriebel, A. R., "Analysis of Normal Shock Waves in Particle-Laden Gas", ASME Paper No. 63 -WA-13, 1963.

23. Clinch, J. M., and Karplus, H. B., "An Analytical Study of the Propagation of Pressure Waves", NASA-CR-54015, May 31, 1963.

24. Semenov, N.I., and Kosterin, S.I., "Results of Studying the Speed of Sound in Moving Gas-Liquid Systems", Teploenergetika 11, #6, 46051, 1964.

25. Deich, M.E., Filippov. G. A., and Stekol'shchikov, E.V., "The Speed of Sound in Two-Phase Media", Teploenergetika 11, #8, 33-36, 1964.

26. Rudiger, G., "Some Properties of Shock Releaxation in Gas Flows Carrying Small Particles", Phys. Fluids. 7, 658-663, 1964.

27. Rudiger, G., and Chang, A., "Analysis of Nonsteady Two-Phase Flow" Phys. Fluids 7, Nov. 1964.

28. Chu, B. T., and Chow, J.C.F., "On a Macroscopic Theory of a Two-Phase Fluid", AIAA 2nd Aerospace Sciences Meeting, New York, Jan. 1965, Paper No. 65-8.

29. F.V.D. Walle, Verheugen, A. J.,Haagh, V. J.M., and Bogaardt, M., "A Study of the Application of Acoustical Methods for Determining Void Fraction in Boiling Water Systems", EUR, 2336, e., June 20-23, 1965.

30. Rudinger, G., "Some Effects of Finite Particle Volume on the Dynamics of Gas-Particle Mixtures", AIAA J. 1217-22, July 1965.

31. Davies, A. L., "The Speed of Sound in Mixtures of Water and Steam," AEEw-M452, Oct., 1965.

32. Deich, M.E., Stekol'shchikov, E.V., and Filippov. G.A., "Step Changes in Specific Heat C_v, Sonic Velocity and Ratio of Specific Heats on the Vapour-Liquid Phase Equilibrium Curve", Teploenergetika 12, #12, 51-54, 1965.

33. Bowles, R. E., and Manion, F. M., "Analysis and Test of Signal Transmission in a Multiphase Fluid Mixture", U.S. Army Aviation Material Laboratories, Report 65-77, Jan. 1966, AD628676.

34. Temkin, S., "Attenuation and Dispersion of Sound by Particulate Relaxation" , Div. of Eng., Brown U., Feb. 1966, AD603026.

35. Temkin, S., and Dobbins, R. A., "Measurements of Attenuation and Dispersion by an Aerosol", Div. of Eng., Brown U., May 1966, AD632911.

36. Dvornichenko, V. V., "The Speed of Sound in the Two-Phase Zone," Teploenergetika, 13, #10, 72-76, 1966.

37. Eddington, R. B., "Investigation of Supersonic Shock Phonemena in a Two-Phase (Liquid-Gas) Tunnel", J.P.L. Tech. Report 32-1096, Mar. 15, 1967.

38. Deich, M.E., Filippov, G. A., Stekol'shchilzov, E. V., and Anisimova, M. P., "Experimental Study of the Velocity of Sound in Wet Steam" Teploenergetika 14, #4, 59-63, April 1967.

39. Zenz, F. A., and Othmer, O. F., "Fluidization and Fluid-Particle Systems", Reinhold Pub. Co., 1960.

40. Forslund, R. P., "Thermal Non-Equilibrium in Dispersed Flow Film Boiling in a Vertical Tube" Sc.D. Thesis, Mech. Eng. Dept., M.I.T., 1966.

41. Isshiki, N., "Theoretical and Experimental Study on Atomization of Liquid Drops in High Speed Gas Stream", Report #35, Transportation Technical Research Institute, Tokyo, Japan.

42. Snyder, G.A.,"Determination of the Drop Size Distribution in Two-Phase Boiling Flow", B.S. Thesis, Mech. Eng. Dept., M.I.T., June 1959.

43. Bergles, A. E., and Suo, M., "Investigation of Boiling Water Flow Regimes at High Pressure"Proceedings of 1966 Heat Transfer and Fluid Mechanics Institute, Ed., Saad, M. A., and Miller, J. A., Stanford Univ. Press, Stanford, Ca., 79-88, 1966, L.C. A50-7899.

44. Alves, G.E., "Co-Current Gas Flow in a Pipe-Line Contactor", Chem. Eng. Prog. 50, 449, 1954.

45. Baker, O., "Simultaneous Flow of Oil and Gas", Oil and Gas J. 53, 185-190, July 1954.

46. Hinkle W. D., "A Study of Liquid Mass Transport in Annular Air-Water Flow" Sc. D. Thesis Nuc. Eng. Dept., M.I.T., May 1967.

47. Arnold, C. R., and Hewitt, G. F., "Further Developments in the Photography of Two-Phase Gas-Liquid Flow", A.E.R.E. R 5318, Harwell, England, Jan. 1967.

48. Arnold, C. R., and Hewitt, G. F., "Two-Phase Annular Flow", (Axial View), 16 mm film, Atomic Energy Research Establishment, Harwell, England, 1966.

49. Griffith, P., and Wallis, G. B., "Two-Phase Slug Flow", J. Heat Transfer, 83, No. 3, Series C. 307, Aug. 1961.

50. Morse, P. M., and Ingard, K. U., "Theoretical Acoustics", McGraw-Hill New York, 1968, L. C. 67-15428.

51. Shapiro, A. H., "The Dynamics and Thermodynamics of Compressible Fluid Flow" Vols. I and II, Ronald Press, New York, 1953.

52. Chu, F. K. H, "Miniature Piezoelectric Pressure Transducers for Dynamic Pressure Field Measurements in a Small Turbine", M.I.T. Engineering Projects Laboratory, Memorandum M-9821- 1, July 6, 1964.

53. Baganoff, D., "Pressure Gauge with One-Tenth Microsecond Rise Time for Shock Reflection Studies", Rev. Sci. Inst., Vol. 35, No. 3, 288-295, March 1964.

54. Gouse, S. W., Jr., "Void Fraction Measurement", M.I.T. Engineering Projects Laboratory, Report No. DSR 8734-2, April, 1964.

55. Hubbard, M.G., and Dukler, A.E., "The Characterization of Flow Regimes for Horizontal Two-Phase Flow", Proceedings of 1966 Ht. Trans. and Fluid Mech Institute Ed.,Saad,M.A. and Miller, J.A,,Stanford Univ. Press, Stanford, Cal. 1966, LC A50-7899.

56. Solomon, J.V., "Construction of a Two Phase Flow Regime Transition Detector" S.M. Thesis, M.I.T., June 1962.

57. Fiori, M.P., and Bergles, A.E., "A Study of Boiling Water Flow Regimes at Low Pressure", M.I.T. Engineering Projects Laboratory, Report No. 5382-40, Feb. 1966.

58. Lees, L., "Viscous-Inviscid Flow Interactions at Supersonic Speeds", Univ. of Notre Name. Ht. Trans. and Fluid Mech. Lab. Lecture Notes, April 10-11, 1967.

59. Crocco, L. "Considerations on the Shock Boundary Layer Interaction", Proc. Conf. on High Speed Aeronautics, Polytechnic Institute of Brooklyn, 75-112, Jan. 20-22, 1955.

60. Lees, L. and Reeves, B. L., "Supersonic Separated and Reattaching Laminar Flows," AIAA J. 2, 1907-1920, 1964.

61. Bennett, A.W., et. al., "Flow Visualization Studies of Boiling at High Pressure" AERE-R 4874, Harwell, England March 1965.

62. Haberstroh, R.D., and Griffith, P., "The Transition from the Annular to the Slug Flow Regime in Two-Phase Flow" M.I.T. Engineering Projects Laboratory Report 5003-28, June, 1964.

63. Johnson, H. A., and Abou-Sabe, A.H.A., "Heat Transfer and Pressure Drop for Turbulent Flow of Air-Water Mixtures in a Horizontal Pipe" Trans. ASME 74, 977-987, 1952.

64. Gill, L.E., and Hewitt, G. F., "Sampling Probe Studies of the Gas Core in Annular Two Phase Flow Part 3" A.E.R.E. -M1202 Harwell, England, July 1967.

65. Alexander, L.G., and Coldren, C. L., "Droplet Transfer from Suspending Air to Duct Walls" Industrial and Engineering Chemistry 43, No. 6, 1325-1331, 1951.

66. Donaldson, C. DuP. and Sullivan, R.D., "The Effect of Wall Friction on the Strength of Shock Waves in Tubes and Hydraulic Jumps in Channels" NACA TN 1942 Sept. 1949.

67. Hollyer, R. N., "A Study of Attenuation in the Shock Tube" Univ. of Mich. Eng. Research Institute Project M 720-4, July 1953.

68. Fauske, H. K., "Two-Phase Two-and One-Component Critical Flow",Proceedings of the Symposium on Two Phase Flow. Vol. I. Exeter, England 21-23 June 1965.

69. Gouse, S.W., Jr., "An Introduction to Two Phase Gas Liquid Flow" MIT Engineering Projects Laboratory Report 8734-3, June 1964.

70. Bergelin, O. P., and Gazely, C., "Co-Current Gas-Liquid Flow", Ht. Trans. and Fluid Mech. Inst. Berkely Cal., 5-18, 1949.

BIOGRAPHICAL NOTE

The author was born in New Orleans, Louisiana on August 11, 1936. He attended the public elementary schools of that city and the Alcée Fortier High School. In 1953 he moved with his family to Washington, D.C. and graduated in 1954 from the Woodrow Wilson High School.

He attended the United States Naval Academy in Annapolis, Maryland graduating with distinction in June 1958.

He served at sea as an officer in the Destroyer Force U.S. Atlantic Fleet from 1958 until 1963 when he entered the Massachusetts Institute of Technology under the U.S. Navy's Post Graduate Education Program. In June of 1966 he received a Master of Science degree in Mechanical Engineering and a Naval Engineers degree.

The author is an associate member of the Society of Naval Architects and Marine Engineers. He is also a member of Sigma Xi and Tau Beta Pi.

He is married to the former Ann Webster Hogan of Princeton, New Jersey.